ENGINEERED NANOFLUIDS FOR HEAT TRANSFER PROCESS INTENSIFICATION

by

HAJAR ALIAS

Submitted in accordance with the requirements for the degree of Doctor of Philosophy

The University of Leeds
School of Process, Environmental and Materials Engineering

October 2006

The candidate confirms that the work submitted is her own and that appropriate credit has been given where reference has been made to the work of others

ACKNOWLEDGEMENTS

I am very grateful to my supervisor, Dr. Yulong Ding for the opportunity to undertake this study and for his continuous advice, support and encouragement. I have the pleasure of thanking Professor Richard A. Williams for his invaluable help and advice throughout my study. This has been a wonderful experience that will remain in my mind.

I would like to thank the Ministry of Science, Technology and Innovation (MOSTI) of Malaysian Government and Universiti Teknologi Malaysia (UTM) for the financial support.

I would like to convey my gratitude to the staffs of Institute of Particle Science and Engineering of SPEME for their moral support and help during my time here.

I would also like to express my appreciation and thankful to all members of the group especially Dr. Dongsheng Wen, Dr Muzhong Shen, Wei Yang, and Yi Jin for the cooperation and help during my working in the lab.

My heartfelt thanks go to my sisters and brother for their love and support.

Special thanks and love to my beloved husband Shadan, whose love shines through his patience, support and understanding throughout my journey.

ABSTRACT

Heat transfer equipment is one of the main unit operations in many industrial processes such as heating, cooling, transportation and power generation. Thus, convective heat transfer plays a major role in the heat equipment. In the past years, liquids such as water, oil and ethylene glycol had been used as the heat transfer fluids. These fluids have a major drawback since they possess low thermal conductivity. Thus innovation in developing advanced heat transfer fluids is needed in many industrial applications so that more energy efficient and compact systems can be achieved. This is the main impetus of this work.

A nanofluid is a liquid suspension that consists of nano-sized solid particles. In this work, carbon nanotubes (CNT) and titanium dioxide (TiO_2) were utilized in formulating nanofluids. The shape and morphology of these nanoparticles make it a challenge in producing long term stable nanofluids. CNT nanofluids were produced using sonication and higher shear mixing, while the TiO_2 nanofluids were produced by using the beads mill. The CNT nanofluids dispersion stability was enhanced by the aid of gum arabic surfactant and the TiO_2 was stabilized by means of electrostatic stabilization mechanism at pH = 11.0.

The nanofluids were characterised using electron microscopy and size analyzer. The multi-wall CNTs have a diameter of < 10nm and length up to micron size, thus the aspect ratio is huge. The primary particles of TiO_2 have an average diameter of 30-40 nm.

The heat transfer study involves several measurements and analysis: i) the thermal conductivity measurements, ii) viscosity analysis and iii) convective heat transfer measurements. A significant enhancement was observed for thermal conductivity of CNTs nanofluids, where nanoparticles concentration of 0.25 wt %, 25% enhancement was observed. On the other hand, for concentration of 0.2 wt% of TiO_2 nanofluids, a maximum of 3.2% enhancement was observed, both measurements were conducted at 25°C.

The viscosity of CNT and TiO_2 nanofluids showed shear thinning behaviour. The viscosity decreases with increasing shear rate, and decreases with increasing temperature. The viscosity of CNTs nanofluids was much greater than that of TiO_2 nanofluids. At shear rate greater than 150 s^{-1}, the TiO_2 nanofluids behaved like Newtonian fluids and the viscosity approached the viscosity values of water.

The heat transfer behaviour of nanofluids was investigated for various experimental conditions such as flow conditions (Reynolds Number), nanoparticle concentration, pH, and particle size. For flow in 45 mm diameter pipe, the heat transfer coefficient decreases with increasing axial direction from the entrance, and increasing Reynolds Number. A significant enhancement for heat transfer coefficient was observed for CNT nanofluids. At Re = 800, a maximum of 350% enhancement of heat transfer coefficient was observed for 0.5wt % of CNTs. As the concentration increases, the maximum enhancement occurred at increasing axial direction along the pipe. On the other hand, the maximum enhancement (~16%), was observed at x/D = 150 for the TiO_2 nanofluids. Moreover, the heat transfer coefficient of TiO_2 increases with decreasing particle size for Reynolds Number $\geq$ 2000.

Apart from the thermal conductivity of nanoparticles, several other possible mechanisms are believed to be operating towards the enhancement of heat transfer coefficient. These include changes in the boundary layer thickness, particle migration and re-arrangement, thermal conduction increase due to shear and aspect ratio of nanoparticles.

TABLE OF CONTENT

LIST OF TABLES

LIST OF FIGURES

LIST OF SYMBOLS

Notation

A	-	tube cross sectional area
c_p	-	specific heat capacity, J/kg·K
d_p	-	particle diameter
D	-	diameter of tube
h	-	heat transfer coefficient, W/m^2·K
k	-	thermal conductivity, W/m·K
L	-	length of tube
n	-	particle shape factor, $n = 3/\psi$
Nu	-	Nusselt Number, $Nu = \frac{hD}{k}$
Pe	-	Peclet Number, $Pe = \frac{\mu L}{\alpha}$
Pr	-	Prandlt Number, $Pr = \frac{\nu}{\alpha}$
q	-	heat flux
Re	-	Reynolds Number, $Re = \frac{\rho u D}{\mu}$
S	-	perimeter of tube
T	-	temperature
u	-	fluid velocity
x	-	axial distance

Greek letters

α	-	thermal diffusivity
δ_t	-	thickness of thermal boundary layer
ϕ	-	particle volume fraction
η	-	viscosity, kg/m·s
μ	-	dynamic viscosity, Pa·s
ν	-	fluid kinematic viscosity

ρ	-	density, kg/m^3
ψ	-	particle sphericity, ratio of surface area of a sphere with volume of particle

Subscripts

cl	-	cluster
eff	-	effective property
f	-	fluid
in	-	inlet
p	-	particle
w	-	wall

CHAPTER ONE

INTRODUCTION

1.1 Background of research

Heat transfer equipment is one of the most important unit operations in many industries. Thus heat transfer fluids play a vital role in many processes such as heating and cooling processes, chemical processes and power generation. Conventionally, the fluids commonly used as the medium include water, oil and ethylene glycol. However, these fluids have poor heat transfer properties. Particularly, the thermal conductivities of these fluids are low and this has limited the thermal performance of some heat transfer equipment. Thermal conductivity and heat transfer coefficient of fluids play an important role in the development of energy-efficient and compact heat transfer equipment. A lot of efforts have been carried out to improve and optimise the equipment and operation as well as heat transfer fluid.

One significant consideration in achieving efficient and compact heat transfer equipment is to increase the thermal conductivity of the heat transfer fluids. This could be done by suspending metal or metal oxide particles in the base liquid. This is partially due to the fact that metal and metal oxide have higher thermal conductivity. For instance, water has a thermal conductivity of 0.6 W/m·K and copper has the a value of 386 W/m·K. When the micro-meter sized particles were 'in fashion', many attempts were made to employ microparticles in liquid suspensions. A study of fluids with suspended particles of micro and millimeters had been carried out by Ahuja (1975(a)

and 1975(b)) and Sohn and Chen (1981). Unfortunately, such suspensions suffer a number of drawbacks such as clogging, fouling and other related problems. Further studies have shown improvement on suspension stability where utilizing much smaller size particles. The bottleneck started to be eliminated when new dimension in science, such as nanotechnology come into the scene. The concept of using particles of nanometer dimensions was materialised by a series of research works pioneered at the Argonne National Laboratory, USA approximately a decade ago, and since then the term 'nanofluids' attracts great attention of both physics and engineering communities (Choi, 1995; Eastman et. al, 1997; Eastman et. al, 1999). The credit should also go to Masuda et. al who had started a work on the nanofluids in Japan in 1993 (Masuda et. al, 1993).

1.2 Nanofluids in the attention

Nanofluids are liquid suspensions that consist of nano-sized solid particles. Since a decade ago, research interest in nanofluids has rapidly increased. In the early stages, lots of the researches were mainly devoted to the production techniques and syntheses. Production of stable nanofluids remains a challenge due to the fact that nanoparticles form agglomeration and aggregates, and thus the size could be much bigger than the primary particles. A single route was predominantly employed at that stage where solid nanoparticles, produced from a separate synthesis, were suspended in the base liquid. Two step procedures were then used in which the first step involved producing the nanoparticles and secondly suspending them in liquids. The nanoparticles used in these studies include metal, metal oxide as well as carbon

nanotubes. Recently diamond and titanium dioxide nanotubes have also been added to the list of nanoparticles to produce nanofluids.

The research on nanofluids continued on to the study of its novel properties and characteristics. One of the properties that were measured and predicted in the early stages was thermal conductivity. Nanofluid, if properly engineered, could exhibit a thermal conductivity that is significantly higher than the base liquid (Choi, 1995; Lee et. al, 1999; Li and Xuan, 2002; Putra, 2002). This extraordinary property of nanofluid has gained an attractive research interest especially in the development of advanced heat transfer fluids. Therefore, the innovation of nanofluid has opened a new dimension for heat transfer enhancement. Recent literatures have revealed that high thermal conductivity enhancement can be achieved by adding even a very small amount ($\leq$ 5 volume %) of nanoparticles (Lee and Choi, 1996; Choi et. al, 2002; Li and Xuan, 2002; Das et. al, 2003c; Hwang et. al, 2005). These remarkable findings somehow vary in terms of the percentage of enhancement, ranging from as low as 5% to as high as 200%. Mathematical models were also developed to predict the thermal conductivity of nanofluids (Wang et al, 2003; Xue, 2003; Xue et. al, 2004). However, there was inconsistency in the observed properties and several issues have been raised to understand the behavior of nanofluids.

Besides thermal conductivity, there are few publications on the convective heat transfer of nanofluids (Xuan and Li, 2003; Wen and Ding, 2004b; Ding et. al. 2006; Heris et. al 2006). Experiments were conducted to measure the convective heat transfer coefficient of nanofluids under various conditions of flow and temperature.

Mathematical models were also developed in conjunction with the experiments (Buongiorno, 2006; Jou and Tzeng, 2006).

Apart from the thermal properties, there were several reports on the rheology of nanofluids (Park and Cho, 1998; Tepei and Forter-Barth, 2001; Kinloch et. al, 2002; Alias et. al, 2003). The viscosity of nanofluids was reported to have shown pseudo plastic flow behavior. However, there is certain condition such as pH influence where nanofluids could behave differently (Tseng and Wu, 2002).

1.3 Motivation of research

As mentioned above, nanofluids have gained a lot of attention over the past decade. The researches on the properties of nanofluids are still moving on with many new findings and results reported. Having known the basic properties and characteristics of nanofluids, the research trend on nanofluids are being advanced to practical applications on a small scale basis.

However, few works have been done on the convective heat transfer of nanofluids. This behaviour of nanofluids is more important from the industrial point of view. Thus, this has been the main motivation of this research to further study the convective heat transfer of nanofluids. Since this involves a flow system, a rheological study of nanofluids would be necessary. This is because the pressure drop of the flow system is closely related to the fluid rheology. In addition, the flow and heat transfer

behaviour in a flow system are coupled. Thus, relating the rheological behaviour with the thermal behaviour of nanofluid has been another motivation of this work.

1.4 Aims and objectives

The aim of this research is to engineer nanofluids with tailored properties. The specific objectives are:

- To formulate stable nanofluid systems using both metal oxide nanoparticles (TiO_2) and carbon nanotubes.
- To construct and use a robust experimental measurement system to quantify the heat transfer performance of the nanofluids.
- To characterize the nanofluids in terms of size distribution, thermal conductivity and rheological behaviour.
- To investigate the convective heat transfer in both horizontal and vertical configuration pipe systems.
- To provide detailed and more advanced understanding of heat transfer mechanisms in these systems.

1.5 Scope of this work

It is impossible to investigate all ranges of particulates systems within this scope of research. Due to this, this research has been focused on the following aspects.

- **Materials** - Titanium dioxide (TiO_2) and carbon nanotubes have been chosen as the subject matter. This is because little work has been reported on the convective heat transfer of nanofluids made from these materials.

- **Thermal conduction** – A hot wire based probe is chosen for the thermal conductivity measurements. This is because of the easiness for the measurements and fairly good repeatability of the measurements.

- **Rheology** - Steady shear rate increment is used to characterise the flow properties of nanofluids.

- **Convective heat transfer** – Both the horizontal and vertical pipe system are used for the work.

- **Pressure drop** – Measurement of pressure drop for the flow of nanofluids.

1.6 The structure of report

The second chapter follows will review the production and synthesis of nanofluids. Various techniques and methods that have been employed will be discussed. Chapter Three will review some properties and behaviour of nanofluids that have been reported in the literatures. These include thermal conductivity, convective heat transfer and rheology. The thermal conductivity of nanofluids has been a major focus in the previously reported studies. There are also models that have been developed to predict

the thermal conductivity of nanofluids. Moreover, mechanisms aimed at explaining the enhancement of nanofluids thermal conductivity have been discussed in various publications. Convective heat transfer of nanofluids is also gaining more and more research interest. In addition to thermal behaviour, the flow behaviour of nanofluids in terms of rheological properties, have in fact received considerable attention. If nanofluids were to be adopted in industrial applications, these properties have to be tailored to maximize the advantages of nanofluids.

Chapter Four describes the research methodology. A detail description of the experimental procedure will be discussed. The methods of preparation, selection of dispersant system, and experiments will be explained in this chapter. The equipment used for characterization and analysis are also discussed in this chapter. The following Chapter Five focuses on the results and discussion of the work done on carbon nanotubes. This will be followed by results and discussion of titanium dioxide system in Chapter Six. Conclusion will be drawn in Chapter Seven. The final chapter, Chapter Eight will give some recommendations for future research.

1.7 Contribution of research

The main contribution of the research is on the formulation of carbon nanotubes and titanium dioxide nanofluid system. It also provides an insight and knowledge of the convective heat transfer of these nanofluids.

CHAPTER TWO

PRODUCTION AND SYNTHESIS OF NANOFLUIDS : A REVIEW

2.1 Introduction

The successful production and synthesis of nanofluids are crucial in obtaining optimum thermal properties. A lot of efforts have been put on to the synthesis of nanofluids since the research begun approximately a decade ago. Studies to date have reported that various type of nanoparticles which include metal nanoparticles such as aluminium (Al), copper (Cu), iron (Fe), gold (Au), nickel (Ni), and titanium (Ti) have been utilized in the production of nanofluids. Oxide nanoparticles and other metal compound such as alumina (Al_2O_3), copper oxide (CuO), silica (SiO_2), titanium dioxide (TiO_2), and silicon carbide (SiC) are also received as much attention in the synthesis of nanofluids. In addition nanotubes such as carbon and titania nanotubes as well as diamond nanoparticles have also been used to make nanofluids. The formulations of nanofluids have been a real challenge due to various factors such as morphology of nanoparticles/nanotubes, strong interparticle forces and surface properties of nanoparticles. Particles in the liquid move through Brownian motion and collide with each other. Therefore, the stability of the suspension is mainly determined by the interactions during the collision. The particles are either attractive or repulsive to each other depending on the solution chemistry and surface properties of particles. When particles are attractive, they will form aggregates and even strong agglomerates, which have to be overcome during nanofluid production. In achieving stable and even distribution of nanoparticles in nanofluids synthesis, many techniques and methods have

been employed. This chapter will review the methods and techniques that have been so far most commonly used in formulation of nanofluids.

2.2 Formulation of nanofluids

There are several approaches that have been employed to prepare nanofluids. These include the single evaporation process, the two-step process, the direct mixing method, and other methods. They are briefly discussed in the following.

2.2.1 Single-step process

This method has been shown to successfully produce stable nanofluids. It is the single-step evaporation method, which simultaneously makes and disperses nanoparticles directly into a base liquid. The technique was employed at the Argonne National Laboratory, USA. Eastman et. al. (1997) used CuO and Al_2O_3 nano-crystalline nano-powder in these experiments. The schematic diagram of this process is shown in Figure 2.1. The same procedure was also applied by Lee et. al. (1999), Choi and Eastman (2001), and Choi et. al. (2001).

Zhu et. al. (2004) successfully prepared Cu nanofluids by reacting copper sulfate anhydride ($CuSO_4.5H_2O$) and sodium hypophosphite ($NaH_2PO_2.H_2O$) in ethylene glycol. The reaction was carried under irradiation microwave. Stable and non-agglomerated suspension was obtained.

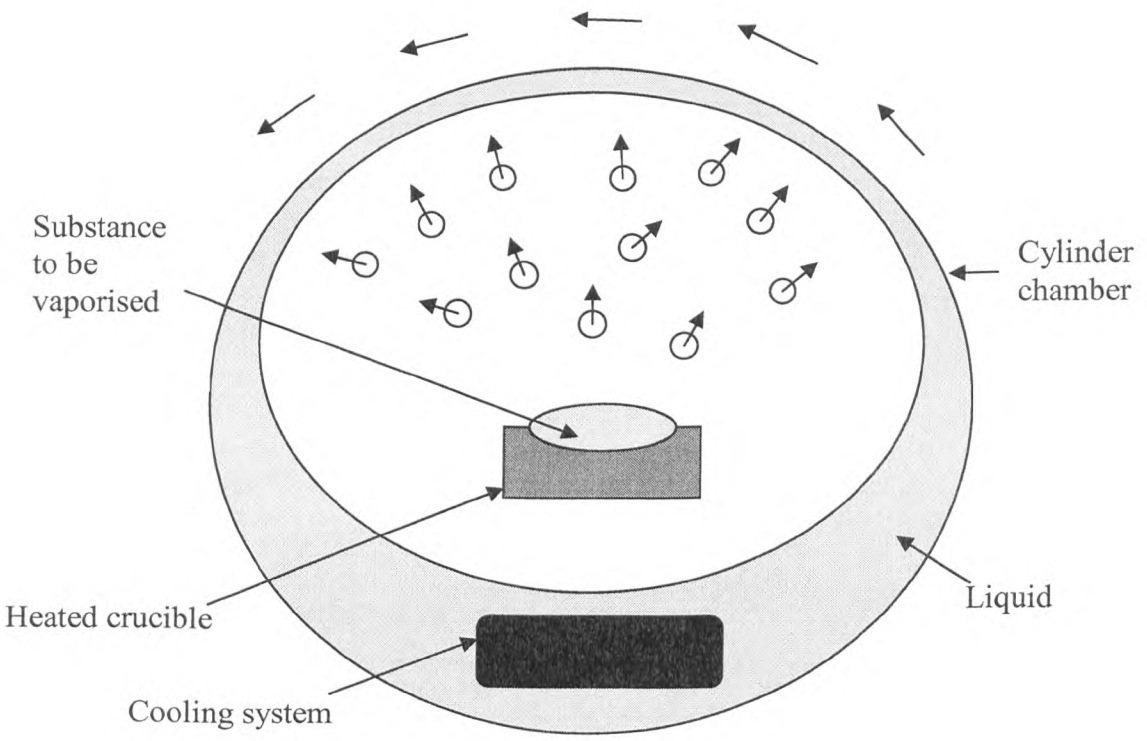

Figure 2.1: Schematic diagram of a single-step process of nanofluids production (Choi, 2002).

2.2.2 Two-step process

In the two-step process, nanoparticles were first produced as dry powder using the gas inert condensation method. Then the nanoparticles were dispersed in the base liquid. Advantages of gas-condensation method over other processing techniques include the ability to produce particles under cleaner conditions. Nanofluids produced by gas condensation method could have good stability and evenness (Li and Xuan, 2000). However, this method is expensive and difficult to satisfy practical application requirement. There are many other techniques that have been employed to produce nanoparticles such as chemical synthesis technique (Gleiter, 1989), aerosol spray drying method (Ashly, 1994) and condensation of metal vapor (Andres et. al, 1981). However, carbon nanotubes have been produced from different techniques which include arc discharge (Iijima, 1991), laser ablation (Scott et. al, 2001), catalytic process (Hernadi, 2002) and chemical vapor deposition (Pan et. al, 1999).

Another successful and well known two-step process in the production of nanofluids is the VEROS method which stands for Vacuum Evaporation on Running Oil Substrate. This method was introduced by Yatsuya et. al. (1978). With this technique, the nanoparticles were produced by direct evaporation in a vacuum onto the surface of running oil. The size distribution of particle produced by this technique was narrow and the particle yield per unit time is higher than that of gas evaporation technique. However, this technique is not suitable for substances of more than one component such as metal oxides. Furthermore, it is difficult to separate the particles from the fluids to obtain dry powder.

The VEROS technique was used by Eastman et. al. (1999) in dispersing Cu nanoparticles. However certain modification was introduced and the running oil was substituted with ethylene glycol instead. The nanoparticles produced by this technique were very small with average diameter of less than 10 nm and very little particle agglomeration.

2.2.3 Three-step process

Wang et. al. (1999) introduced a three steps method for producing Al_2O_3 nanofluids. The first step employs mechanical blending and ultrasonic bath. The nanofluids produced contain both separated individual particles and agglomerations of several particles. The second step involves coating of particles with polymer. Styrene-maleic anhydride was added during the blending process to keep the particles separated. To keep the polymer fully soluble the pH of the solution was kept at 8.5-9.0. In the last step, filtration was applied to removes particles with diameters larger than 1 μm.

2.2.4 Alternative processes

As an alternative for producing nanofluids, direct mixing of nanoparticles in the base liquid can be used. However, using this means of production, an additional aid would be necessary in order to obtain an even distribution and stable suspensions. As mentioned above, particles in suspension attract each other, it is necessary to modify particle surfaces to give repulsion between the particles to enhance stability. The repulsion must be strong enough to overcome the attractive interactions. Stability of suspensions can be obtained through electrostatic stabilization and steric stabilization

(Tadros, 1993; Werth et. al, 2003; Muller, 2004). Therefore, some auxiliary activator and dispersant have been used to enhance the dispersion.

A vast variety of surfactants and dispersants have been used in nanofluids systems which include organic acids, polymer surfactants and salts. They form stable suspension through the mechanism of steric stabilization. Steric stabilization is a mechanism that can explain the ability of certain additives to inhibit coagulation of suspensions. These additives include certain hydrophilic polymers and surfactants with hydrophilic chains. Stabilized system using this mechanism tend to remain well dispersed even at high particle loading or under conditions where the zeta potentials of the surfaces are reduced to near zero.

Quite a few researches have used this technique of stabilization in producing nanofluids. Deiss (1996), used poly ethylene glycol (PEG) and polyacrylamide (PAM) to sterically stabilize TiO_2 nanoparticles suspension. Both PEG and PAM are polymers. Bandyopadhyaya et. al. (2002), reported that gum arabic (GA) gave the longest stabilized nanofluids containing carbon nanotubes (CNT). Different types of surfactant were also tested and compared with GA such as a polysaccharide (Dextrin), a long chain synthetic polymer poly ethylene oxide (PEO), negatively charged sodium dodecyl sulfate (SDS), positively charged cetyltrimethylammoniumchloride (CTAC), dodecyl trimethylammoniumbromide (DTAB) and nonionic pentaoxoethyelenedodecyl ether ($C_{12}E_5$). Islam et. al. (2003) explored the dispersing power of several surfactants to evaluate stabilization characteristics of CNT nanofluids. The surfactant include sodium dodecylbenzenesulfate (NaDDBS), sodium octylebenzene sulfonate (NaOBS),

sodium benzoate ($C_6H_5CO_2Na$), sodium dodecyl sulfate (SDS), and Triton X-100. This study has demonstrated that NaDDBS can stabilize nanofluids for a long period of time.

In addition, to successfully obtain stable nanofluids systems, mixing techniques such as sonication, high shear mixer, or milling are required. Sonication is a method of dispersing using the ultrasonic waves. It is the most commonly used method in the production of nanofluids (Xuan and Li, 2000; Bandyopadhyaya et. al, 2002; Li and Q, 2002; Putra, 2002; Xie et. al, 2002(a) and 2002(c); Alias et. al, 2003; Chon, 2005; Heris et. al, 2006).

Besides sonication, nanofluids have also been produced by using a high shear mixer. The nanofluids systems are well mixed in this method since high frequency of mixing is used (Wen and Ding, 2004(a); Wen and Ding, 2004(b); Wen and Ding, 2005). This method, however, needs certain precaution in order not to mechanically damage the structure and morphology of nanoparticles. Both sonication and high shear mixing processes are simple and relatively cheap. Even so, results have shown that long stable nanofluids can be achieved by these methods.

Wang et. al. (2005) obtained nanofluids by filling CNT with toluene using supercritical CO_2 gas. Prior to the synthesis, the CNT have been produced using a different technique.

2.2.5 Acid treatment process

Stable suspension of nanofluids can also be achieved by techniques such as pH alteration to change the surface charge of particles in aqueous solutions. This is a

mechanism of stabilizing suspensions through the electrostatic repulsion mechanism, in which the particles are surrounded by electrical double layer. Changing the pH would change the surface charge of the nanoparticles. Acid or alkaline is added into the suspensions to adjust the pH level. Nitric acid (HNO_3) and sodium hydroxide (NaOH) were used by Wen and Ding (2006) to adjust the pH of TiO_2 nanofluids. Shaffer and Windle (1999) used acid oxidation treatment to stabilize CNT nanofluids. Esumi et. al. (1996) stabilized CNT nanofluids by using nitric acid (HNO_3) and sodium hydroxide (NaOH). Lee et. al. (2006) adjusted CuO nanofluids by using hydrochloric acid (HCl) and NaOH.

As a conclusion, there have been several techniques and methods to formulate nanofluids. Each of the methods has advantages and disadvantages. Therefore, it is important to have a basic understanding of the characteristics and nature of nanoparticles and the base fluids before one can engage on any method to produce nanofluids. Table 2.1 summarizes some of the techniques and methods that have been employed for formulation of nanofluids. This research will use a few of these techniques to produce CNT-water and TiO_2-water nanofluids. The chapter follows will review the characteristics and behaviour of nanofluids that have been reported in the literature.

Table 2.1: Review of nanofluids production.

No.	Literature	Nanoparticles used	Method of nanofluids production
1.	Esumi, et. al. (1996)	CNTs	Chemical treatment
2.	Eastman, et. al. (1997)	Cu, CuO and Al_2O_3	Gas condensation and VEROS method.
3.	Lee, et. al. (1999)	CuO and Al_2O_3	Production of oxide nanoparticles and dispersed in the base fluid.
4.	Shaffer, M.S.P. and Windle, A.H. (1999)	CNTs	Acid oxidation treatment.
5.	Xuan, Y and Li, Q. (2000)	Cu	Ultrasonic vibration
6.	Choi et. al. (2001)	CNTs	Production of CNT in a chemical-vapour-deposition reactor and dispersed in base fluid
7.	Choi et. al. (2001)	Cu, CuO and Al_2O_3	Two methods : 1. Preparation of nanoparticles using inert gas condensation (IGC) and dispersed in base fluid. 2. Preparation of nanoparticles using VEROS method and dispersed in base fluid.

Table 2.1: Review of nanofluids production (continued).

No.	Literature	Nanoparticles used	Method of nanofluids production
8.	Hirai, H and Yakura, N. (2001)	Pd	Alcohol reduction method.
9.	Bandyopadhyaya, et. al. (2002)	CNTs	Sonication method.
10.	Choi, et. al. (2002)	Cu and CNTs	Cu- Direct evaporation method CNT – production of CNT and dispersed in base fluid
11.	Kinloch, et. al. (2002)	CNTs	Acid oxidation treatment.
12.	Li, Q and Xuan, Y. (2002)	Cu	Ultrasonic vibration.
13.	Putra, N.S.D. (2002)	CuO and Al_2O_3	Ultrasonic vibration.
14.	Saito, et. al. (2002)	CNTs	Chemical treatment
15.	Xie, et. al. (2002b)	$\propto$-Al_2O_3	Ultrasonication.
16.	Xie, et. at. (2002c)	Al_2O_3	Production of nanoparticles and dispersed in the base fluid.
17.	Yerushalmi-Rozen, R. and Regev, O. (2002)	CNTs	Ultrasonic vibration.

Table 2.1: Review of nanofluids production (continued).

No.	Literature	Nanoparticles used	Method of nanofluids production
18.	Islam, et. al. (2003)	CNTs	Sonication method.
19.	Jiang, et. al. (2003)	CNTs	Acid oxidation treatment.
20.	Patel et. al. (2003)	Au and Ag	Citrate reduction route
21.	Tseng, W.J. and Lin, K.C. (2003)	TiO_2	Mixing – adsorption of polymeric surfactant.
22.	Xie, et. al. (2003)	CNTs	Acid treatment.
23.	Assael et. al. (2004)	CNTs	Ultrasonication
24.	Wen and Ding (2004a)	CNT, Al_2O_3	Shear mixing
25.	Gibson et. al. (2004)	CNTs	Ultrasonication
26.	Bang and Chang (2005)	Al_2O_3	Ultrasonication
27.	Bonnemann et. al. (2005)	Cu and Ag	Cu - Peptization Ag – Thermal decomposition

Table 2.1: Review of nanofluids production (continued).

No.	Literature	Nanoparticles used	Method of nanofluids production
28.	Lou et. al. (2005)	Cu	Submerged arc nanoparticle synthesis system (SANSS)
29.	Manna et. al. (2005)	$Al_{70}Cu_{30}$	Two-step method
30.	Wang et. al. (2005)	CNTs	Supercritical CO_2: nanochemical reaction.
31.	Chopkar et. al. (2006)	$Al_{70}Cu_{30}$	Two-step method
32.	Lee et. al. (2006)	CuO	Acid-alkaline treatment
33.	Mamut, E. (2006)	Cu	Single-step process – VERL device
34.	Wen and Ding (2006)	TiO_2	Direct mixing and acid treatment

CHAPTER THREE

PROPERTIES AND BEHAVIOUR OF NANOFLUIDS : A REVIEW

3.1 Introduction

Extensive research conducted on nanosized powder preparation and processing technology in recent years has provided an opportunity to apply this emerging nanotechnology to thermal engineering. For instance, improvements to make heat transfer equipment more energy efficient would be crucial. Conventional heat transfer fluids such as water, mineral oil and ethylene glycol play a very vital role in many industrial processes. The poor heat transfer properties of these commonly used fluids are a primary obstacle to high compactness and effectiveness of heat exchangers. Many initiatives and approaches at utilizing solids particle suspensions as heat transfer media were developed. When particles of the order of millimeters and micrometers are suspended in liquid, severe problems could occur such as increased pressure drop, clogging of flow channels, and erosion of the pipelines. Furthermore, they often suffer from instability and associated problems. Although these suspensions have better thermal conductivity, they are not practical. Hence, a solution to some of these problems was found when much smaller particles are added instead.

Since the word 'nanofluids' was coined and associated research was started, the number of publications increase every year. In the early stage of the research, most studies on nanofluids were focused on the production of nanofluids and their thermal conductivities. As the time goes by, more research work is directed to areas associated

the applications of nanofluids. This chapter will review the literature on properties and behaviour of nanofluids.

3.2 Thermal conductivity of nanofluids

Theoretical and experimental studies have shown that suspensions containing solid particles have significantly higher thermal conductivities than the base fluids without particles. Unfortunately, suspended particles of micrometer dimensions may cause some severe problems such as abrasion and clogging in small passages. Moreover, large particle suspensions have a poor stability the coarse grained solid particles settle out under gravity eventually. Nanofluids have been shown to exhibit superior thermal conductivity yet without suffering particle settling. It is well known that metal in liquid have a thermal conductivity several orders of magnitude higher than pure liquid. For example, at the room temperature copper has a thermal conductivity of approximately 700 higher than that of water. Furthermore, the thermal conductivity of metal materials is much greater than that of nonmetallic materials. Therefore, the thermal conductivity of liquids having suspended solid metal particles is expected to be higher than the conventional fluids. In most studies, the thermal conduction of nanofluids is characterized by the effective thermal conductivity, k_{eff}, which is a function of the thermal conductivity of particles, k_p, the thermal conductivity of the base fluid, k_f, the concentration of particles, and other properties of the base liquid and particles, for instance, particle shape, solution pH and others.

Many studies have devoted to the prediction and measurement of the thermal conductivity of nanofluids and the literature is seen to increase. Nanofluids containing

metal nanoparticles are studied by few groups around the world. The method used to measure thermal conductivity in many studies is the transient hot-wire method (Healy et. al, 1976). Other methods include the steady-state parallel-plate technique (Wang et. al, 1999) and the temperature oscillation technique (Putra, 2002; Das et. al, 2003c; Bhattacharya et. al, 2004; Bhattacharya, 2005).

Eastman et. al. (1997) studied the thermal conductivity of copper (Cu) nanofluids in water. Xuan and Li (2000) studied nanofluids of Cu in water and transformer oil. Thermal conductivity of Cu-ethylene glycol nanofluid was measured by Eastman et. al. (2001). All these studies reported enhanced thermal conductivity despite to different extents. Several factors were investigated by these authors such as particle concentration and size which will be discussed in Section 3.3. Other metals investigated include iron (Fe) (Hong et. al, 2005), gold (Au) (Patel et. al, 2003; Putnam 2006) and silver (Ag) (Patel et. al, 2003). Despite the high percentage of thermal enhancement observed by earlier research, a different scenario was observed in a recent work (Putnam et. al, 2006). The nanofluids containing ~0.001 volume % gold nanoparticles did not show significant enhancement (< 2%). This is a direct conflict of results measured by Patel et. al. (2003) where 5% - 21% thermal conductivity enhancement was observed for particle concentration of 0.00026 by volume. The results from the experimental data of these researchers are shown in Figure 3.1.

The difference results obtained in these researches may be due to different technique employed in the nanofluids production and different physical properties of surfactant. For example, Eastman et. al. (1997) employed the VEROS technique, Xuan and Li (2000) utilized the sonication method while Patel et. al. (2003) applied the citrate

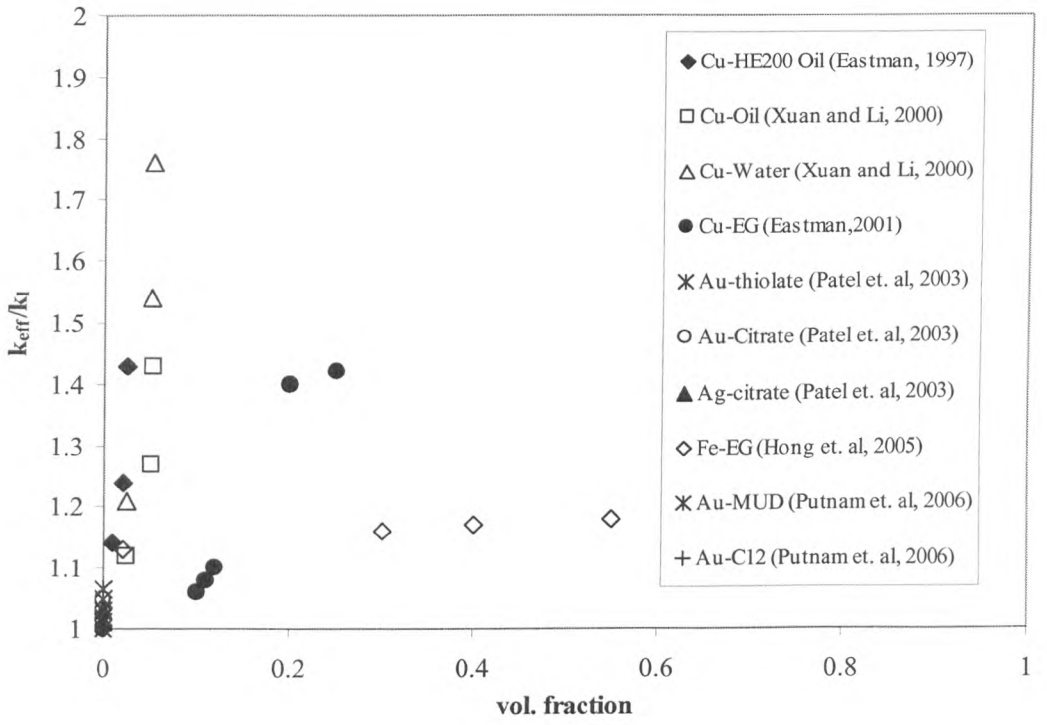

Figure 3.1: The experimental data on thermal conductivity of nanofluids containing metal nanoparticles. (Note : EG = Ethylene glycol, MUD = 11-mercapto-1-undecanol, C12 = toluene).

reduction method. The accuracy and reliability of theses results are unknown as they are not been reported. The temperature at which the data were taken was also slightly different between these results. The error estimated in these results is approximately 5%-10%.

The thermal conductivity of nanofluids containing metal oxide nanoparticles was also measured by many researchers. The three oxide nanoparticles that are very commonly investigated are Al_2O_3, CuO and TiO_2. An earlier work by Eastman et. al (1997) have demonstrated that the thermal conductivity of CuO-water nanofluids could be enhanced by 60% by adding 5 volume % of nanoparticles. The enhancement was also observed for Al_2O_3-water nanofluids, although less significant than that of CuO. A similar work was also conducted by Eastman et. al. (1999). These works showed that the thermal conductivity of nanofluids increased linearly with particles loading. Kwak and Kim (2005) observed that even at very low volume fraction (0.1%), the thermal conductivity of Cu-EG nanofluids was increased by 2.6%.

Wang et. al. (1999) measured the thermal conductivity of Al_2O_3 (28 nm diameter) and CuO (20nm diameter) that are dispersed in several fluids; water, vacuum pump liquid, engine oil and ethylene glycol (EG). The results showed that the effective thermal conductivity for all the nanofluids measured were higher than that of the respective fluids. The experimental data were compared to those of Masuda et. al. (1993) and Lee et. al. (1999) results. The comparison indicated a possible relation between the effective thermal conductivity and the nanoparticle size. The thermal conductivity was observed to increase with increasing particles size. The experimental data measured were found to be lower than the thermal conductivities values predicted

by several existing models. This indicates that there are deficiencies in the models and therefore are insufficient to describe the heat transfer behaviour of nanofluids. Thus new model is needed which should account for factors such as motion and structuring of nanoparticles.

Putra (2002) and Das et. el. (2003c) studied the heat conduction of water-based nanofluids containing CuO (28.6 nm) and Al_2O_3 (38.4 nm) over a temperature range of 21°C to 51°C. The thermal conductivity of the nanofluids was enhanced as a function of both volume fraction and temperature. The data were compared with the Hamilton-Crosser model, a mathematical model that predicts the thermal conductivity of solid-liquids mixture (Hamilton-Crosser, 1962). At room temperature, the Al_2O_3-water nanofluids agree with the Hamilton-Crosser (H-C) prediction whereas at other temperature they did not agree. It would somewhat be accidental since Wen and Ding (2004b) observed a contradict results where the thermal conductivity of Al_2O_3-water nanofluid, measured at room temperature failed to agree with H-C prediction. Chon et. al (2005) observed that the thermal conductivity of nanofluids was enhanced with increasing temperature and decreasing particle size. For such occurrences, the Brownian velocity is believed to be the key mechanism on the temperature dependence of nanofluids thermal conductivity and will be discussed in more detail in Section 3.5.

Thermal conductivity of TiO_2-water nanofluids was studied by Mushed et. al. (2005). Two morphologies of nanoparticles were investigated; i) spherical shape of 15nm diameter and ii) rod-like shape with 10nm x 40nm dimension. The investigation showed that the thermal conductivities of TiO_2 nanofluids are higher than the base liquid. For a particle volume fraction of 5%, the enhancement achieved was 27.9% for

nanofluids consisting of spherical particles and 32.8% enhancement was observed for cylindrical particles. The thermal conductivities were also affected by the morphology of the nanoparticles where the thermal conductivity of spherical shape nanoparticles was always higher. The results were compared with several models. It was found that the experimental results were higher than those predicted by the models. An earlier work on TiO_2-water nanofluids observed 10% enhancement for a particle loading of 4.35 volume % (Masuda et. al, 1993).

Nanofluids containing other compound of metal such as carbides were also studied in several works. Xie et. al. (2002a) and Xie et. al. (2002d) measured the thermal conductivity of SiC nanofluids where EG and water were utilized as the base liquids. Two types of SiC nanoparticles were investigated; one having a spherical shape with 26 nm average diameter and the other is cylindrical shape with average diameter of 600nm. The experiments showed that even at small amount of particle loading (4.2 volume %), the thermal conductivities of the nanofluids systems were significantly higher than that of the respective base liquids and the enhancement increased linearly with particle volume fraction. The results were compared with the Hamilton-Crosser model. It was found that the model fitted well for large particle (600nm) but inadequate for nanofluids made of smaller nanoparticles. A recent work on $Al_{70}Cu_{30}$ alloy in ethylene glycol observed a sigmoidal nature of thermal conductivity enhancement. A very significant increased (> 200%) was reported for 1.5 volume % of particles (Chopkar et. al, 2006). The results of the experimental data of some studies on oxide metal and other compound are shown in Figure 3.2 to give better insight of the findings.

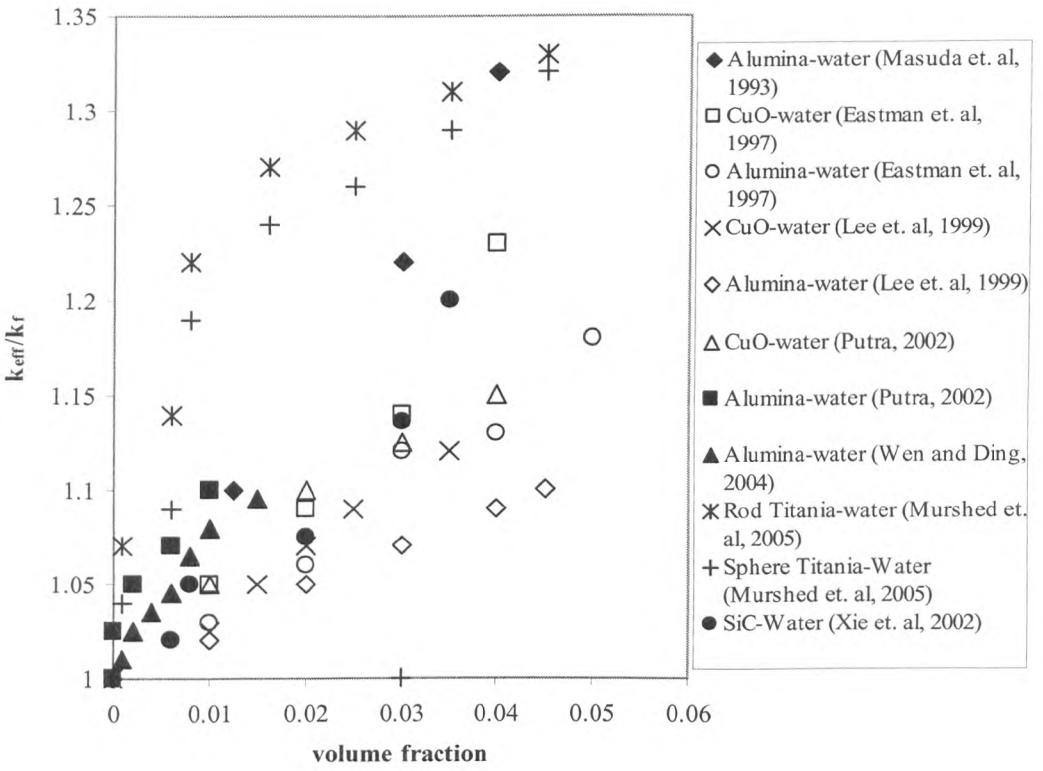

Figure 3.2: The experimental data of thermal conductivity of nanofluids containing oxide and other metal compound.

The thermal conductivity of carbon nanotubes (CNTs) nanofluids also received much attention in the literature. CNTs were first discovered by a Japanese physicist (Iijima, 1991). Since then, a lot of reports on the thermal conductivity of CNTs were published. Experimental measurements have indicated that CNTs possess high thermal conductivity (Berber et. al, 2000; Xie et. al, 2000; Kim et. al, 2001).

Having such a high thermal property, introducing CNTs in nanofluids would be an extra advantage to their thermal conductivity. Choi et. al. (2001) studied the thermal conductivity of multi-wall CNT dispersed in oil. A significant extent of enhancement of thermal conductivity (~160%) was observed for 1 volume % of CNT. A lower enhancement (~20%) was observed by Xie et. al. (2003) for the same CNT volume fraction. However, the experimental conditions of these work are unidentical, thus, direct comparison could not be made. Biercuk et. al. (2002) measured thermal conductivity of CNTs-Epoxy composites and observed ~125% thermal conductivity enhancement for 1 weight % of CNT loading. Wen and Ding (2004a) also observed the enhancement even though at a lower of 30%-40% magnitude.

Assael et. al. (2004) studied the thermal conductivity of multi-wall CNTs-water nanofluids with 0.1 weight % of Sodium Dodecyl Sulfate (SDS) as a dispersant. Maximum thermal conductivity enhancement was observed for 0.6 volume % of CNTs loading. The experiments were then repeated but hexadecyltrimethyl ammonium bromide (CTAB) and nanosphere AQ was used as a dispersant instead of SDS (Assael et. al, 2006). In addition to multiwall CNTs, the thermal conductivity of nanofluids containing double-wall CNTs were also investigated. For the same volume fraction, the maximum enhancement achieved was 34% with CTAB and CTAB was found to be

better dispersant for both double-wall and multi-wall CNTs. Recently, Hwang et. al (2006) investigated the thermal conductivity of several nanofluids (CNT-water, CuO-water, SiO_2-water and CuO-EG) and reported that the CNT nanofluids showed the highest thermal conductivity enhancement. At 1 volume % of particle loading, the thermal conductivity increased to 11%.

Liu et. al. (2005) experimentally measured the thermal conductivity of multi-wall CNT in ethylene-glycol (EG) and synthetic oil. They observed that the thermal conductivity enhancement increased almost linearly with the volume fraction. For 1.0 vol. %, 12.4% of enhancement was observed for CNT-EG nanofluids, while for 2.0 vol. % of CNT-synthetic oil nanofluids, 30% enhancement was observed.

It can be seen that the experimental data on CNTs nanofluids thermal conductivity are widely varied between the researchers. Several factors may influence such phenomena. These include the preparation technique, the CNTs structure and dimension, the CNTs thermal properties and the chemistry of the dispersant. Figure 3.3 illustrates some the experimental data on thermal conductivity of nanofluids containing CNTs.

Many studies on thermal conductivities of nanofluids have reported a significant enhancement. Fundamentally, the thermal conductivity of nanoparticles depends on their size, which may be even much lower than the bulk value because of the boundary scattering of phonon and electrons. Therefore, with this argument, the thermal conductivity of nanoparticles suspension would then be reduced if particles are smaller

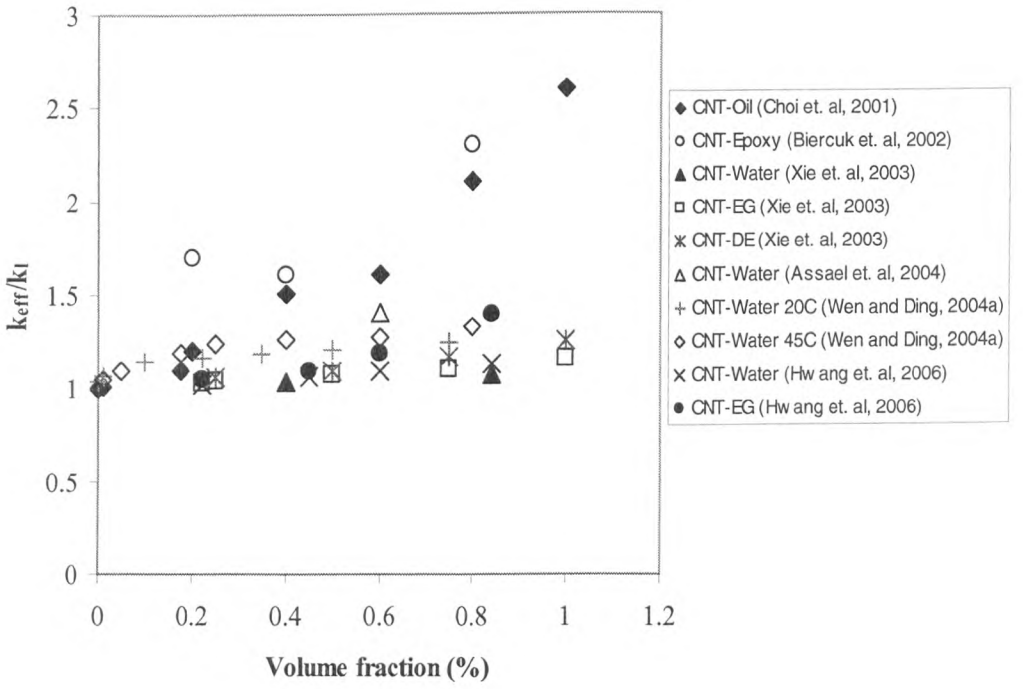

Figure 3.3: Comparison of experimental data of CNT nanofluids. (Note: EG=ethylene glycol, DE = decene)

than the mean free path of the energy carrier. In most publications, the thermal conductivity of the bulk material is often used since there is very limited data on the thermal conductivity of nanoparticles. These results suggest that there is an urgent need to develop new measurement techniques that takes into account these factors and able to predict nanofluid thermal conductivity.

3.3 Factors affecting the thermal conductivity of nanofluids

Several parameters have been looked into in the work on the effective thermal conductivity of nanofluids. These include particle size, particle loading (volume fraction), morphology, type of base fluids, type of nanoparticles, and solution chemistry.

3.3.1 The effect of particle size

The most significant factor affecting the thermal conductivity of nanofluids is the particle size. Several studies have found that thermal conductivity increases with decreasing particle size. Masuda et. al. (1993) measured thermal conductivity of alumina nanofluids with nanoparticle diameter of ≈13nm and observed a 30% enhancement of effective thermal conductivity. On the other hand, Lee et. al. (1999) measured the same type of nanofluids, but alumina size slightly bigger (≈40 nm). Only a 10% enhancement was observed for the same volume fraction of nanoparticles (4.3 volume %). An even greater enhancement was reported for Cu nanofluids, where just a 0.3 volume fraction of 30nm Cu nanoparticles led to thermal conductivity increase of up to 40% (Eastman, 2001). This was attributed to the increase in the specific surface area which increases as particles size decreases.

3.3.2 The effect of particle concentration

Another important factor that affects the thermal conductivity of nanofluids is the particle volume fraction. The thermal conductivity of nanofluids increases with increasing volume fraction of nanoparticles. Wang et. al. (1999) reported that the effective thermal conductivity of ethylene glycol increased 26% when approximately 5 volume % of Al_2O_3 powders were added, whereas 40% increase was observed when approximately 8 volume % of Al_2O_3 powders were added. Xuan and Li (2000) reported that the effective thermal conductivity of water-Cu nanofluids varied from 1.24 to 1.78 when the volume fraction of Cu nanoparticles increased from 2.5% to 7.5%. Choi et. al. (2001) observed that when 5 volume % of nanocrystalline CuO particles were suspended in water, the improvement in thermal conductivity reached 60%. Another remarkable enhancement was reported by Choi et. al. (2002). They found that nanofluids containing ~1 volume % of 26 nm carbon nanotubes could enhance the thermal conductivity by 160%. Nevertheless, all studies showed that the ratio of the thermal conductivity of nanofluids increases almost linearly with the volume fraction.

3.3.3 The effect of particle shape

Not only particle size plays a role in thermal conductivity enhancement, particle shape does too. A study on this factor was conducted by Xie et. al. (2002). Thermal conductivity of nanofluids containing SiC nanoparticles having a cylindrical and spherical shape was measured. The results showed that the thermal conductivities enhancement were larger for cylindrical shape as compared to spherical shape. A similar conclusion was drawn for thermal conductivity measurement of spherical and

rod-like TiO_2 nanofluids (Murshed et. al, 2006). With these findings, it seems not surprising that nanofluids containing carbon nanotubes can exhibits a significant thermal conductivity enhancement (Choi, 2001; Xie et. al, 2003; Wen and Ding, 2004a) even with low percentages of particle loading.

3.3.4 The effect of base liquid

The effective thermal conductivity of nanofluids increases with increasing thermal conductivity of the base fluid. However, the ratio of the effective thermal conductivity of nanofluids to that of the base liquid decreases with increasing thermal conductivity of the base liquid. Lee et. al. (1999) and Xie et. al. (2002) studied two nanofluids made of water and ethylene glycol. They reported that percentage of the thermal conductivity enhancement of ethylene glycol based nanofluid, was always higher than that of the water based systems. Wang et. al. (1999) reported that the thermal conductivity enhancement was the highest for ethylene glycol and engine oil based nanofluids, whereas that for the pump oil based nanofluid was the lowest. This result seems to be consistent with other work by Xie, et. al. (2002) for water and ethylene glycol based nanofluid, where percentage of the thermal conductivity enhancement of SiC-ethylene glycol nanofluid was slightly higher than that of SiC-water nanofluids. Given that, the thermal conductivity of water, engine oil, and EG are 0.613 W/m·K, 0.145 W/m·K and 0.256 W/m·K respectively, the above conclusion does not held for the mineral based oil. The exact reason is unclear. Thermal conductivity of nanoparticle seems to give more impact towards the thermal conductivity of nanofluids. Physical interaction between the nanoparticle and the base liquid may also play a role.

3.3.5 The effect of nanoparticle material

The thermal conductivity of nanofluids should be related to the properties of nanoparticles used. For instance, the thermal conductivities of Cu and Fe are 400 W/m·K and 80 W/m·K, respectively. One therefore would expect that nanofluids containing Cu nanoparticles to have a thermal conductivity higher than that of Fe nanofluids, given other conditions. However, this does not seem to be the case. As Xie et. al. (2005) reported, the nanofluids containing Fe nanoparticles showed a higher thermal conductivity than nanofluids containing Cu nanoparticles. The exact reason for this is unclear. Solution chemistry, the material density and the crystalline structure are believed to play a role.

3.3.6 The effect of pH

The pH of nanofluids is also affecting the thermal conductivity of nanofluids. Xie et. al. (2002) observed that the enhanced thermal conductivity ratio of Al_2O_3-water nanofluids decreased with increasing pH value (pH 2 -12). However, there is inconsistency with results obtained by Lee et. al. (2006). They found that the effective thermal conductivity of CuO-water nanofluids decreased with increasing pH, from pH 2 to pH 8, and increased above pH 8. These results indicate that the surface charge of nanoparticles may play a role in which affects nanoparticle structuring, hence the thermal conductivity of nanofluids.

3.4 Model for thermal conductivity of nanofluids

After the measurements of nanofluids thermal conductivity were made, many researchers have attempted to theoretically calculate the thermal conductivity. Thermal conductivities of mixtures have been studies for more than a century. As discussed previously, thermal conductivity of nanofluids is believed to be dependent on several parameters such as thermal conductivities of base fluid and the nanoparticles, particle volume fraction, the surface area, the shape of nanoparticles as well as the temperature. However, the conventional models of the effective thermal conductivity for solid-liquid suspensions fail to predict the thermal conductivity of nanofluids satisfactorily. Maxwell's model (Maxwell, 1904) was among the first for predicting both the effective electrical conductivity and thermal conductivity of a random suspension of spherical particles. The theory is expressed as follows:

$$\frac{k_{eff}}{k_f} = \frac{k_p + 2k_f - 2\phi(k_f - k_p)}{k_p + 2k_f - \phi(k_f - k_p)} \qquad \text{Eq. 3-1}$$

where k_{eff} is effective thermal conductivity, k_f is thermal conductivity of base liquid, k_r is the ratio of thermal conductivity of particle and base liquid and ϕ is the volume fraction. Maxwell model can satisfactorily predict thermal conductivity of large particle suspensions at low concentrations. Wang et. al. (1999) observed that the experimental data of low concentration Al_2O_3-EG nanofluids did not fit in this model. This suggests that the particle size do matter in the calculation of nanofluids thermal conductivity.

Hamilton and Crosser (H-C) developed a model for effective thermal conductivity of solid-liquid mixtures for non-spherical particles as in the following:

$$\frac{k_{eff}}{k_f} = \frac{k_p + (n-1)k_f - (n-1)(k_f - k_p)\phi}{k_p + (n-1)k_p + \phi(k_f - k_p)} \qquad \text{Eq. 3-2}$$

where n is the shape factor given by $n = 3/\psi$, and ψ is the particle sphericity (Hamilton and Crosser, 1962). Even with the additional factor included, just like the Maxwell model, the H-C model is capable of predicting the thermal conductivity of suspensions containing large particles. It appears to be inadequate for nanofluids with smaller particles. Xie et. al. (2002) used the H-C equation to compute the thermal conductivity of SiC nanofluid. They reported that the equation is adequate of predicting the thermal conductivity of 600 nm particles, but failed for 26 nm sized particles. This is because the heat transfer between the particles and the fluid takes place at the particle-surface interface. The heat transfer is expected to be more efficient and rapid for a system with large interfacial area. If the size of the dispersed particles were large, the volume effect of the particles becomes dominant. Since, the H-C model focuses on the effect of the particle shape on the surface area, hence it is capable of predicting the thermal conductivities of 600nm SiC nanofluids. Similar finding was reported by Lee et. al.(1999), where the H-C equation was applied for predicting the thermal conductivities of CuO and Al_2O_3 nanofluids. The prediction was satisfacory for large agglomerated Al_2O_3 (~100nm) but inadequate for CuO particles (<100nm). Choi et. al. (2001) observed that the effective thermal conductivity of CNT-oil suspension did not fit not only to this model, but several other conventional models as well such as those by Davis (1986), Bonnecaze and Brady (1990), and Lu and Lin (1996). These findings indicate

that other characteristics and properties of nanofluids should be included in the empirical models to calculate the thermal conductivity of nanofluids.

Yu and Choi (2003) developed a modified version of Maxwell model, considering the effect of nano-layer that forms at the nanoparticle-liquid interface (Figure 3.4). Nano-layer is the layering of the liquids at the interface of nanoparticles and the bulk liquid. The solid-like nano-layer is assumed to have a thermal conductivity (k_{layer}) higher than that of the bulk liquid and thermal transport in nanofluids is diffusive. The nanoparticle of radius r, and the thin nano-layer of thickness l, form a particle with a thermal conductivity k_{pe}. Based on the effective medium theory, the thermal conductivity correlation is as the following:

$$k_{pe} = \frac{\left[2(1-\gamma)+(1+\beta)^3(1+2\gamma)\right]\gamma}{-(1-\gamma)+(1+\beta)^3(1+2\gamma)} k_p \qquad \text{Eq. 3-3}$$

where $\gamma = k_{layer}/k_p$ is the ratio of nano-layer thermal conductivity to particle thermal conductivity and $\beta = l/r$, where l is the nano-layer thickness. If $k_{layer} = k_p$, then Eq. 3-3 reduces to

$$k_{eff} = \frac{k_{pe}+2k_f+2(k_{pe}-k_f)(1+\beta)^3\phi}{k_{pe}+2k_f-(k_{pe}-k_f)(1+\beta)^3\phi} k_f \qquad \text{Eq. 3-4}$$

The model predicted the experimental data (Cu-EG and CuO-EG nanofluids) quite well and most effective when the particle diameter is < 10 nm. This suggests that the presence of nano-layer contributes to the enhancements of nanofluids thermal

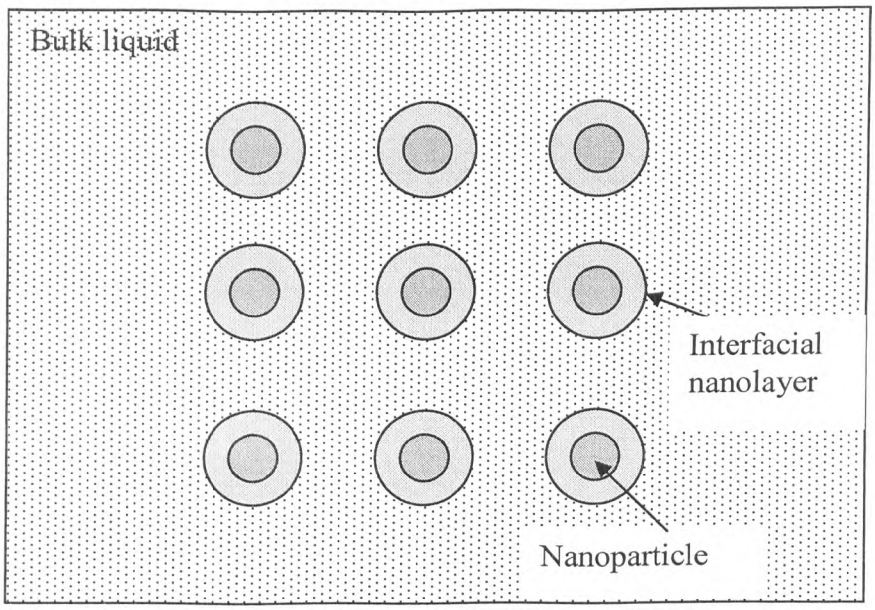

Figure 3.4: The schematic structures of nanoparticles suspended in a base liquid (nanofluids).

conductivity. However, the model did not satisfactorily predict Cu-EG nanofluids with surfactant and thus indicates that the chemistry of surfactant should be considered. This model is also limited only to spherical particle, thus it is inadequate to predict CNTs nanofluids thermal conductivity. More recently, the nano-layer theory has been suggested to be physically unsound (Evans et. al, 2006).

Xue (2003) proposed a model for effective thermal conductivity of nanofluids based on Maxwell theory and average polarization theory. This model considers the interface effect between the solid particles and the base fluids in nanofluids, identical to the nano-layer structure as proposed by Yu and Choi (2003). The particle and interfacial layer are assumed to form an elliptical complex nanoparticle. The effective thermal conductivity of this model is expressed as follows:

$$9\left(1-\frac{\phi}{\lambda}\right)\frac{k_{eff}-k_f}{2k_{eff}+k_f}+$$

$$\frac{\phi}{\lambda}\left[\frac{k_{eff}-k_{c,x}}{k_e+B_{2,x}(k_{c,x}-k_{eff})}+4\frac{k_{eff}-k_{c,y}}{2k_e+(1-B_{2,x})(k_{c,y}-k_{eff})}\right]=0 \qquad \text{Eq. 3-5}$$

where $\lambda = abc/[(a+t)(b+t)(c+t)]$, t is the interfacial thickness and a,b,c are the half-radii of the elliptical complex nanoparticles. $k_{c,j}$ is the effective diaelectric constant and $B_{2,x}$ is the depolarization factor component of the elliptical particle along the j-symmetrical axis, derived from the average polarization theory. The model was tested on CNT-oil and Al_2O_3-water nanofluids. It was observed that the measured data was in good agreement with the model when the interfacial thickness, t = 3nm. The model also satisfactorily predicted the nonlinear increase of CNT-oil nanofluids thermal

conductivity. However, Yu and Choi (2004) found that this model is inaccurate for CNT-oil nanofluids because the *depolarization factor* and the *semi-axis a* values used were incorrect. Therefore the validity of this model needs to be re-established.

The interfacial/nano layers formed in nanofluids are considered again in a modified H-C model developed by Yu and Choi (2004). Similar with H-C theory, this model include the non-spherical factor of nanoparticles. The effective thermal conductivity of nanofluids is expressed as:

$$k_{eff} = \left(1 + \frac{n\phi_{eff} A}{1 - \phi_{eff} A}\right) k_f \qquad \text{Eq. 3-6}$$

where the parameter A is defined as

$$A = \frac{1}{3} \sum_{j=a,b,c} \frac{k_{p,j} - k_f}{k_{p,j} + (n-1)k_f} \qquad \text{Eq. 3-7}$$

and

$$\phi_{eff} = \frac{\sqrt{(a^2 + t)(b^2 + t)(c^2 + t)}}{\sqrt{abc}} \qquad \text{Eq. 3-8}$$

is the equivalent volume concentration of complex ellipsoids particles, an imaginary structure of elliptical particles. The shape factor, n, in H-C model is modified to consider more general rod-like particles. The shape factor, n, is expresses as $n = \psi^{-\alpha}$ where α is an empirical parameter and ψ is the particle sphericity. The model was compared with CNT-oil nanofluids measured data with α = 1 and 1.55. This model predicted the data quite well but failed to predict the nonlinearity thermal conductivity enhancement. It was suggested that the α value of CNT should be > than 1. The

modified H-C model has shown that the interfacial layers play an important role in the enhanced thermal conductivity of nanofluids. However, this model needs to be improved for the extreme case of nanotubes and other non-spherical particles.

Xue and Xu (2005) porposed a model based on Bruggeman model (Bruggeman, 1935), in which the interfacial shell/nano layer was also considered. The nanoparticle and the interfacial shell were considered as a 'complex nanoparticle' and the effective thermal conductivity correlation was established as follows:

$$\left(1-\frac{\phi}{\alpha}\right)\frac{k_{eff}-k_f}{2k_{eff}+k_f} + \frac{\phi}{\alpha}\frac{(k_{eff}-k_2)(2k_2+k_1)-\alpha(k_1-k_2)(2k_2+k_{eff})}{(2k_{eff}+k_2)(2k_2+k_1)+2\alpha(k_1-k_2)(k_2-k_{eff})} = 0 \qquad \text{Eq. 3-9}$$

The model was compared to the measured data of CuO-water and CuO-EG nanofluids and good agreement was evident.

Xie et. al. (2005) also investigated impact of interfacial layer on the enhancement mechanism of nanofluids thermal conductivity. The effective thermal conductivity derived from the Fourier's law of heat conduction gives the following expression:

$$k_{eff} = \left(1+3\Theta\phi T+\frac{3\Theta^2\phi_T^2}{1-\Theta\phi_T}\right)k_f \qquad \text{Eq. 3-10}$$

with

$$\Theta = \frac{\beta_{lf}\left[\left(1+\gamma^3 - \frac{\beta_{pl}}{\beta_{fl}}\right)\right]}{(1+\gamma)^3 + 2\beta_{lf}\beta_{pl}}; \qquad \gamma = \frac{\delta}{r_p}; \qquad \phi_T = \phi(1+\gamma)^3$$

$$\beta_{lf} = \frac{k_1 - k_f}{k_1 + 2k_f}; \qquad \beta_{pl} = \frac{k_p - k_1}{k_p + 2k_1}; \qquad \beta_{fl} = \frac{k_f - k_1}{k_l + 2k_1} \qquad \text{Eq. 3-11}$$

where δ is the nano-layer thickness and r_p is the original particle radius. It was observed that the model predicts some experimental data (Cu-EG, CuO-EG, Al_2O_3-water) quite well. However, they also claimed that the model is inconsistent with some other experimental data.

This model was re-visited to consider the effects of micro-convection due to the Brownian motion of nanoparticles (Ren et. al, 2005). With this consideration Eq, 3-10 was modified to:

$$k_{eff} = \left(1 + F(Pe) + 3\Theta\phi T + \frac{3\Theta^2\phi_T^2}{1-\Theta\phi_T}\right)k_f \qquad \text{Eq. 3-12}$$

with

$$F(Pe) = 0.0556Pe + 0.1649Pe^2 - 0.0391Pe^3 + 0.0034Pe^4 \quad ;$$

$$Pe = \frac{uL}{\alpha_f}\phi_T^{0.75} \quad ; \qquad L = (r_p + \delta)\left[\frac{4\pi}{3\phi_T}\right]^{1/3} \qquad \text{Eq. 3-13}$$

where α_f is the diffusivity of the base liquid. With δ = 2nm, the model predicts the effective thermal conductivity of nanofluids quite well.

The models that emphasize the interface layer seem to be promising but there is a controversial issue raised by other groups (Xue et. al, 2003; Xue et. al, 2004) which will be discussed in Section 3.5.

Based on the Maxwell model, Xuan et. al. (2003) developed another theoretical model to analyze the enhancement mechanism of nanofluids thermal conductivity. In this work, the suspended particles are believed to randomly move in Brownian motion. During this motion, some particles may collide with each other and form aggregates. The clusters of two or more particles move slower than a single particle. If the clusters are large enough they may even sedimentate by gravity. The enhancement of thermal conductivity is believed to decrease as more cluster form in the suspension. Using the Fourier's law energy flux, the effective thermal conductivity enhanced by the Brownian motion is expressed as follows:

$$k_{eff} = \frac{1}{2}\rho_p \phi c_p \sqrt{\frac{k_B T}{3\pi r_c \eta}} \qquad \text{Eq. 3-14}$$

Thus, the Maxwell model can be re-expressed as follows:

$$\frac{k_{eff}}{k_f} = \frac{k_p + 2k_f - 2\phi(k_f - k_p)}{k_p + 2k_f + \phi(k_f - k_p)} + \frac{1}{2}\rho_p \phi c_p \sqrt{\frac{k_B T}{3\pi r_c \eta}} \qquad \text{Eq. 3-15}$$

where k_B is the Boltzmann constant, r_c is the radius of clusters, and η is the liquid viscosity. Note that the temperature effect is taken into account. The model satisfactorily predicted the experimental data of Cu-water nanofluids. This observation suggests that apart from the parameters in the Maxwell model, the thermal conductivity

of nanofluids is also a function of density, viscosity, the specific heat of the particles and the radius of the clusters. The smaller the cluster radius the larger effective thermal conductivity can be achieved. Therefore, the low percentage of thermal conductivity enhancements from some experimental data may due to the forming of large aggregates and cluster in the nanofluids. If this is so, the preparation techniques need to be improved for better size distribution of particles. Although the temperature is incorporated, the dependence is too weak.

The role of Brownian motion of nanoparticles in nanofluids is no doubt to be very important. Several other models were developed based on this argument. Jang and Choi (2004) proposed a model based on kinetics, Kapitza resistance, and convection. The prediction of thermal conductivity of nanofluids is continuing as it is necessary to understand the mechanism lying behind the behaviour. The particles in the suspension are believed to collide in four modes of energy transport; 1) collision between the base liquid molecules, 2) thermal diffusion in suspended nanoparticles, 3) collision between nanoparticles in the Brownian motion, and 4) thermal interaction of dynamics nanoparticles with the base liquid molecules. The effective thermal conductivity of nanofluids is expressed as follows:

$$k_{eff} = k_f(1-\phi) + k_p\phi + 3C\frac{d_f}{d_p}k_f Re_{dp}^2 Pr\phi \qquad \text{Eq. 3-16}$$

where $\overline{C}$ is propotional constant, Pr is the Prandtl Number, Re_{dp} is the Reynolds Number defined by

$$Re_{dp} = \frac{\overline{C} d_p}{\nu}; \qquad \overline{C} = \frac{D_0}{l_f} \qquad \text{Eq. 3-17}$$

where $\overline{C}$ is the random motion velocity of nanoparticles, ν is dynamics viscosity of the base liquid, l_f is the mean free path, $D_0 = k_B T/3\pi\mu d_p$, and k_B = 1.3807 x 10^{-23} J/K is the Boltzmann constant. The prediction was compared to experimental data of nanofluids (Cu-EG, CuO-water, CuO-EG, Al_2O_3-water). Excellent agreement was evident for all the nanofluids. This model validates the size and temperature dependence of nanofluids. As the temperature increase, the particles move more rapidly and increasing the Brownian motion. As a result, the convection effects increases, hence increases the conductivities.

The argument that Brownian motion of nanoparticles contributes to the thermal conductivity enhancement was experimentally validated by Chon et. al. (2005). Based on the Buckingham-Pi theorem, an empirical correlation was established to show that the effects of particle size and temperature on nanofluids thermal conductivity. The correlation is:

$$\frac{k_{eff}}{k_f} = 1 + const.\left(\frac{Pr(T)^{0.9955} T^{1.2321}}{d_p^{0.369} k_f(T)^{0.7476} \mu^2(T)} \right) \qquad \text{Eq. 3-18}$$

with

$$Pr = \frac{\mu}{\rho_f \alpha} \quad ; \quad Re = \frac{\rho_f k_B T}{3\pi\mu^2 l_f} \quad ; \quad \mu = A \cdot 10^{B/(T-C)}$$

where l_f ($l_f = 1/\sqrt{2n} \cdot \pi d_f^2$) is the mean free path of the base liquid, A,B, and C are constant associated with the base liquid. The model was compared to experimental data

of three batches (11, 47, and 150 nm) of Al_2O_3-water nanofluids and good agreement was achieved.

Bhattacharya et. al. (2004) used the Brownian dynamics simulation to calculate the effective thermal conductivity of nanofluids. Based on the Newton's equation of motion, the correlation is expressed as follows:

$$k_{eff} = \phi k_p + (1-\phi)k_f \qquad \text{Eq. 3-19}$$

where k_p is the conductivity due to the positions and motions of the particles in the liquid defined as

$$k_p = \frac{1}{k_B T^2 V}\sum_{j=0}^{n}\langle Q(0)\cdot Q(j\Delta T)\rangle \Delta t \qquad \text{Eq. 3-20}$$

where T is temperature, V is the volume of the domain, n is the number of time step , ΔT is the time step and $\langle Q(0)\cdot Q(j\Delta T)\ \Delta T\rangle$ is the time-autocorrelation function of $Q(t)$. The simulation results are nearly in full agreement with the Cu-EG nanofluids and within 3% varied with the Al_2O_3-EG nanofluids.

A comprehensive model was proposed by Kumar et. al. (2004) to account for the thermal conductivity in nanofluids. The effect of particle size, concentration, motion and temperature are taken care in the model. To account for all the effects, two aspects are considered: 1) stationary particle model and 2) moving particle model

developed from the Stokes-Einstein formula. The effective thermal conductivity correlation is expressed as

$$k_{eff} = k_p + c\frac{2k_B T}{\pi\eta d_p^2}\frac{\phi r_f}{k_f(1-\phi)r_p}k_b \qquad \text{Eq. 3-21}$$

where c is a constant, η is the dynamic viscosity, T is the temperature, d_p is the particle diameter, and r_p is the particle radius. The data was compared with experimental data of Au-toluene nanofluids and good agreement was achieved. The thermal conductivity enhancement increases with temperature. As the temperature increases, the viscosity of liquid decreases and thus the Brownian motion increases. However, the validity of this model is yet to be further investigated especially for high concentrated nanofluids since the concentration of tested nanofluids was too low.

Similar parameters were incorporate by Koo and Kleinsteuer (2004) and Koo (2005) in developing the model for nanofluids thermal conductivity. The micro-mixing resulting from the Brownian motion was taken into account and the correlation can be expressed as:

$$k_{eff} = \frac{k_p + 2k_f + 2(k_p - k_f)\phi}{k_p + 2k_f - (k_p - k_b)\phi}k_f + 5\times10^4 \beta\phi\rho_p c_p\sqrt{\frac{k_B T}{\rho_p D}}f(T,\phi) \qquad \text{Eq. 3-22}$$

where β is the fraction of the liquid volume V_f, which travels with a particle. It will decrease with particle volume fraction, α. It can be seen that this model incorporates

the Maxwell model, as shown in the first term of Equation 3.22. The function, f(T,ϕ) was assumed to vary with particle volume fraction as the following relation:

$$f(T,\phi) = (-6.04\phi + 0.475)T + (1722.3\phi - 134.63) \qquad \text{Eq. 3-23}$$

The data satisfactorily agreed with a few sets of experimental data. The Brownian motion effect was observed to become more effective at high temperature.

Later, the model was re-visited to check for the effect of thermo-phoresis and osmo-phoresis (Koo and Kleinsteuer, 2005). The thermo-pherotic thermal conductivity, k_{TP}, is defined as

$$k_{TP} = \frac{1}{6\pi}\frac{\phi k_B}{\mu}\frac{3k_{kc}}{k_d + 2k_c}\left(1\times10^5 \rho_f c_f\right)\nabla T \qquad \text{Eq. 3-24}$$

where k_c is the thermal conductivity of the continuous phase, k_d is the thermal conductivity of the discrete phase and ∇T is the temperature gradient in the base liquid. The thermal conductivity due to the osmo-phoresis, derived from the van't Hoff's equation for osmotic pressure, is defined as

$$k_{OS} = \frac{1}{3\pi}\frac{\phi^2 k_B}{\mu}\frac{3k_c}{k_d + 2k_c}\left(1\times10^5 \rho_f c_f\right)\nabla T \qquad \text{Eq. 3-25}$$

The model was tested on Cu-water nanofluids with 1% concentration, d_p = 10 nm, k_{TP} = 5.1 x 10^{-10}, ∇T = 3.2 x 10^5 and k_{OS} = 1 x 10^{-10}. It can be seen that the k_{OS} value is very

low and negligible. The impact of Brownian motion is more dominant than the thermo-phoretic and osmo-phoretic effects. The Brownian motion effect on thermal conductivity decreases with particle concentration, and shows a transition region between 0.55 and 1.0%.

Prasher et. al. (2005) proposed another mechanism for the nanofluids thermal conductivity enhancement. Neglecting the impact of interfacial layer, they proposed three other mechanisms for thermal energy transport in nanofluids: 1) translational Brownian motion, 2) the existence of an interparticle potential, and 3) convection due to the Brownian motion. The modification of Maxwell model leads to the following correlation:

$$\frac{k_{eff}}{k_f} = (1 + A\mathrm{Re}^{m} Pr^{0.333} \phi)\left[\frac{(1+2\alpha)+2\phi(1-\alpha)}{(1+2\alpha)-\phi(1-\alpha)}\right] \qquad \text{Eq. 3-26}$$

with

$$\alpha = 2R_b k_m / d \; ; \qquad Re = \frac{1}{\nu}\sqrt{\frac{18k_B T}{\pi \rho_p d_p}} \qquad \text{Eq. 3.27}$$

where R_b is the interfacial thermal resistance.

Recently, Prasher et. al. (2006), introduce a convective-conductive model that captures the effects of particle size, thermal interfacial resistance between particle and liquid, temperature, choice of base liquid and others. Based on the Maxwell-Grant conduction model and the Brownian convection effect, an empirical correlation, called multisphere Brownian model (MSBM), was established for the effective thermal conductivity of nanofluids. The Eq. 3-26 have been re-casted to:

$$\frac{k_{eff}}{k_f} = \left(1 + ARe^m Pr^{0.333}\phi\right)\left[\frac{\left[k_p(1+2\alpha)+2k_m\right]+2\phi\left[k_p(1-\alpha)-k_m\right]}{\left[k_p(1+2\alpha)+2k_m\right]-\phi\left[k_p(1-\alpha)-k_m\right]}\right] \qquad \text{Eq. 3-28}$$

where *km* ($k_m = k_f[1+(1/4)Re \cdot Pr]$) is the matrix thermal conductivity. The validity of this model very much depends on the constant A, m and R_b values. The model was tested on nanofluids with different base liquid and good agreement was evident. It was shown that the convection due to the Brownian motion contributes to the mechanism in nanofluids thermal conductivity enhancement.

Several models that account the Brownian motion of nanoparticles in nanofluids have shown that Brownian motion constitutes a key mechanism in the enhancement of nanofluids thermal conductivity. The role of Brownian motion and a controversial issue raised by Evans et. al. (2006) will be discussed in the next section.

Wang et. al. (2003) used the effective medium approximation and the fractal theory to predict the effective thermal conductivity of nanofluids. This model takes into account the process of nanoparticles clustering, particles size as well as the surface adsorption. The effective thermal conductivity of nanofluids is expressed as:

$$\frac{k_{eff}}{k_f} = \frac{(1-\phi)+3\phi\int_0^\infty \frac{k_{cl}(r)n(r)}{k_{cl}(r)+2k_f}dr}{(1-\phi)+3\phi\int_0^\infty \frac{k_{cl}n(r)}{k_{cl}(r)+2k_{f1}}dr} \qquad \text{Eq. 3-29}$$

where r is the radius of nanoparticle clusters, k_{cl} is the thermal conductivity of cluster and $n(r)$ is the log normal distribution function. The liquid molecules on the particle surface are assumed to be adsorped on the particle surface and form single layer. The model was tested with CuO-water nanofluids, but the measured value did not quite fit in the model. Moreover, the model was not tested with other nanofluids. Therefore further research work is needed for validity of the clustering argument.

In summary, the theoretical models developed have shown that the effective thermal conductivity of nanofluids is not mainly a function of the physical parameters of the nanoparticles and the base liquid. In fact, it is also governed by some other nanoscale structure and microscopic conditions of the suspended nanoparticles. Although some models are applicable to a specific set of data, they have provided certain understanding of nanofluids behaviour. Note that most of the models pay least attention to the properties and surface chemistry of dispersant and coating material and their effects on the effective thermal conductivity of nanofluids. Figure 3.5 compares results of the effective thermal conductivity of CuO nanofluids from a few selective models. The models of nanofluids effective thermal conductivity are summarised in Table 3.1.

3.5 Mechanism for thermal conductivity enhancement

There are several possible mechanisms lie behind the thermal conductivity enhancement, some of which have been briefly discussed in the previous section.

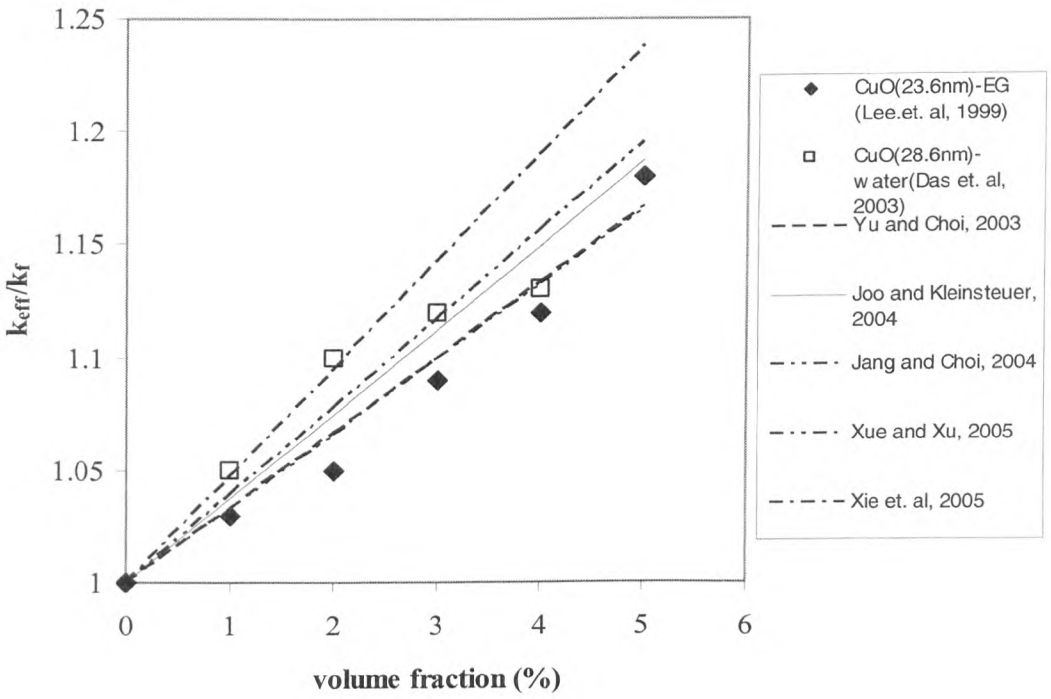

Figure 3.5: Comparison of experimental data and effective thermal conductivity models for CuO nanofluids.

Table 3.1: Mathematical models of thermal conductivity

No.	Reference	Expressions	Remarks
1.	Maxwell (1904)	$\frac{k_{eff}}{k_f} = \frac{k_p + 2k_f - 2\phi(k_f - k_p)}{k_p + 2k_f - \phi(k_f - k_p)}$	1. Spherical particles are assumed. 2. Accurate to order ϕ^1, applicable to $\phi \leq 1$ or $\lvert\alpha-1\rvert \leq 1$. ϕ = volume fraction of particle in suspension
2.	Hamilton-Crosser (1962)	$\frac{k_{eff}}{k_f} = \frac{k_p + (n-1)k_f - (n-1)(k_f - k_p)\phi}{k_p + (n-1)k_p + \phi(k_f - k_p)}$	1. Spherical and nonspherical particles are considered : n = 3 for spheres, n=6 for cylinders. 2. Accurate to order ϕ^1, applicable to $\phi \leq 1$ or $\lvert\alpha-1\rvert \leq 1$.
3.	Bruggeman (1935)	$\phi\left(\frac{k_p - k_{eff}}{k_p + 2k_{eff}}\right) + (1-\phi)\left(\frac{k_f - k_{eff}}{k_f - 2k_{eff}}\right) = 0$	Spherical particles
4.	Yu and Choi (2003)	$k_{eff} = \frac{k_{pe} + 2k_f + 2(k_{pe} - k_f)(1+\beta)^3\phi}{k_{pe} + 2k_f - (k_{pe} - k_f)(1+\beta)^3\phi} k_f$	Modified version of Maxwell model. Effect of nano-layer considered. Most effective for < 10 nm particles
5.	Xue (2003)	$9\left(1 - \frac{\phi}{\lambda}\right)\frac{k_{eff} - k_f}{2k_{eff} + k_f} + \frac{\phi}{\lambda}\left[\frac{k_{eff} - k_{c,x}}{k_e + B_{2,x}(k_{c,x} - k_{eff})} + 4\frac{k_{eff} - k_{c,y}}{2k_e + (1 - B_{2,x})(k_{c,y} - k_{eff})}\right] = 0$	Based on Maxwell model. Interfacial layer considered. Most effective when the interfacial thickness is 3 nm.

Table 3.1: Mathematical models of thermal conductivity (continued)

No.	Reference	Expressions	Remarks
6.	Yu and Choi (2004)	$k_{eff} = \left(1 + \frac{n\phi_{eff} A}{1 - \phi_{eff} A}\right) k_f$	Modified H-C model Interfacial layer and non sphericity of particles considered.
7.	Xue and Xu (2005)	$\left(1 - \frac{\phi}{\alpha}\right)\frac{k_{eff} - k_f}{2k_{eff} + k_f} + \frac{\phi}{\alpha}\frac{(k_{eff} - k_2)(2k_2 + k_1) - \alpha(k_1 - k_2)(2k_2 + k_{eff})}{(2k_{eff} + k_2)(2k_2 + k_1) + 2\alpha(k_1 - k_2)(k_2 - k_{eff})} = 0$	The expression depends on the thermal conductivity of solid, base liquid, their volume fraction, particle size as well as the interfacial properties.
8.	Xie et. al. (2005)	$k_{eff} = \left(1 + 3\Theta\phi T + \frac{3\Theta^2\phi_T^2}{1 - \Theta\phi_T}\right) k_f$	Based on Fourier's law Interfacial layer considered.
9.	Ren et. al. (2005)	$\frac{k_{eff}}{k_f} = \left[1 + F(Pe) + 3\Theta\phi_T + \frac{3\Theta^2\phi_T^2}{1 - \Theta\phi_T}\right]$	Nanolayer and Brownian convection considered.
10.	Xuan et. al. (2003)	$\frac{k_{eff}}{k_f} = \frac{k_p + 2k_f - 2\phi(k_f - k_p)}{k_p + 2k_f + \phi(k_f - k_p)} + \frac{1}{2}\rho_p \phi c_p \sqrt{\frac{k_B T}{3\pi r_c \eta}}$	Modified version of Maxwell model. Brownian motion and aggregation considered.

Table 3.1: Mathematical models of thermal conductivity (continued)

No.	Reference	Expressions	Remarks
11.	Jang and Choi (2004)	$k_{eff} = k_f(1-\phi) + k_p\phi + 3C\frac{d_f}{d_p}k_f \,\mathrm{Re}_{dp}^2 \,\mathrm{Pr}\,\phi$	Brownian motion effects considered
12.	Chon et. al. (2005)	$\frac{k_{eff}}{k_f} = 1 + const.\left(\frac{\mathrm{Pr}(T)^{0.9955}\,T^{1.2321}}{d_p^{0.369}\,k_f(T)^{0.7476}\,\mu^2(T)}\right)$	Brownian motion effects considered
13.	Bhattacharya et. al. (2004)	$k_{eff} = \phi k_p + (1-\phi)k_f$	Brownian dynamics simulation
14.	Kumar et. al. (2004)	$k_{eff} = k_p + c\frac{2k_BT}{\pi\eta d_p^2}\frac{\phi r_f}{k_f(1-\phi)r_p}k_b$	Stationary and moving particle model.
15.	Koo and Kleinsteuer (2004)	$k_{eff} = \frac{k_p + 2k_f + 2(k_p - k_f)\phi}{k_p + 2k_f - (k_p - k_b)\phi}k_f + 5\times10^4\,\beta\phi\rho_p c_p\sqrt{\frac{k_BT}{\rho_p D}}f(T,\phi)$	Brownian motion effects considered

Table 3.1: Mathematical models of thermal conductivity (continued)

No.	Reference	Expressions	Remarks
16.	Koo and Kleinsteuer (2005)	$k_{TP} = \frac{1}{6\pi}\frac{\phi k_B}{\mu}\frac{3k_{kc}}{k_d + 2k_c}\left(1\times10^5 \rho_f c_f\right)\nabla T$ $k_{OS} = \frac{1}{3\pi}\frac{\phi^2 k_B}{\mu}\frac{3k_c}{k_d + 2k_c}\left(1\times10^5 \rho_f c_f\right)\nabla T$	Additional effect of thermo-phoresis and osmo-phoresis to previous model (Koo and Kleinsteuer, 2004).
17.	Prasher et. al. (2005)	$\frac{k_{eff}}{k_f} = (1+A\mathrm{Re}^{\mathrm{m}}Pr^{0.333}\phi)\left[\frac{(1+2\alpha)+2\phi(1-\alpha)}{(1+2\alpha)-\phi(1-\alpha)}\right]$ $\alpha = 2R_b k_m / d$	Brownian convection effect considered. A = constant, m = constant
18.	Wang et. al. (2003)	$\frac{k_{eff}}{k_f} = \frac{(1-\phi)+3\phi\int_0^\infty \frac{k_{cl}(r)n(r)}{k_{cl}(r)+2k_f}dr}{(1-\phi)+3\phi\int_0^\infty \frac{k_{cl}n(r)}{k_{cl}(r)+2k_{f1}}dr}$	Predict dilute suspension of non metallic nanoparticles.

3.5.1 Role of Brownian motion

In the previous section, it can be seen that quite a number of publications developed the effective thermal conductivity models based on the hydrodynamics effects of Brownian motion of nanoparticles. The main basis of their arguments is directly connected to the vigorous collision between the particles during the random motion. The collisions then enable transportation of heat between the colliding particles to occur, and thus increasing the thermal conductivity of the fluids.

The Brownian motion is also believed to produce micro-convection of the liquid at the nanoscale. With the small size of nanoparticles, the random motion is increased and the micro-convection effect becomes dominant, thus increasing the thermal conductivity. Therefore smaller particles size will give thermal conductivity enhancement (Jang and Choi, 2004). The Brownian velocity increases with increasing temperature and decreasing particle size. The argument that the thermal conductivity enhancement due to convection was also proposed by Prasher et. al. (2005). Their findings have shown the enhancement is at least one order of magnitude higher than other mechanisms.

A controversy raised by Evans et. al. (2006) suggested that the Brownian motion contribution towards the enhanced thermal conductivity is small. The argument was supported by the results from molecular dynamics simulation of nanofluids model. In the simulation, the liquid and nanoparticles are assumed to be in same phase, thus the whole liquid is diffused together with the nanoparticles. Both the liquid and the nanoparticles have the same velocity. At low volume fraction, the nanoparticles carry

much less heat than the surrounding liquid. From these assumptions, the ratio of the Brownian-motion-induced thermal conductivity, κ_B to the thermal conductivity of the base liquid, κ_f is < 1%. Therefore the contribution of particle motion in the nanofluids is not a key mechanism to thermal transport. The simulation agrees with the experimental results of low volume fraction nanofluids (Eastman et. al, 2001; Patel et. al, 2003; Putnam et. al, 2006).

To further support the argument, molecular dynamics simulation was done once again on the heat flow of nanofluids. The nanoparticles can be divided into three categories based on the solid-fluid interaction strength: 1) non wetting, 2) weakly-wetting and 3) wetting particles. The thermal transport results showed that the thermal conductivity of nanofluids with non wetting and weakly wetting particles is slightly lower than that of nanofluids with wetting particles. The three categories of particles exhibit different interfacial thermal resistance. There is only small thermal conductivity difference between the three categories of particles and the base liquid. From the effective medium theory, the thermal conductivity ratio of nanofluids to the base liquid can be deduced to

$$\frac{k_{nf}}{k_f} = 1 + 3f\left(\frac{\gamma - 1}{\gamma + 2}\right) \qquad \text{Eq. 3-30}$$

where f is the volume fraction and γ is the ratio of particle radius to the equivalent matrix thickness. From Eq.3-30, when γ = 1, there is no thermal conductivity enhancement at all, and when γ<1, the addition of particles will reduce the nanofluids thermal conductivity. The simulation has shown that the Brownian-motion-induced did not have a significant enhancement to the nanofluids thermal conductivity.

As a conclusion, the Brownian motion may have an impact on the effective thermal conductivity of nanofluids. To reject the argument may be unjustified since there are models that have proved its effects. The extent of the impact to all nanofluids system is uncertain and therefore more understanding of the nanofluids behaviour is required.

3.5.2 The effect of solid-liquid interface layer

As discussed in Section 3.4, at least five models have been discussed have shown the effect of interfacial/nano-layer that forms at the interface between the particle and the bulk liquid. These models have shown that the interfacial layer plays an important role in the enhancement mechanism of nanofluids effective thermal conductivity. The interfacial layer, having the thermal conductivity, k_{layer} ($k_{layer} > k_f$) acts as a thermal bridge and increases the thermal conduction from the particles to the liquid. The effective thermal conductivity increases with increases in the nano-layer thickness. It was suggested that the effective thermal conductivity of nanofluids could further be increased by manipulating the nano-layer.

However, these arguments were opposed by Xue et. al. (2003) where they found that the nano-layer has little effect on the thermal transport of nanofluids. From the molecular dynamics simulation, it was found that the nano-layer has almost the same temperature as the bulk liquid. The study on the intermolecular interactions between the solid and liquid regimes has found that the atomic bonding at the particle-matrix interfaces in nanofluids will exhibit high thermal resistance. This argument is again supported by Xue et. al. (2004) where they found that the structure of nano-layer

exhibits weak ordering and essentially limited to single atomic layer. Note that these studies are specific to simple (mono-atomic) liquid. They might not be true for other nanofluids involving more complex liquid such as liquid with long chain molecules.

Thus, by manipulating the thickness of nano-layer may not enhance nanofluids thermal conductivity. Alternatively, there may be an optimum nano-layer thickness that is essential for the interface nano-layer to make a significant impact on the effective thermal conductivity of nanofluids. Hence this opens an opportunity in the research area for instance, to manipulate the thermal conductivity of the nano-layer.

3.5.3 The effects of particles clustering

Clusters of particle are formed from the attachment due to collision in the Brownian motion. During clustering, nanoparticles form percolating patterns that provide paths for rapid heat transfer. Choi et. al. (2002) studied the relation between the thermal conductivity and effective volume of the clusters. When the packing fraction was decreased, the effective volume of clusters increased, thus enhancing thermal conductivity. If the particles do not need to be in physical contact, an increase in thermal conductivity could take place since heat flows rapidly within the clusters.

As pointed out by Xuan et. al. (2003), the effective thermal conductivity of Cu-water nanofluids without aggregation would be higher than that with aggregation. From the effective medium theory simulation (Keblinski et. al, 2002; Keblinski et. al, 2005), it was shown that the effective thermal conductivity of nanofluids would be higher in a loosely packed clusters than that of closely packed (Figure 3.6).

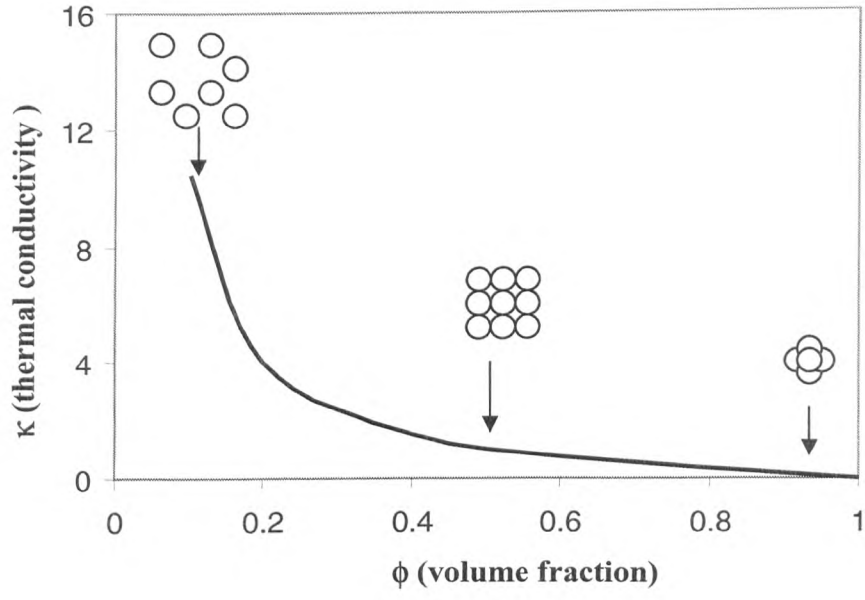

Figure 3.6: Schematic diagram of thermal conductivity enhancement due to particle clustering

3.5.4 The effect of ballistic phonon transport

Energy transport across a material consists of two natures, diffusive and ballistic (Aitcheson et. al, 2002). Nanoscale heat transfer differs from that of larger scale mainly due to the size effect. In bulk materials, heat transfer processes are dominated by the internal scattering which is considered as diffusive transport. Ballistic transport is movement of carrier without any collision or scattering. In nanoscale particles, phonons transport of nanoparticles is contributing to the enhanced thermal property of nanofluids.

Phonons are the quantum of vibrational energy in a solid. Since the coherent length of thermal phonons is short, phonons can be considered as discrete particles. Thermal conductivity can also be explained by phonons interactions. As the particle size decreases, the frequency of the phonon boundary collision increases. The interface scattering of phonons and the associated thermal boundary resistance can dominate heat conduction in nanoparticles. Around nanoparticles, phonons become rarefied when their mean free path is comparable or larger than the nanoparticles themselves, which indirectly increases the thermal resistances (Chen, 2000). Based on the kinetic theory, mean free path (Λ) of phonon can be related to the thermal conductivity through

$$\Lambda = \frac{3k}{Cv} \qquad \text{Eq. 3-31}$$

where k is thermal conductivity, C is the specific heat per unit volume and v is the speed of sound. When particle size is smaller than Λ, the transport of heat in solids not in diffusive manner but of a ballistic nature or in other words, scattering is negligible or absent.

These mechanisms are believed to be a factor that constitutes the enhancement of nanofluids thermal conductivity. Whether each mechanism contributes a significant impact is unclear, therefore more research is required to understand the thermal transport of nanofluids.

3.6 Convective heat transfer of nanofluids

Most work on nanofluids has been concerned on the heat conductivity of nanofluids. The convective heat transfer of nanofluids has received comparatively lesser attention, despite its engineering importance. One of the earliest works on forced convection of nanofluids was done by Lee and Choi (1996). The performance of microchannel heat exchangers was compared using water and two different nanofluids, NF_2 and NF_3 as the working fluid. The thermal conductivities of NF_2 and NF_3 are two and three times higher than that of water, respectively. They showed that by using nanofluids, the thermal resistances are reduced by a factor of 2.

Pak and Cho (1998) experimentally investigated turbulent friction factor and heat transfer behaviours of Al_2O_3-water and TiO_2-water nanofluids in circular pipe. The viscosities of 10 vol. % Al_2O_3 and TiO_2 nanoparticles were 200 times higher than water for Al_2O_3 and 3 times higher for TiO_2. The hydrodynamics entry section was long enough (x/D = 157) to accomplish fully develop flow. The heat transfer test section had a dimension (x/D) of 330. They found that the Darcy friction factors for the nanofluids coincided with the Kays' correlation for turbulent flow in a single phase fluid. The Darcy friction factor decreased (0.05-0.02) with increasing Reynolds Number (3000-100000 s^{-1}). The Nusselt Number for the nanofluids increased (10^1 – 10^3) with

increasing volume fraction and Reynolds Number. A new Nusselt Number (Nu) correlation was suggested as

$$Nu = 0.021 Re^{0.8} Pr^{0.5} \qquad \text{Eq. 3-32}$$

valid for volume concentration of 0-3%, the Reynolds Number of (10^4-10^5) and Prandtl Number (6.54-12.33). Since the viscosities were higher than water, based on Equation 3-32, the Nu is expected to decrease. Therefore, the heat transfer coefficient should decrease since h is directly proportional to Nu. Thus is it justified that the heat transfer coefficient of the nanofluids in the experiment was 12% smaller than that of water.

Xuan and Li (2000) developed a model to estimate the convective heat transfer coefficient and friction factor of nanofluids in a tube. The nanofluid sample used was Cu nanoparticles dispersed in de-ionized water. This study reported that the heat transfer coefficient of nanofluids changed with flow velocity as well as volume fraction. The convective heat transfer coefficient of the nanofluids was higher than that of the base liquid, for instance a 2% by volume of nanofluids gave a 39% enhancement. The enhancement was attributed to the high thermal conductivity of nanofluids, random movement particles, and the dispersion effect of the nanoparticles. The results also showed that the nanofluids did not cause significant increase in pressure drop. Further experiments were carried out by Xuan and Li (2003) to investigate the convective heat transfer and flow features of nanofluids. Similar conclusion was obtained.

Chien et. al. (2003) used Au-water nanofluid to measure the thermal resistance of a disk-shaped miniature heat pipe (DMHP). Their results showed that the Au-water

nanofluid had a lower thermal resistance under any charge volume, for example a decrease of 40% in thermal resistance could be achieved. Au-water nanofluid was also used by Tsai et. al. (2004) to measure the thermal performance of conventional circular heat pipe. Their results also revealed that the thermal resistance of the heat pipe with nanofluids was lower than that of water, with at least 20% reduction. The reduction of thermal resistance was due to the bombardment of vapor bubbles by the suspended nanoparticles. The nucleation size of vapor bubble is much smaller for nanofluids than that without them. Ma et. al. (2006) developed an ultrahigh-performance cooling device, called nanofluid oscillating heat pipe (OHP), utilizing Au as the working medium. They found that, at the input power of 80.0W, the nanofluid could reduce the temperature difference between the evaporator and condenser from 40.9 to 24.3°C. These findings have shown that nanofluids have an excellent cooling performance.

Yang et. al. (2005) reported experimental results of convective heat transfer coefficient of graphite nanoparticles dispersed in liquid for laminar flow tube. The results illustrated that heat transfer coefficient increased with Reynolds number and the particle volume fraction. However, the heat transfer enhancement was small (15%) when the liquid temperature increased (70°C). At lower temperature (50°C), the heat transfer coefficient is 22% higher than the base liquid (water). Wen and Ding (2004b) studied the heat transfer coefficient at the entrance region of a horizontal tube. Alumina nanoparticles were used in the work. Apart from the results that the heat transfer coefficient increased with increasing Reynolds number and volume fraction, they also found that the enhancement was more profound in the entrance region.

The CuO (50-60nm) and Al_2O_3 (20nm) in water nanofluids systems were investigated by Heris et. al. (2006). The laminar flow of nanofluids in a circular tube was examined. The results showed that for both nanofluids systems, the heat transfer coefficient increased with increasing particle size and Peclet Number. Peclet Number (*Pe*) is defined as Reynolds Number multiply by Prandtl Number ($Pe = Re \cdot Pr$). They also found that, for the same Peclet Number, the Al_2O_3-water nanofluids showed more enhancement than that of CuO-water nanofluids. For example at Peclet Number 5000, when Al_2O_3-water concentration changed from 0.2% to 2.5%, the heat transfer enhancement increased from 1.05 to 1.29, while for CuO-water nanofluids the increased was from 1.06 to 1.23. This may be due to the size factor and higher viscosity of CuO which affecting the heat transfer coefficient. The viscosity of CuO and Al_2O_3 was 1.7 mPa·s and 1.5m Pa·s respectively.

Maiga et. al. (2004) investigated the laminar forced convection flow inside a uniformly heated tube. Al_2O_3-water and Al_2O_3-EG were used as the working nanofluids. Their results showed that the addition of nanoparticles had increased the heat transfer at the tube wall for both laminar and turbulent regimes. However, the addition of nanoparticles induced drastic effects on the wall shear stress. The Al_2O_3-EG nanofluids seemed to have better heat transfer enhancement than that of Al_2O_3-water. Unfortunately it is the one that induced more drastic effects on the wall shear stress. In the turbulence regimes, the heat transfer increased was more profound with increasing Reynolds Number.

Further investigation was done by Maiga et. al. (2005) which include radial flow. Apart from the results obtained previously, they also observed for radial flow,

both Reynolds Number and the distance separating the disks did not have a significant impact on the heat transfer.

Buongiorno (2006) analyzed the effects of various particle migration mechanism on the convective heat transfer. He considered effects of inertia, Brownian diffusion, thermophoresis, diffusiophoresis, magnus effect, fluid drainage and gravitational force. Among these factors, Brownian diffusion and thermophoresis were concluded to be the dominant in effecting the forced convective heat transfer.

Few works have devoted to the natural convective heat transfer. An experimental study on convective heat transfer of nanofluids was conducted by Putra et. al. (2003). Two nanofluids (Al_2O_3-water and CuO-water) flowing in a horizontal cylinder were observed. Several parameters such as particle concentration, particle type and geometry of cylinder were investigated at steady-state conditions. The convective heat transfer of nanofluids was found to be lower than the base liquid. In addition, the convective heat transfer was also found to deteriorate with increasing particle concentration, aspect ratio of cylinder and density of particles. The deterioration of smaller sized CuO nanofluids was higher than that of Al_2O_3. This is because the density of CuO was higher than Al_2O_3. The error of the experiment was estimated to be below 5%.

A contradict findings was observed by Khanafer et. al. (2003) where nanofluids was utilized in a two-dimensional enclosure. In the model developed, the results showed that the heat transfer rate increased with increasing nanoparticles volume fraction at any Grashof Number, and this is a total disagreement with Putra et. al.

(2003). A similar work was done by Jou and Tzeng (2006) and the results showed that by increasing the buoyancy and volume fraction of nanoparticles, the heat transfer coefficient was increased.

Wen and Ding (2005) investigated the natural convective heat transfer of TiO_2 – water nanofluids. Their results showed that convective heat transfer decreased with increasing particle concentration, an agreement to Putra et. al. (2003) finding. They proposed several mechanisms for the observation such as nanofluids properties, convection due to concentration difference, pH influence, and particle-surface interactions. Recent work by Wen and Ding (2006) obtained similar conclusion.

3.7 Mathematical model for convective heat transfer of nanofluids

Some empirical models have been developed based on the experimental data, theoretical analysis and even modeling. Earliest attempts were done by Pak and Cho (1999) and Xuan and Roetzel (2000). The model was derived using two approaches in these attempts. Nanofluids were treated as a single phase fluid in the first approach while the other treated nanofluids as a solid-liquid mixture. Later on, Xuan and Li (2000) established a correlation for the forced convective heat transfer coefficient based on the experimental work done on Cu-water system. The correlation included factors such as Brownian motion, friction between the fluid and particles, etc. The correlation was further improved by incorporation the micronvection and microdiffusion effects (Xuan and Li, 2003).

Kim et. al. (2004) introduced a new factor f, defined as the ratio of the Raleigh Number of nanofluids to that of the based liquid, and proposed a new relationship for natural convection of nanofluids. A macroscopic view of heat transfer in nanofluids was studied by Xuan et. al. (2005). The external and internal forces that act on the suspended nanoparticles were considered as well as the thermal interactions between the solid and fluid particles. The Lattice Boltzmann model was used to describe the heat transfer and flow of the nanofluids. The findings revealed that the convective heat transfer is enhanced with increasing volume fraction, for example, the Nusselt Number with 1 vol. % of nanoparticles is 27% higher than that of water.

Table 3.2 summarizes the correlations for the convective heat transfer coefficient in terms of Nusselt Number reported in the literature. Note that these models are based on the single-phase assumptions. They are only applicable to conditions under which they were established. A fundamental understanding of the enhancement mechanism is needed to establish a more generic model.

3.8 Viscosity of nanofluids

The rheology of suspensions has been the subject of numerous researches, mainly because of its obvious importance in a wide range of industrial applications. A thorough understanding of the dispersion and resultant flow behaviour of nanoparticle suspensions is critically important before they can be applied in the practical applications. Therefore, the measurement of rheological properties of a suspension can help to develop a better product, predict its end use performance and predict the physical properties of a product during and after processing.

Table 3.2: Convective heat transfer correlation in terms of Nusselt Number

$$Nu = \frac{hD}{k}$$

No.	Reference	Correlation	Remarks
1.	Park and Cho (1998)	$Nu = 0.021 Re^{0.8} Pr^{0.5}$	Re = Reynolds Number Pr = Prandtl Number
2.	Xuan and Li (2000)	$Nu = \frac{\sum_{m=1}^{\infty} X(\bar{x}) / \left[X(0) - X'(0)/Pe^*\right]}{\sum_{m=1}^{\infty} \left[X(x) / \left[X'(0)/Pe^*\right]\right] / \beta_m^2}$	Pe = Peclet Number
3.	Xuan and Roetzel (2000)	$Nu = \left[1 + C^* Pe^n f'(0)\right] \theta'(0) \mathrm{Re}^m$	
4.	Li and Xuan (2002)	For laminar flow $Nu = 0.4328(1.0 + 11.285 \phi^{0.754} Pe_p^{0.001}) \mathrm{Re}_{nf}^{0.333} \mathrm{Pr}_{nf}^{0.4}$	
5.	Putra (2002) and Putra et. al. (2003)	$Nu = C\, Ra^n$	Ra = Rayleigh Number

Table 3.2: Convective heat transfer correlation in terms of Nusselt Number (continued).

No.	Reference	Correlation	Remarks
6.	Xuan and Li (2003)	$Nu = 0.0059(1.0 + 7.628\phi^{0.6886} Pe_d^{0.001}) \mathrm{Re}_{nf}^{0.9238} \mathrm{Pr}_{nf}^{0.4}$	Correlation establish for turbulence flow
7.	Kim et. al. (2004)	$Nu_{nf} = A\, Ra_{nf}^m = A\, Ra_f^m f^m = Nu_f f^m$ $\frac{h_{nf}}{h_f} = f^m \left(\frac{k_{nf}}{k_f} \right)$	

When subjected to shear, suspensions show different responses to deformation rate depending upon the general physical and chemical characteristics of the system. This include particle size and particle size distribution, particle shape, solid phase volume, surface charge heterogeneity, range and magnitude of various forces between the suspended particles and type of the dispersing agents used to stabilize the dispersion. Suspensions of particles in shear flows experience several forces such as hydrodynamic forces which include the viscous drag force and particle-particle interaction through flow field induced by neighbouring particles. Other forces are electrostatic, steric, London-van der Waals attractive forces, forces due to the gravitational, inertia, electroviscous, and thermal or molecular collisional effects (Zaman et. al, 2002).

Only few literatures discussed in the previous sections have studied the rheology of nanofluids. However, there have been numerous other publications on rheology of suspensions. Pak and Cho (1998) investigated the viscosity of Al_2O_3-water and TiO2-water nanofluids. The results showed that at 10% volume fraction, the viscosities of Al_2O_3-water and TiO2-water nanofluids were 200 and 3 times greater than that of water. The viscosities were measured using a Brookfield rotating viscometer with cone-and-plate geometry. Putra et. al. (2003) studied the rheological behaviour of Al_2O_3-water nanofluids and found that at low volume fraction (1% and 4%), the nanofluids showed Newtonian behaviour in the range of the shear rate studied (10-1000s^{-1}). For instance, at 60°C, the viscosity of 1 volume fraction of Al_2O_3 was at 0.7 mPa·s between shear rate of ~70-700s^{-1}. The viscosities measurements were made using a disc type rotating rheometer. Heris et. al. (2006) used a cylindrical rheometer observed that for low concentration (< 5 vol %) of Al_2O_3-water and CuO-water nanofluids. They also observed that the viscosities increased with particles volume fraction and the viscosity

of CuO nanofluids increased more significantly than that of Al_2O_3. These findings have indicated that viscosity of nanofluids depended on the volume fraction of nanoparticles.

Tseng and Wu (2002) studied the rheology of Al_2O_3-water nanofluids at pH 2.0 and pH 11.0. The average particle size investigated was ~37nm. The pH was adjusted by adding HCl or NH_4OH. Nanoparticle suspensions at pH 2.0 generally showed that the viscosity decreased with increasing shear rate in a shear rate range of 70-200 s^{-1}. This indicated that particle structures were broken into smaller ones as the shear rate increased. The suspensions showed an apparent shear thickening when the shear rate exceeds a critical level. The critical shear rate for the dilatant transitions increased with particle volume fraction. Quite different behaviour was shown by suspensions at pH 11.0. At lower volume fractions (ϕ = 0.03 and 0.06), the suspensions exhibited rheological properties similar to those of pH 2.0, with a transition from shear thinning to shear thickening. However, for $\phi \geq 0.11$, the suspensions were pseudoplastic in character over the entire shear rate and no transition was observed. This indicated that the suspensions were flocculated over the entire investigated shear rate (1-1000s^{-1}).

Tseng and Lin (2003) investigated the rheological behaviour of TiO_2-water nanofluids. The average particle size of TiO_2 was 7-20 nm. The nanofluids generally showed a pseudoplastic flow behaviour over the entire shear rate investigated (0-1200 s^{-1}) for all particle volume fractions (ϕ = 0.05-0.12). The shear thinning flow behaviour revealed that the particle aggregates in the suspension were broken down into smaller flow units by the applied forces, so that the resistance to flow was reduced, leading to a lower viscosity as the shear rate increased. A thixotropic behaviour was also observed for particle volume fraction higher than 0.1. This indicated that particle aggregations

existed in the suspensions, and nanoparticles interaction increased with the increased particle volume fraction.

Chen et. al. (1998) investigated the stability and rheology of concentrated (>50%) TiO_2 dispersions. The dispersion was found to be non-Newtonian and the increase in viscosity was more significant at higher volume fraction. A remarkable shear thinning characteristics was observed for shear rate range of 0-500s^{-1}. The viscosity decreased with increasing surfactant (SDS) indicate that a strong adsorption of SDS on the surface of TiO_2. The stability of the suspension was depended on the pH value. Mushed et. al (2005) characterized the rheology of TiO_2-water (spherical and cylindrical shape). They found that the viscosity of spherical TiO_2 nanoparticles in water is higher than that of cylindrical TiO_2 in water. Moreover, the viscosity increased was more significant for the spherical TiO_2 nanoparticle suspension. Wen and Ding (2006) investigated the viscosity of TiO_2-water nanofluids (pH 3.0) and shear thinning behaviour was observed for shear rate range of 0-400s^{-1}.

Kinloch et. al. (2002) studied the rheological behaviour of carbon nanotubes/water dispersions. A shear thinning behaviour was observed for all particle loading (0.05 vol. % to 9.20 vol. %). The pseudoplastic character was observed over the whole range of shear rate (0.1 – 1000 s^{-1}). A thixotropic behaviour was observed for volume fraction higher than 4.5%. Alias et. al. (2003) studied the rheological behaviour of CNTs nanofluids. The pseudoplastic behaviour was found but none of the nanofluids showed any thixotropic behaviour for the same shear rate range.

The rheology of CNT nanofluids was studied by Yang et. al. (2005). The dispersion also exhibit shear thinning behaviour in steady shear measurement. The result also showed that the ultrasonication time changes the rheological behaviour of the dispersion. This was attributed to the fact that the sonication alters the aspect ratio of the tube. Yang et. al. (2006) investigated the thermal and rheological properties of CNT-oil nanofluids with polyisobutene succinimideas the dispersant. Without the dispersant, the viscosity of nanofluids was quite high ($5x10^5$ Pa·s) at low stress (0.1 Pa). Addition of dispersant reduced the nanofluids viscosity to < 0.5 Pa.s at a stress of 0.07 Pa. A strange behaviour was observed where for the highest (8wt. %) and lowest (0.3 wt. %) concentration, the viscosity showed a clear shear thinning, while for 0.3 wt. % concentration, the nanofluids behaved like a Newtonian fluid. Nanofluid with 3 wt. % dispersant concentration gives the minimum viscosity (~0.1 Pa·s) at a low stress (0.07 Pa). For dispersant concentration of below and above 3 wt. %, the viscosities were higher. This suggests that at low dispersant concentration, less polymer molecules were adsorbed to the CNT surface, thus reduced protection towards agglomeration. At higher dispersant concentration, bridging flocculation could occur between the polymer chain and form agglomerates. The agglomeration can be reduced by the fluid motions under high shear rates.

The thermal conductivity ratio (k_{nf}/k_f) was a minimum at 3wt % dispersant loading. This suggests that the dispersant provided good steric hindrance between the nanotubes and reduced the contact between them. At higher dispersant loading, the thermal conductivity increased due to the larger agglomeration forming and promoted the nanotubes contact. They also observed that ultasonication time could reduce the agglomerates and the aspect ratio of nanotubes.

Shin and Lee (2000) also studied the relation of thermal and rheological properties relation, but focused on larger particle size (25-300 μm). When subjected to shear, the thermal conductivity of suspension for particle size of 25 μm remained constant even for 10% volume fraction of particles. On the other hand, suspension made of 100 μm, the thermal conductivity increased linearly with the shear rate in a shear rate between 50-220s^{-1}. The thermal conductivity reached a plateau at shear rate higher than 220 s^{-1}. For larger particle size (180 and 300 μm), the thermal conductivity of suspensions strongly depend on the shear rate. The degree of shear rate dependence increased with the particle size. The results were consistent with the experiments conducted by Ahuja (1975). This phenomenon may cause an overestimation of heat transfer rate for high shear flows.

From these studies, several conclusions can be drawn on the rheological behaviour of nanofluids. The viscosity of nanofluids is depended on volume fraction, particle size, particle shape, types of particle, pH and dispersant loading.

3.9 Potential application of nanofluids

Due to the size factor, nanoparticles appear to be suited for applications in which fluids flow through small channels. Nanoparticle suspensions, if properly engineered, are stable, thus will not clog the channel. Therefore, the findings of nanofluids could impact many industrial sectors, including transportation, electronics, energy supply, electronics, textiles, and paper production. Successful design of nanofluids will encourage the current trend in miniaturization. For instance, small microchannel and

heat exchangers could be designed and utilized. Nanofluids can also act as a lubricating medium because of their small sizes.

Lee and Choi (1996) estimated the performance of microchannel heat exchangers using nitrogen, water and nanofluids as the working fluids. The heat exchangers were used for cooling of silicon mirrors used in the X-ray sources. Again, Jang and Choi (2006) used a nano-sized metal (Cu and diamond) particles suspension as new coolant in microchannel heat exchanger. When nanofluids were used, the thermal resistances were reduced and the power densities were increased. The nanofluids enhanced the cooling rates during the operation of the cooling system. The pumping power of 2.25W was enhanced by 10% with the nanofluids. They concluded that nanofluids can offer significant benefits in cooling technology. Nanofluids can also be used in engines, superconducting magnets, and in supercomputers, where densely packed chips generate much heat. It may also be used in fiber-forming processes or in reducing size of current industrial cooling instruments. Furthermore, by passing the nanofluids through small channels, the possibility of thermal distortion and flow-induced vibration could be eliminated (Eastman et. al, 2002).

Faulkner et. al. (2003) used nanofluids in cooling the microwave electronics. A suspension of ceramic-based nanoparticles was used in the design. No problems were encounter with the nanofluids and flow in the micro-channels. It is a good evidence that nanofluids can improve the heat flux in heat transfer fluids. At temperature 125°C, the system was observed to dissipate heat fluxes between 243-320 W/cm^2.

Ali et. al. (2004) added nanoparticles suspensions to the falling films dessicant to study the heat and mass transfer enhancements. A comparative numerical study was employed in the parallel and counter-current flow configurations. They reported that the dispersion factor appeared to have an effect on enhancing the heat transfer between air and liquid desiccant at the interface. By adding Cu nanoparticles in the suspension, the dehumidification and the cooling rates were enhanced.

3.10 Conclusions

The properties and behaviour of nanofluids are discussed in this chapter. Many researchers have given more attention to the measurements and calculation of nanofluids thermal conductivity. This can be seen that the publications on thermal conductivity of nanofluids outnumbered that on the convective heat transfer studies and the trend tends to continue as in current situation.

The work on modeling the thermal conductivity of nanofluids is progressing. Several conventional theories of thermal conduction have been modified to include certain characteristics of nanofluids. It can be seen that certain models can satisfactorily agreed with only some experimental data. Therefore no concrete conclusions can be drawn whether the models are accurate. The proposed mechanisms of the thermal conductivity enhancements with some controversial issues have been discussed. Nevertheless, those models have provided some basic understanding of the enhancement mechanism of nanofluid thermal conductivity. This suggests that the prediction and calculation of nanofluids thermal conductivity remains a challenge in research. This will give better knowledge that underlies the nanofluids behaviour.

The research on the convective heat transfer has provided some insight of the heat transfer performance of nanofluids. However, few works have devoted to the investigation of nanofluids convective heat transfer; hence no concrete conclusions can be drawn regarding the general heat transfer behaviour of nanofluids. Thus more research is required for further understanding of nanofluids.

CHAPTER FOUR

EXPERIMENTS

4.1 Introduction

The details of experiments and research methodology will be described in this chapter. This includes characterization of nanoparticles, materials used, experimental devices and procedures, and data collection.

4.2 Materials

Two types of nanoparticles were used in this work. They are carbon nanotubes (CNTs) and titanium oxide (TiO_2). CNTs are in the form of multi-wall nanotubes (Figure 4.1) while TiO_2 nanoparticles are spherical in shape (Figure 4.2). The details of these nanoparticles are listed in Table 4.1. Distilled water (DW) was used as the base liquid.

In order to obtain a stable suspension, a choice of surfactants and dispersants was used in the preparation of nanofluids. They are oleic acid, gum arabic (GA), sodium dodecyl benzene sulfonate (NDDBS), sodium laurate salt and succinimide for carbon nanotubes nanofluids. Hydrochloric acid, nitric acid and sodium hydroxide were used to manipulate the nanofluids to pH ~2.00 and ~11.00, respectively. The details of these chemical are shown in Table 4.2.

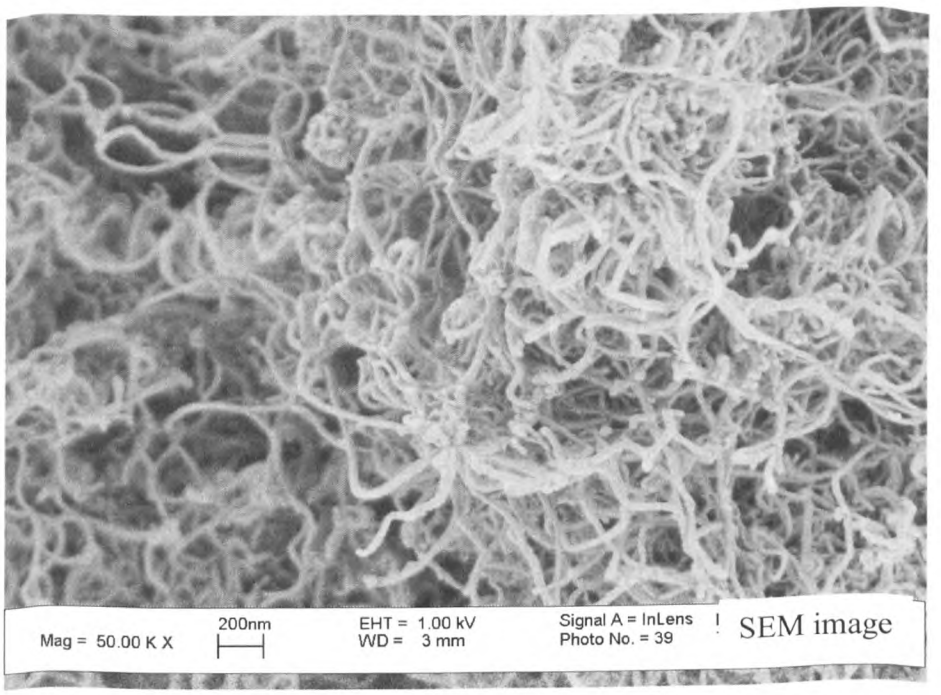

(a)

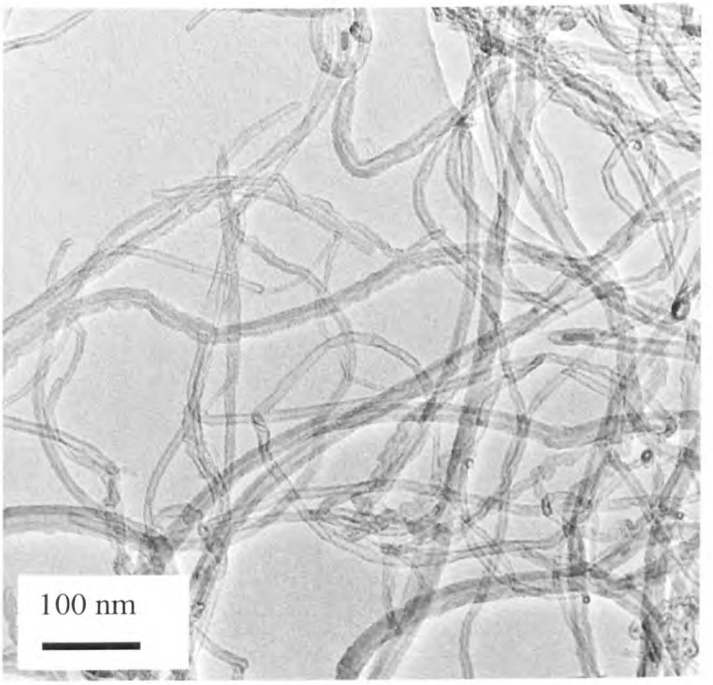

(b)

Figure 4.1: Images of carbon nanotubes as received: (a) SEM image of CNTs and (b) TEM image of CNTs.

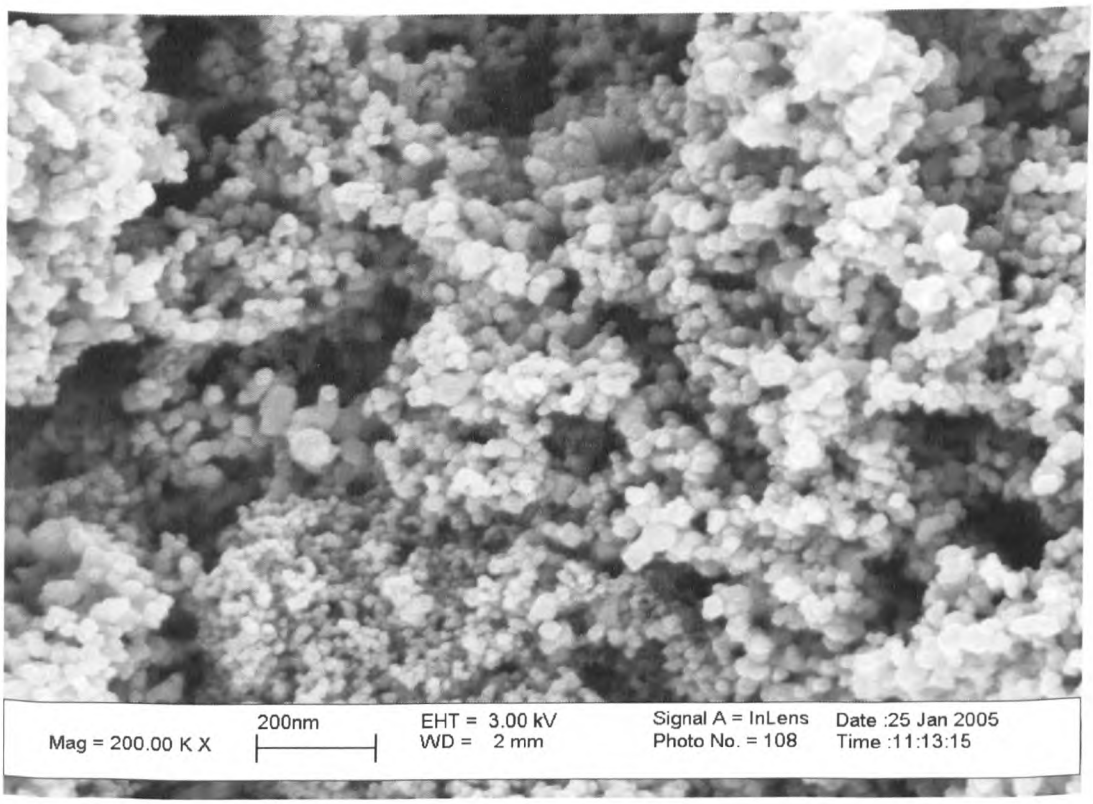

Figure 4.2: The TiO_2 nanoparticles as received.

Table 4. 1: Nanoparticles studied and their shape, size and manufacturer.

Nanoparticles	Shape	Size	Manufacturer
Titanium dioxide	Spherical	20 nm diameter	P25, Degussa, Germany.
Carbon nanotubes	Multiwalled cylindrical	20-60nm diameter	Tsinghua-Nafine Nano-Powder Commercialization Engineering Centre, China

Table 4.2: A list of surfactants and dispersants and their manufacturers.

Surfactant/ Dispersant	Chemical Formula	Description	Manufacturer
Gum Arabic	Complex mixture of arabinogalactan oligosaccharides, polysaccharides and glycoproteins	Crystalline powder, slightly beige in colour	Beecroft Scientific, UK
Oleic Acid	$C_{17}H_{33}COOH$	Clear liquid, colourless with fatty odour	Fischer Scientific, UK
Sodium Laurate Salt	$C_{12}H_{23}NaO_2$	Solid, white in colour and odourless	Fischer Scientific, UK
Sodium dodecyl benzene sulfonate (NDDBS)	$C_{12}H_{25}C_6H_4SO_3$ Na	Crystalline powder, white or light yellow flakes	Fischer Scientific, UK
Hydrochloric acid	HCl	Colourless	Fischer Scientific, UK
Nitric acid	HNO_3	Colourless	Fischer Scientific, UK
Sodium hydroxide	NaOH	Colourless	Fischer Scientific, UK

4.3 Instruments and procedures

Different techniques were applied to formulate the nanofluids. They are sonication, high shear mixing and milling.

4.3.1 Ultrasonication

Bath sonication is a mechanical method of mixing using the ultrasonic vibration. Ultrasonic sound waves enter the liquid within the tank and create an effect called cavitation, the rapid formation and collapse of microscopic bubbles. The bubbles travel at high speed around the tank causing them to implode, against the surface of the test tube immersed, energy release which gradually mixes the suspension inside the test tube.

Sonication technique was used because the technique is simple, easy, and inexpensive. Moreover, previous researches have shown that stable nanoparticle suspension could be achieved by ultrasonication. An ultrasonic bath was used to sonicate the raw nanoparticles as well as the suspension. The instrument used was ultrasonic bath Model MU from Clifton (Figure 4.3). The sonicator can be timed for a maximum of 15 minutes. The tank was filled to certain height so that the suspensions containers are immersed in the liquid and even energy was distributed.

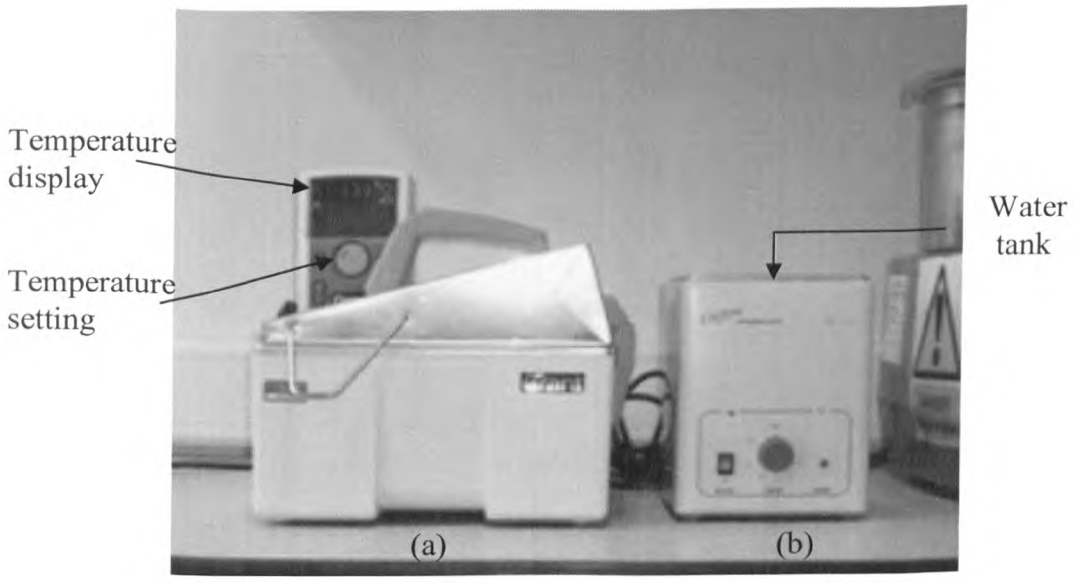

Figure 4.3: Ultrasonic bath : (a) water bath (Grant, UK) for sample heating and (b) sonication bath (Clifton, UK) for sonication of raw CNTs.

4.3.2 High shear mixing

High shear mixing is another mechanical method of mixing. Unlike ultrasonication, in this method, the suspensions are directly contacted with the mixer. High shear force is applied through a nozzle to generate high shear rate, by means of the rotor and stator. In this work, a high-performance dispersing instrument from IKA, UK, model T25 Ultra Turrax (Figure 4.4) was used to homogenizely mix the nanofluids. The device can disperse liquids for a maximum of 2000 ml. The homogenizer had a gap of 0.5 mm between the rotor and stator. The mixing speed ranges from 6500 to 24000 revolutions per minute which can provide a shear rate of 10 000 s^{-1} to 40 000 s^{-1}.

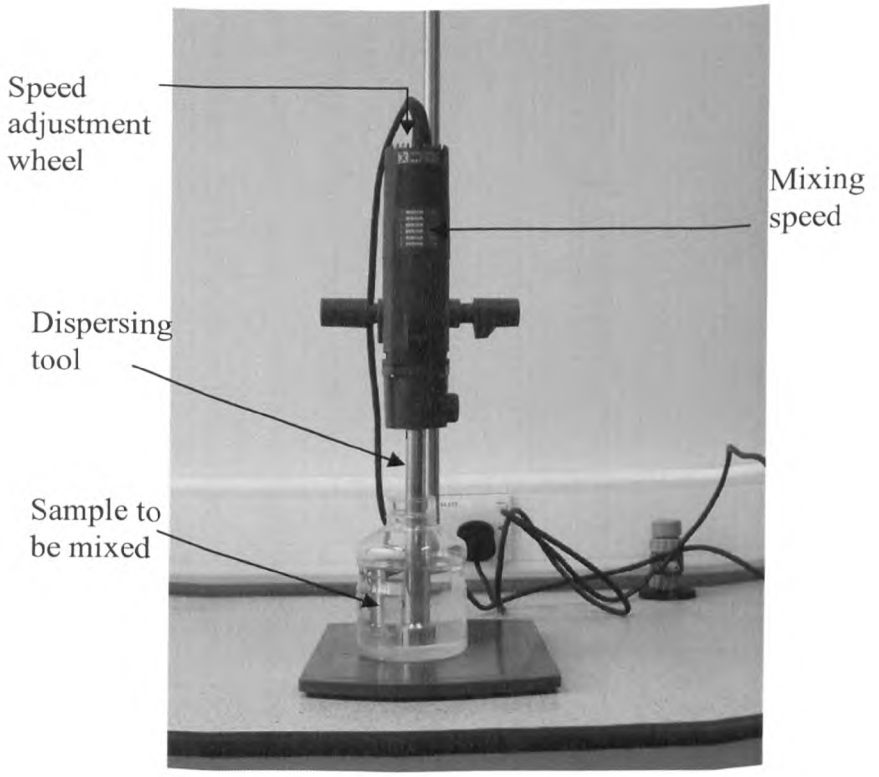

Figure 4.4: High shear mixer for CNTs nanofluids production.

4.3.3 Beads mill mixing

In beads mill mixing, the suspensions have a direct contact with the milling medium. In this method, the suspensions are mixed and agitated in the presence of small ceramics (YS2) beads. The nanoparticles are broken into smaller size by the high shear gradients and collisions with the beads. A large number of small beads will be more effective because of the increased collisions between the beads and the particles.

In this work, the beads mill, also called Dyno-Mill, is manufactured by W. A. Bachofen of Switzerland (Figure 4.5). It consists of a horizontal cylindrical container equipped with motor-driven shaft and impellers. The device can operate continuously. A specially designed agitator discs, mounted symmetrically on a shaft, transfer the energy required for dispersion to the spherical 0.1 mm zirconia grinding beads. An external pump feeds the product into the mill for continuous operation in a 0.6 liter grinding container. The jacketed chamber is cooled via an external chiller to keep the material at optimal temperatures. In this work, this equipment is specially used for TiO_2 nanofluids production. Nanofluids were pumped into the mixing chamber and recycle back into the mixer for continuous operation.

4.3.4 Electron microcopy

The morphology of different nanoparticles is different, which may contribute to the observed thermal behaviour. Thus characterization of the sample is needed. The Scanning Electron Microscopy (SEM) was used to give images of nanoparticle under

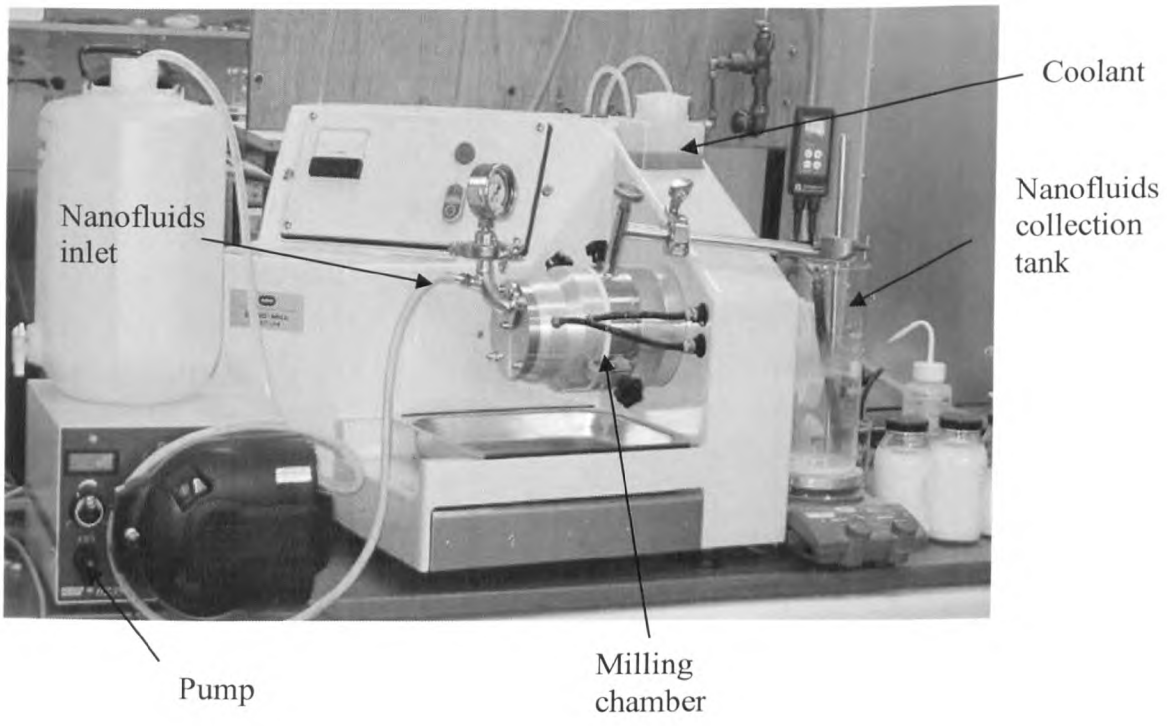

Figure 4.5: Beads mill for titanium dioxide nanofluids production.

study. The equipment used for this purpose is the FEGSEM Model Leo 1500 with a Philips Column and spatial resolution of 1.2 nm at 20 kV .

The SEM images can give the shape as well as the size of nanoparticles. From Figure 4.1, it can be seen that CNTs are entangled and the tubes are micrometers in length. Figure 4.2 shows that TiO_2 nanoparticles are spherical with primary particle size of 30-40 nm but form some degree of agglomerates even to the size of micrometers.

Transmission Electron Microscopy (TEM) images were also taken for some CNTs sample and for this purpose a TEM instrument Model Philips 2000 was used. It uses field emitter, operated at 200kV and fitted with a Gatan GIF 200 Imaging filter.

4.3.5 Thermal conductivity measurements

The instrument used to measure the thermal conductivity of nanofluids is the model KD2 from Labcell, Ltd, UK (Figure 4.6). It is a compact, portable meter which consists of a hand-held read out and a single-needle probe. The probe, having a dimension of 60-mm length and 1.28-mm diameter, is inserted into the medium that to be measured. The device measures thermal conductivity and thermal resistivity at the same time. Thermal resistivity is a measure of the ability of a material to impede the flow of heat, or in other words, thermal resistivity is the reciprocal of thermal conductivity. The operating environment is within a temperature from -20°C to 80°C.

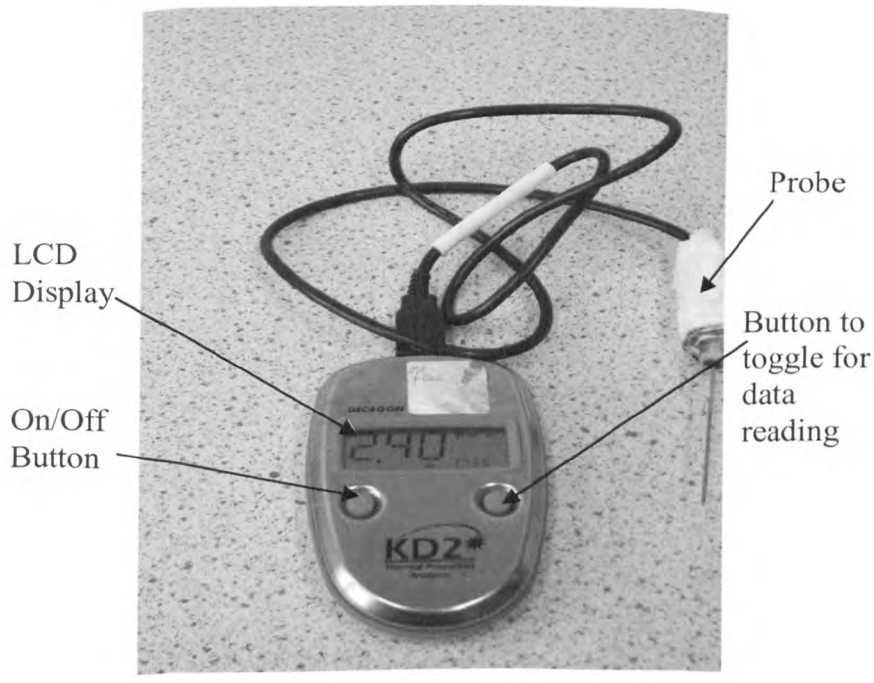

(a)

(b)

Figure 4.6: (a) Thermal conductivity device and (b) thermal conductivity measurement on sample.

The KD2 sensor needle contains both a heating element and a thermosistor. When a measurement is begun, the microcontroller waits for 30 seconds for temperature stability. Then a known amount of current is applied to a heater in the probe that has an accurately known resistance. The microprocessor calculates the amount of power supplied to the heater. The probe thermosistor then measures the changing temperature for 30 seconds while the microprocessor stores the data. It then monitors the rate of cooling for another 30 seconds. At the end of the reading, the controller computes the thermal conductivity using the change in temperature (ΔT) vs. time data. The thermal resistivity is calculated as the reciprocal of thermal conductivity. For multiple measurements, it is important to wait at least 5 minutes between readings. This is to allow enough time for the sample's temperature to equilibrate from the previous reading. For maintaining equilibrium temperature, the samples were placed in a water bath.

At least five measurements were taken for each data set at a given temperature to ensure the uncertainty of measurements within 5%. The device is calibrated using water as the reference materials. Five readings were taken at room temperature (k = 0.592, 0.604, 0.615, 0.622, 0.63 W/m·K)). This gives an average value of 0.6126 W/m·K. Comparing with the value given by the manufacturer (k_{water} = 0.61 W/m·K), this gives an error of ~0.5%.

The principle of the measurement is based on the radial heat conduction in a homogeneous, isotropic medium, given by

$$\frac{\partial T}{\partial t} = \kappa\left(\frac{\partial^2 T}{\partial r^2} + \frac{1}{r}\frac{\partial T}{\partial r}\right) \qquad \text{Eq. 4-1}$$

where T is temperature (°C), t is time (s), κ is thermal diffusivity(m^2/s), and r is radial distance (m). When a long, electrically heated probe is introduced into a medium (sample), the temperature will rise from an initial temperature T_0. Due to surrounding temperature, at some distance, r, within the probe, the temperature of the probe is

$$T - T_0 = \left(\frac{q}{4\pi k_m}\right) E_i\left(\frac{-r^2}{4\kappa t}\right) \qquad \text{Eq. 4-2}$$

where q is heat produced per unit length per unit time (W/m), k_m is the thermal conductivity of the medium (W/m·K), and E_i is the exponential integral function

$$-E_i(-a) = \int_a^{\infty}\left(\frac{1}{u}\right)\exp(-u)du = -\gamma - \ln\left(\frac{r^2}{4\kappa t}\right) + \frac{r^2}{4\kappa t} - \left(\frac{r^2}{8\kappa t}\right) + \ldots \qquad \text{Eq. 4- 3}$$

with $a = r^2/4\kappa t$ and γ is Euler's constant (0.5772…). When t is large, the second order term in Eq. 4-3 approaching zero and can be eliminated. Combining Eq.4-2 and Eq. 4-3 gives

$$T - T_0 = \left(\frac{q}{4\pi k_m}\right)\left(\ln(t) - \gamma - \ln\left(\frac{r^2}{4\kappa}\right)\right) \qquad \text{Eq. 4-4}$$

T-T_0 (ΔT) and $ln\ (t)$ in Eq. 4-4 can be linearly related ($y = mx+c$) with a slope $m=q/4\pi k_m$. From linear regression of (ΔT) on ln (t), the thermal conductivity can be obtained from

$$k_m = \frac{q}{4\pi m} \qquad \text{Eq. 4-5}$$

4.3.6 Rheology analysis

For rheological analysis purposes, a high resolution CVO 120 Bohlin Instruments rheometer from Malvern Instruments, UK was used. It is an integrated system consists of a rheometer, a temperature control unit, a coolant, compressed air and a computer for data acquisition system (Figure 4.7a). Many measuring systems can be used on the rheometer. For this research, a mooney cell was predominantly used as this applies to relatively homogeneous shear rate across the sample. The gap between the measuring system and the plate was set to 70 μm (Figure 4.7b). This geometry is excellent in preventing water loss due to evaporation during the experiments. A Bohlin V6.32.1 software accompanied this instruments for data analysis.

The measurement started with loading of sample into the lower measuring system. Sample of 2.5 ml was loaded into the measuring system for each test run. Then slowly lower the upper measuring system in placed by pressing the down arrow in the control panel. Then the test parameter was set up from the software. For this research, the viscometry test protocol was selected. The test setting was then determined which include the controlled mode, the temperature control mode, the equilibrium time, the delay time and the shear stress test range.

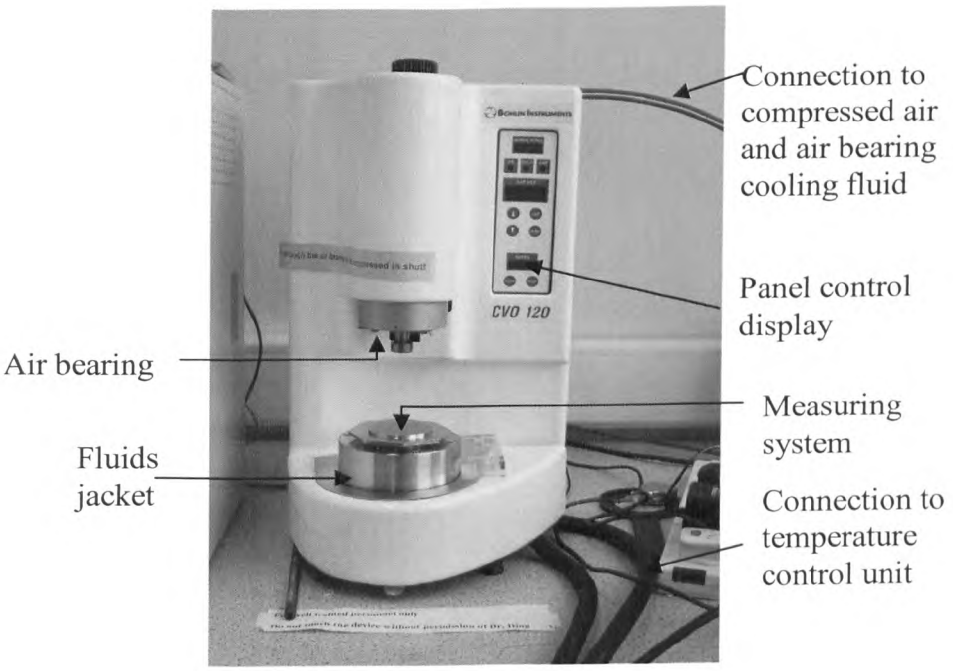

(a)

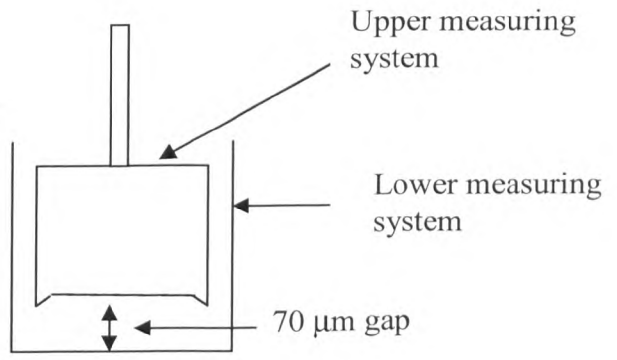

(b)

Figure 4.7: (a) CVO rheometer for rheological analysis and (b) the mooney cell measuring system

Measurements were taken in steady mode. The viscosity measurements were taken in a series of temperatures from 20°C to 40°C. By applying a controlled stress mode, the shear stress was increased systematically in a stepwise manner during the measurement. The samples were being held as each step (shear stress) for typically 120 seconds. The data were automatically generated by the software by recording the shear rate ($\dot{\gamma}$), viscosity (η) and the shear stress (σ).

Calibration of the rheometer was done by running a viscosity test of oil which is a Newtonian fluid. The actual viscosity of the oil is 1 Pa·s. Figure 4.8 shows the viscosity measurement of the oil and it shows that the data obtained from the rheometer was reliable with error estimate is less than 5%.

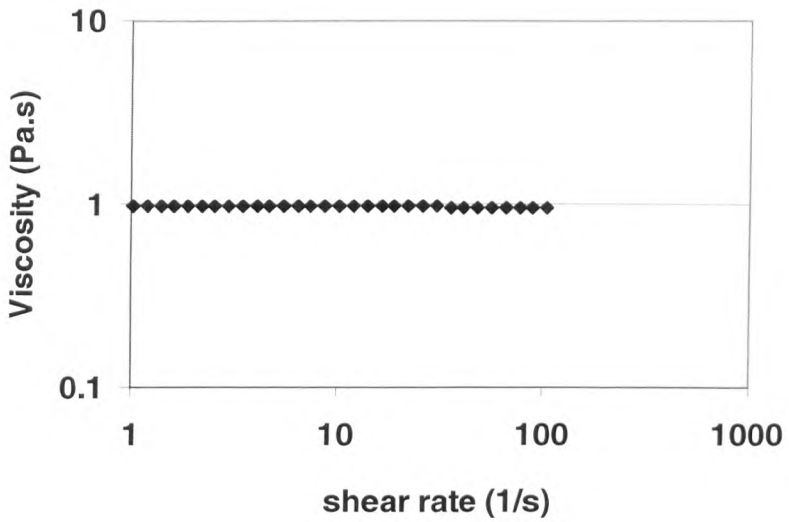

Figure 4.8: Calibration of rheometer using a Newtonian fluid.

4.3.7 Nanoparticle sizing

TiO_2 nanofluids particles size was measured using the Nanosizer ZS from Malvern Instruments, UK (Figure 4.9). The device is accompanied by Nanosizer software version 4.10. The instrument is capable of measuring particle size from 0.6 nm to 6 μm using Dynamic Light Scattering (DLS) method. DLS theory is a well established method for measuring small particle size. DLS measures Brownian motion and relates this to the size of particles. Brownian motion is the movement of particles due to the bombardment by the solvent molecules that surround them. The smaller the particle, the faster the Brownian motion will be. Smaller particles with less inertia are moved further by the solvent molecules and move more rapidly.

The Nanosizer ZS uses a monochromatic coherent He-Ne laser (4 mW) with a fixed wavelength of 633 nm as the source of light. The scattered light is detected by an avalanche photodiode at an angle of 173° and this is known as backscatter detection. The optics are not in contact with the sample. By using this detection, the laser does not have to travel through the entire sample and thus multiple scattering can be minimized. Fluctuations in the intensity of scattered light are converted to electrical pulses, which are fed into a correlator. The correlator then compares the intensity at a certain time intervals. An autocorrelation function will be generated which is passed to a computer where data analysis is performed. In the Nanosizer ZS software, the mean diameter (z-average) and the width distribution are obtained from cumulants analysis. The size distribution displayed is a plot of the relative intensity of light scattered by particles in various size. The plot is known as intensity distribution.

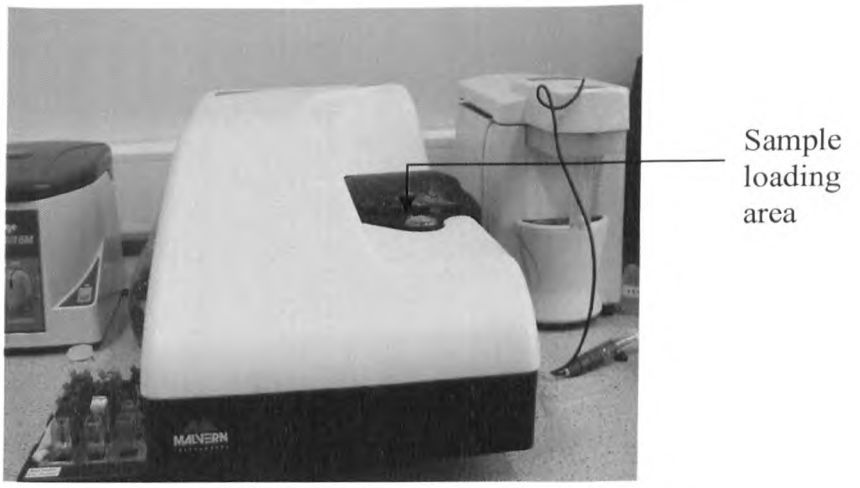

Figure 4.9: Nanosizer Zeta Series for particle size measurements.

4.3.8 Convective heat transfer experiment

The experimental system for measuring the convective heat transfer coefficient is similar to the one used by Wen and Ding (2004b), and is shown in Figure 4.10. It consisted of a flow loop, a heating unit, a cooling part, and a measuring and control unit. The flow loop included a pump with a built-in flowmeter, a reservoir, a collection tank and a test section. A horizontal copper tube with 970mm length, 4.5 ± 0.02mm inner diameter, and 6.4 ± 0.05mm outer diameter was used as the test section. The whole test section (copper tube) was heated by a flexible heater (Watlow, UK) linked to a DC power supply (TTi Ex 752m, RS, UK). The power supply was adjustable and had a maximum power of 300W. There was a thick thermal isolating layer surrounding the copper tube to reduce heat loss along the test section. Five T-type thermocouples were mounted on the test section at axial positions of 118 mm (T1), 285 mm (T2), 524 mm (T3), 662 mm (T4) and 782 mm (T5) from the inlet of the test section to measure the wall temperature distribution. An additional two T-type thermocouples were inserted in the flow at the inlet and outlet of the test section to measure the bulk temperature of the nanofluids. The pump (520S, Watson-Marlow) used in this work was of peristaltic type with flowrate controlled by the rotational rate. The maximum flowrate the pump could deliver was 3.5 liter/minute. There was a three-way valve in the flow loop for flowrate calibrations and flow system cleaning between runs using the same nanofluid. The schematic diagram of the experimental rig is shown in Figure 4.11.

Another experimental system was set up based on the same principle as in Figure 4.10. Instead of having a horizontal pipe, the other rig was set up vertically. The vertical pipe had a length of 184 cm for the test section, while other dimensions remain

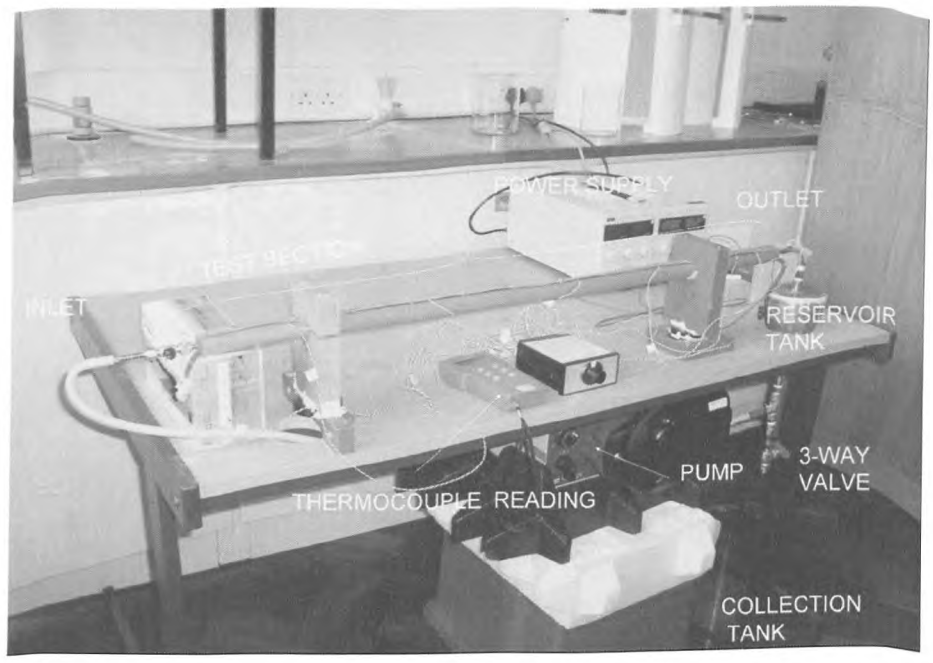

Figure 4.10: Convective heat transfer experimental rig.

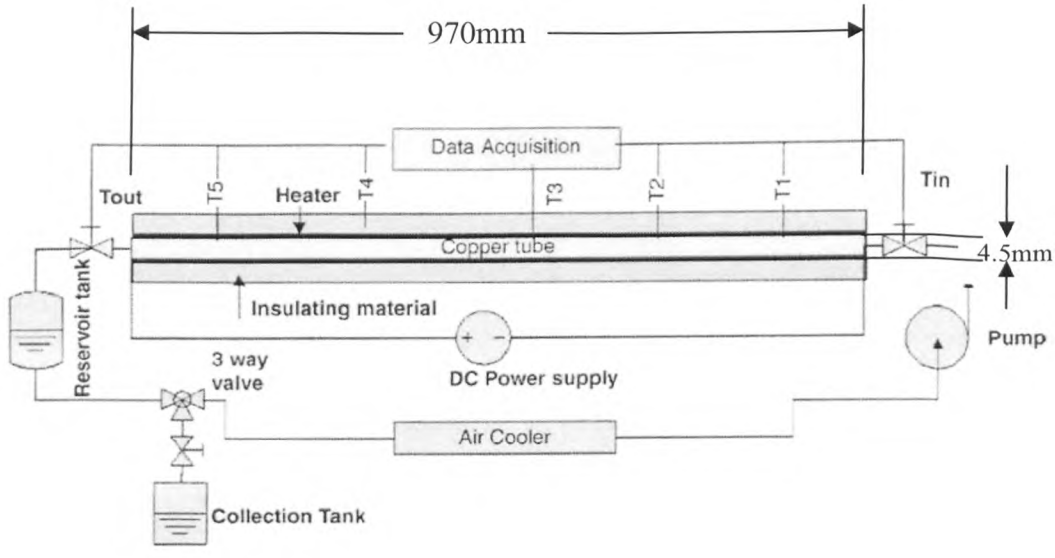

Figure 4.11: Schematic diagram of the convective heat transfer experimental rig.

the same. Seven T-type thermocouples were mounted on the test section at axial positions of 200 mm, 400 mm, 600 mm, 1000 mm, 1400 mm, 1600 mm, and 1800 mm from the inlet of the test section to measure the wall temperature distribution. An additional two T-type thermocouples were also inserted in the flow at the inlet and outlet of the test section to measure the bulk temperature of the nanofluids.

In the heat transfer experiments, the pump rotational rate, voltage and current of the DC power supply were recorded and the temperature readings from seven thermocouples were registered by a data acquisition system. As the pump performance was sensitive to the fluid viscosity at a given rotational speed, calibration was needed. The amount of nanofluids flowed in a time period of 1 minute was weighed before and after each experiment. This is to ensure that the same amount of nanofluids flowed through the test section during the experiments. This gives an accuracy of nanofluids flow rate better than 4.6%. The thermocouples were calibrated in a thermostat water bath and the accuracy was found to be within 0.1K.

4.4 Nanofluids formulation

Two different techniques were employed to formulate CNT-DW nanofluids and TiO_2-DW nanofluids.

4.4.1 CNT-DW nanofluids

Distilled water and multi-walled carbon nanotubes were used to produce nanofluids. The carbon nanotubes (CNTs) were provided by the Tsinghua Nafine

Nano-powder Commercialization Engineering Centre (China) and were used as received. They were produced catalytically from hydrocarbon materials on nano-catalyst under high pressures.

It is known that CNTs have a hydrophobic surface, which is prone to aggregation and precipitation in water in the absence of a dispersant or surfactant (Hilding, et. al, 2003; Zhang, 2004). Lots of effort were therefore made in the initial stage of the work, searching for an appropriate dispersant. Several samples of CNT nanofluids were produced with sodium laurate (SL), sodium dodecyl benzene sulfonate (SDBS) and gum arabic as the dispersants. All the suspensions were stored at the ambient temperature and checked periodically for visual changes. Photos of samples were taken using a digital camera. After a certain period of time, some suspensions were settled (Figure 4.12). Sample with gum arabic remained suspended after one month at stationary state. Therefore, gum arabic was chosen as the dispersant for CNTs nanofluids.

Then the optimum concentration of gum arabic was determined. CNTs nanofluids were produced with several compositions of gum arabic (0.1, 0.25, 0.5, 0.75, 1.0 wt %). From these series of experiments, it was observed that 0.25wt% gum arabic was the optimum concentration which gave the longest stable nanofluids. Summary of CNT-water nanofluids production is shown in a flowchart shown in Figure 4.13.

(i) (ii) (iii)

(a) Vials containing aqueous dispersion of multi-wall CNTs after homogeneously mixed. These samples were stored at stationary state. Dispersants used were (i) laurate salt, (ii) SDBS and (iii) gum arabic.

(i) (ii) (iii)

(b) Samples of CNTs after one month observation. Nanofluids with gum arabic remained suspended.

Figure 4.12: Samples of nanofluids using different dispersants (a) after mixing (b) after one month at stationary state.

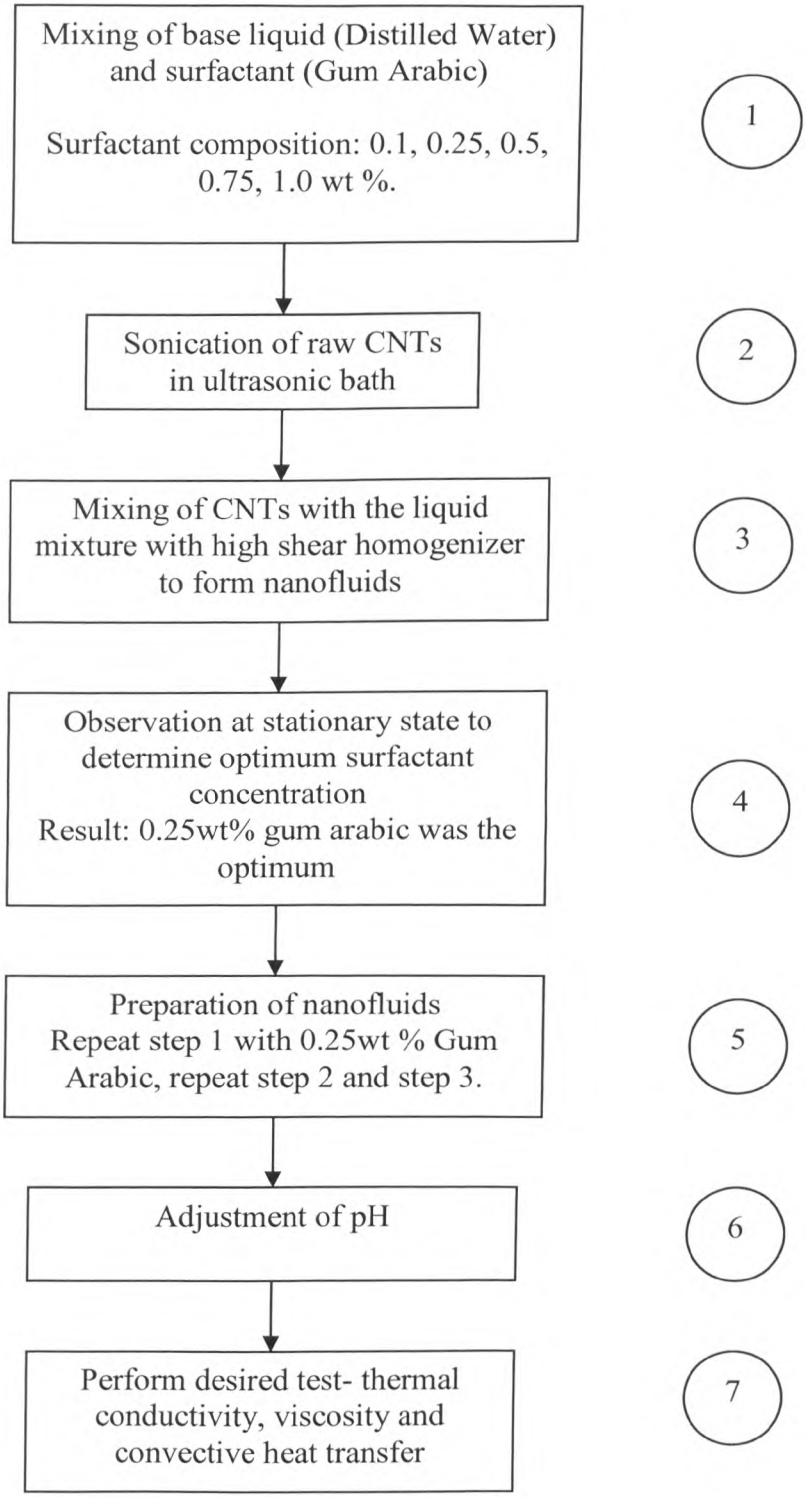

Figure 4.13: Flow chart of CNT-DW nanofluids formulation.

4.4.2 TiO_2-DW nanofluids

Milling technique was used to produce TiO_2 nanofluids system. 0.2 wt % of TiO_2 were added to distilled water. The stabilization was done using sodium hydroxide and the pH was manipulated to 11.00. The nanofluids were milled continuously for 1 hour. TiO_2 particle size was then determined using Nanosizer ZS. If the desired size had not achieved, the milling process was continued for further size reduction. Summary of TiO_2-water nanofluids formulation is shown in Figure 4.14. For TiO_2-DW nanofluids, electrostatic stabilization was employed to obtain stable suspension. Lower pH manipulation was not done because of the sensitivity of beads mill towards strong acid. The samples of TiO_2-DW nanofluids are shown in Figure 4.15. The size distribution of TiO_2 particles is shown in Figure 4.16. The size distribution obtained was based on the average of three measurements. The average diameters (Z-ave) are 90, 120, 180, and 570 nm.

After the formulation of nanofluids, other experiments were done which include thermal conductivity measurements, viscosity measurements and investigation of convective heat transfer. The experiments and test conditions are shown in Table 4.3.

4.5 Convective heat transfer data processing

The local convective heat transfer coefficient *(h)* is defined as

$$h(x) = \frac{q}{T_w(x) - T_f(x)} \qquad \text{Eq. 4-6}$$

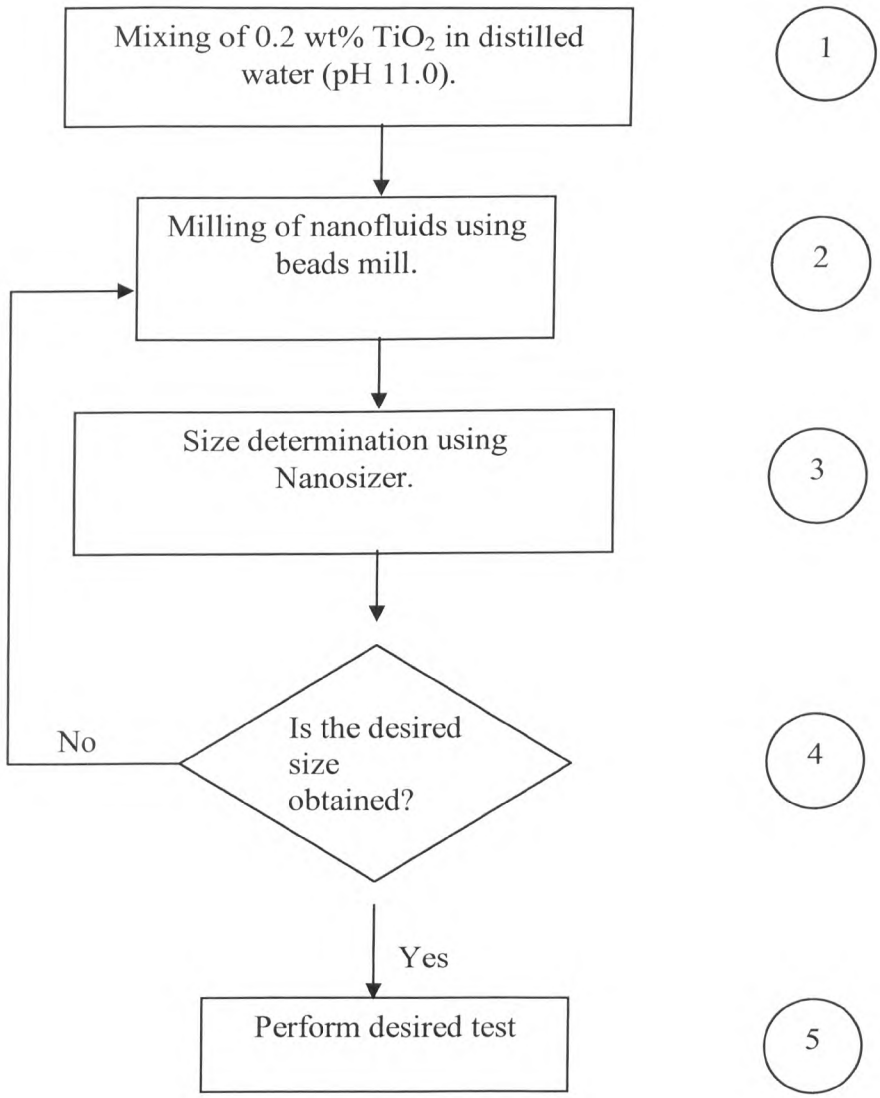

Figure 4.14: Flowchart of TiO_2-DW nanofluids formulation

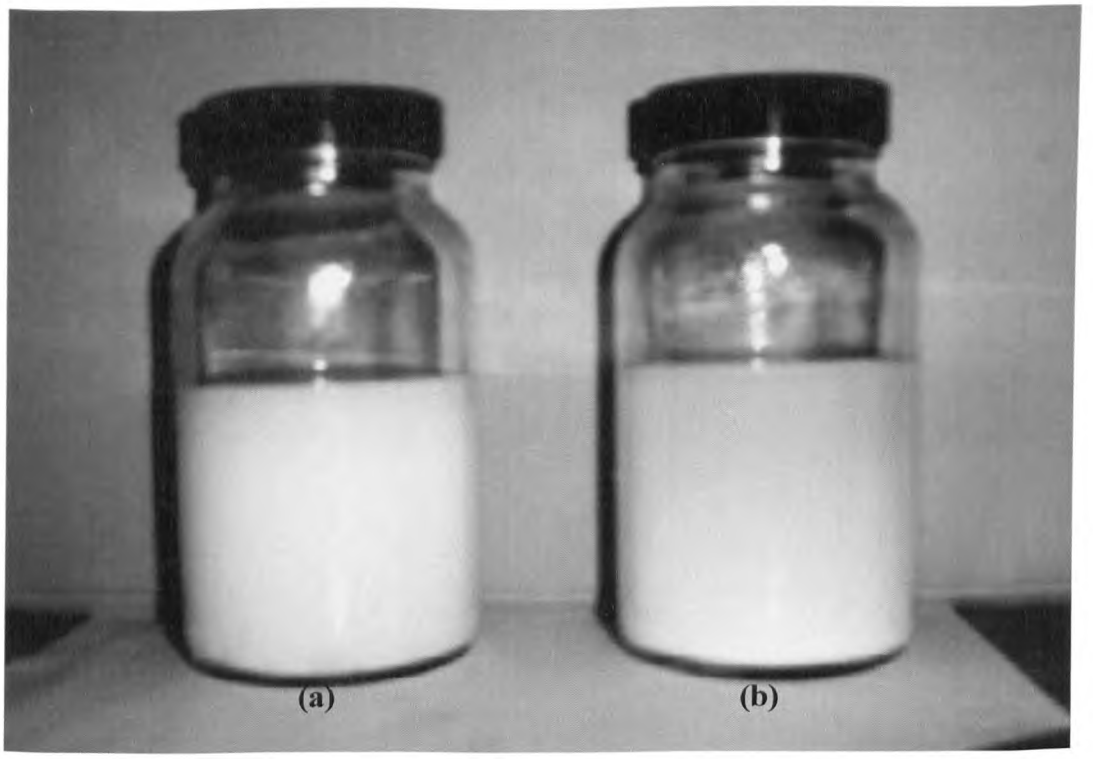

Figure 4.15: Vials containing TiO2-water nanofluids; (a) sample after milling (b) sample after a few months at stationary state.

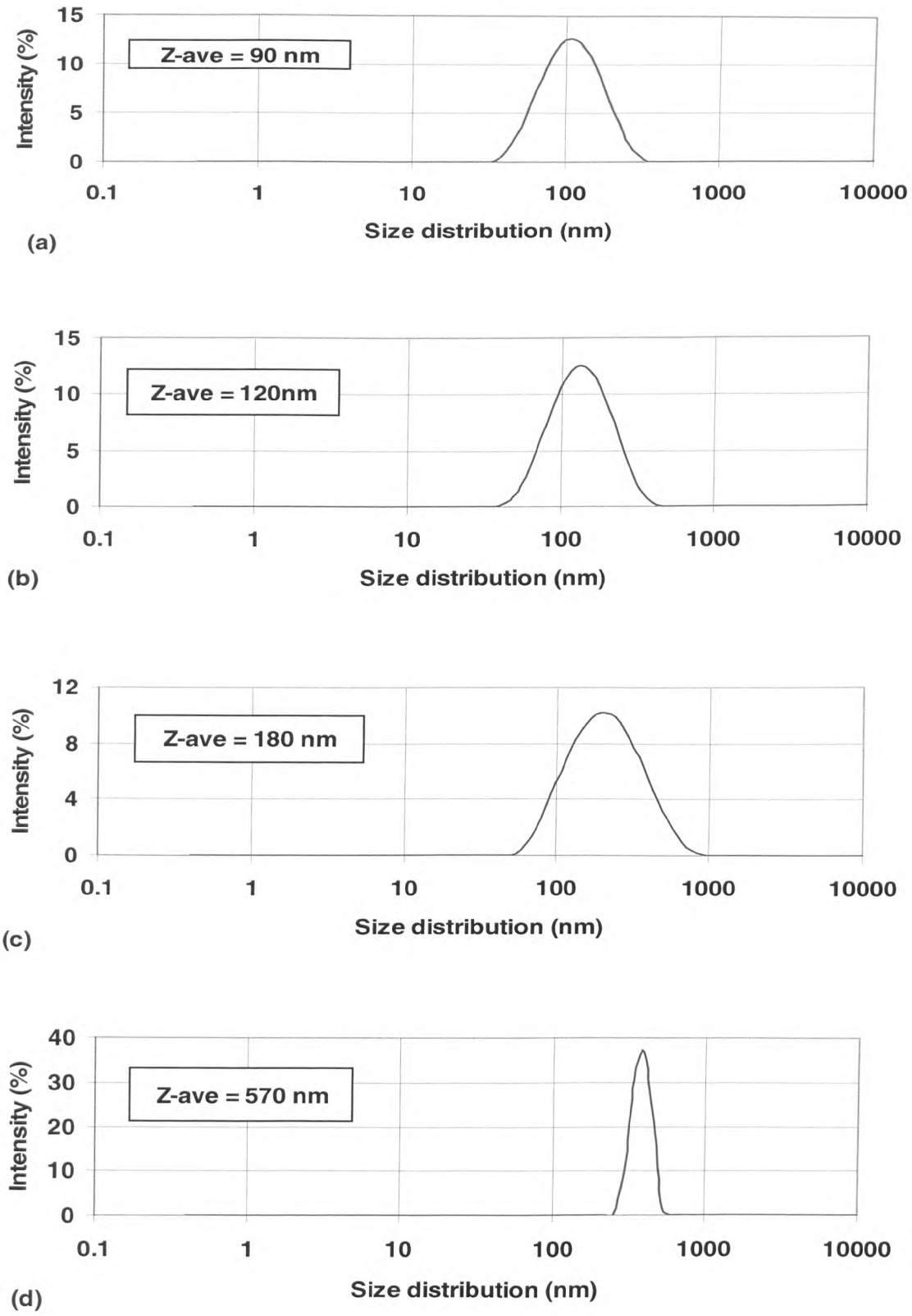

Figure 4.16: Size distribution of TiO2-water nanofluids based on intensity.

Measurements made using Zetasizer (Malvern Instruments).

Table 4.3: Experiments and test conditions.

Nanofluids	Concentration	Particle Size	pH	Surfactant/ Stabilizer	Thermal conductivity	Rheology Test	Convective heat transfer
CNTs-water	0.10wt.%, 0.25wt.%, 0.50wt.%	-	2.0, 6.0, 11.0	Gum Arabic, Acid Hydrochloric, Sodium Hydroxide	T =20°C, 25°C, 30°C	T = 25°C, 40°C	Re = 800, 1000, 1100, 1200
TiO_2-water	0.2wt%	90nm,120nm, 180nm, 570nm	11.0	Sodium Hydroxide	T= 20°C, 25°C, 28°C, 30°C	T = 25°C, 30°C	Re = 900, 1100, 2500,3500

where x represents axial distance from the entrance of the test section, q is the heat flux, T_w is the measured wall temperature and T_f is the fluid temperature decided by the following energy balance

$$T_f(x) = T_{in} + \frac{qSx}{\rho c_p uA} \qquad \text{Eq. 4-7}$$

where c_p is the heat capacity, ρ is the fluid density, A is the cross sectional area, S the perimeter of the test tube, and u is the average fluid velocity. Equation 4.7 is based on the assumption that the heat flux is uniform and zero heat loss through the insulation layer. The deviation to this assumption was assessed by comparing the measured temperature difference between the inlet and the outlet of the test section with the theoretical value calculated by Equation 4.7. It was found that the maximum deviation was lower than 6.2% under the conditions of this work. Equation 4.7 was also used to evaluate the performance of the test rig. This was done by taking the temperature of CNT nanofluids (T_f) after the test. The heat (q) obtained from Eq. 4-7 will then compared with the heat supplied from the heat source. An error estimation between 5-10% was observed.

The convective heat transfer coefficient, h, in Equation 4.6 is usually expressed in the form of Nusselt Number (Nu) as

$$Nu(x) = \frac{h(x)D}{k} \qquad \text{Eq. 4-8}$$

where D is the tube diameter and k is the fluid thermal conductivity. The Nusselts number is related to the Reynolds number defined as

$$Re = \frac{\rho uD}{\mu} \qquad \text{Eq. 4-9}$$

CHAPTER FIVE

HEAT TRANSFER OF AQUEOUS SUSPENSIONS OF CARBON NANTOTUBES (CNT NANOFLUIDS)

5.1 Introduction

This chapter will discuss the experimental work on the convective heat transfer of suspensions of carbon nanotubes (CNT nanofluids). There are several motivating factors that encourage the writer to study the phenomena. Since the production of CNTs is relatively still in a new era, thus, no previous studies have been found in the literature on the convective heat transfer of CNT nanofluids. However, there are some literatures that report the findings of high thermal conductivities of carbon nanotubes, ~3000W/m·K for multi-walled CNTs (Kim et. al, 2001) and ~6000W/m·K for single walled CNTs (Berber et. al, 2000). These finding, therefore, gives a great potential for significant heat transfer enhancement. Apart from that, there have been the inconsistencies in a few reported studies on the convective heat transfer using nanofluids (Pak and Cho, 1998; Xuan and Li, 2003; Yang et. al, 2005; Wen and Ding, 2004b) and for that reason a detail study is essential.

The experimental procedure and data processing method have been discussed in Chapter 4. Therefore, this chapter will focus only on the results and discussion of heat transfer study of CNTs. This chapter is organized in the following manner. Section 2 presents and discusses the results. And finally Section 3 summaries the main conclusions.

5.2 Results and Discussion

5.2.1 Effective thermal conductivity

Figure 5.1(a) shows the effective thermal conductivity of nanofluids as a function of CNTs concentration at three temperatures. The concentration of gum Arabic was 0.25 weight % with respect to water, which was found to give excellent stability to the CNT nanofluids. It can be seen that the effective thermal conductivity increases with increasing temperature and CNT concentration, with the dependence of the conductivity on temperature much more significant. At 20°C and 25°C, the dependence of the effective thermal conductivity levels off at CNT concentration greater than ~0.5 weight %, while this did not occur at 30°C and 35°C. The enhancement of the thermal conductivity, measured at room temperature, shown in Figure 4.4 is slightly higher than that reported by Assael et. al. (2003), Xie, et. al. (2003) and Wen and Ding (2004), but much lower than that reported by Choi et. al. (2001 and Choi et. al (2003). Figure 5.1(b) shows the thermal conductivity increased with increasing temperature and the dependence was nonlinear, a typical observation for CNT nanofluids (Choi et. al, 2001; Xie et. al, 20003; Wen and Ding, 2004).

The exact reason for this discrepancy is unclear but is believed to be associated with the thermal properties of CNTs used, liquid-CNT interfacial resistance, and the aspect ratio of CNTs used (Wen and Ding, 2004a; Wen and Ding, 2005). It should be noted that the base liquid used by Choi et. al. (2001) is oil, which has a much lower thermal conductivity than water; hence the absolute increase in conductivity is not huge.

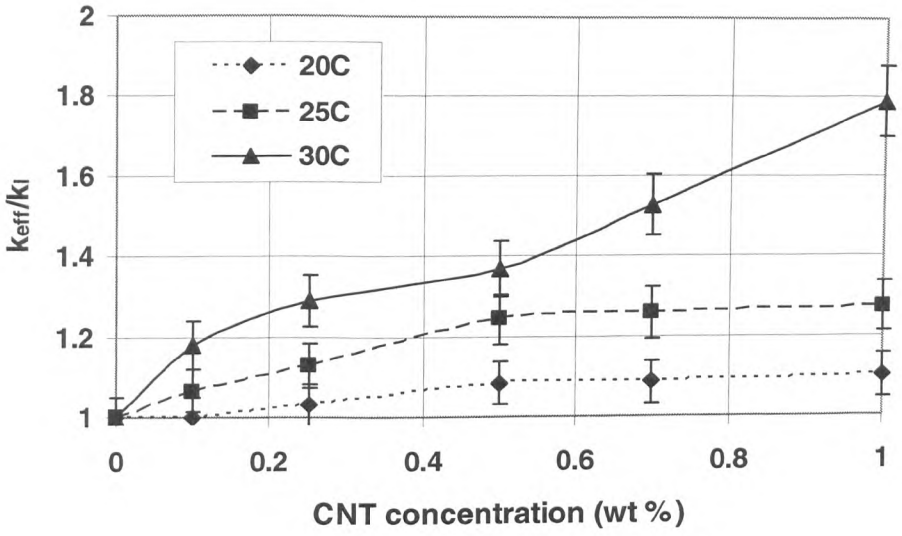

(a) The normalized effective thermal conductivity of CNT nanofluids as a function of concentration.

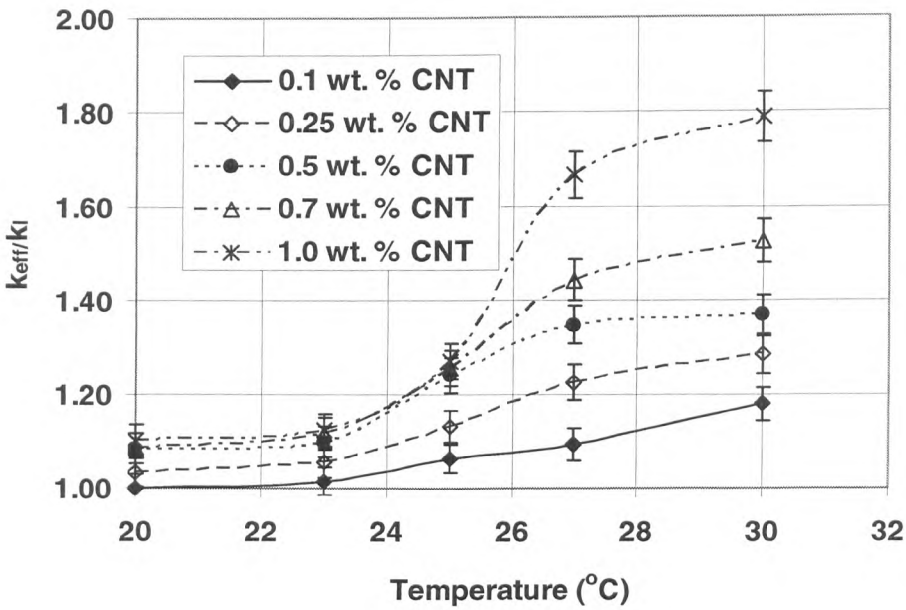

(b) The normalized effective thermal conductivity of CNT nanofluids as a function of temperature.

Figure 5.1: The effective thermal conductivity of CNT nanofluids under different conditions: gum arabic concentration of 0.25 wt.% with respect to water.

Interface thermal resistance can be expressed as the following;

$$q = -G\Delta T \qquad \text{Eq. 5-1}$$

where q is the heat flux, G is the Kapitza conductance and T is temperature. Through molecular modelling, Wen and Ding (2004) found that the presence of surfactant could impose a large thermal resistance to heat transfer. This is due to the phonon-phonon coupling that controlled the CNTs and surfactant molecules. Energy is transferred from high –frequency phonon modes within the CNTs to low frequency modes through the phonon-phonon coupling before being exchanged with the surrounding medium. From this finding, it can be concluded that the lower effective thermal conductivity of CNT nanofluids, in the present work, may partially be due to the phonon-phonon coupling of gum arabic-CNTs.

Zhou and Gao (2006) studied the effective thermal conductivity of non-spherical particles with interfacial thermal resistance. They found that the effective thermal conductivity enhancement was much higher for inclusion that possesses high aspect ratio (cylinder or disk). With this argument, it is expected that the effective thermal conductivity of CNT nanofluids is much higher than that of spherical particles. Differential effective medium theory was used to predict the effective thermal conductivity of CNTs nanofluids. The model was compared with experimental results of CNT-oil nanofluids (Choi et. al, 2001) and CNT-decene nanofluids (Xie et. al, 2003). Note that the aspect ratio in both cases was ~2000 and the thermal conductivity of the base liquid was almost the same, 0.1448 W/m·K and 0.14 W/m·K for oil and decene respectively. Therefore the large discrepancy of these results may results from the different interfacial thermal resistance. The interfacial thermal resistance of, $R_{CNT\text{-}oil}$ =

$1x10^{-8}$ $m^2 \cdot K/W$ and $R_{CNT\text{-}decene} = 4.2 \times 10^{-7}$ $m^2 \cdot K/W$ was estimated for CNT-oil and CNT-decene respectively.

The interfacial resistance is strongly dependent on the type of bonding between the solid and the liquid (Xue et. al, 2003). They found that the solid-liquid bonding can be categories in two regimes; i) the non-wetting region (weak bonding) and ii) the wetting regime (strong bonding). Based on molecular dynamics simulations, they found that there is always a repulsion that preventing the overlaps of the atoms regardless of how small is the solid-liquid interactions. With this argument, even without any solid-liquid attraction, there is still energy transfer from the liquid to the solid. This implies that there is a finite interfacial thermal resistance.

5.2.2 Viscosity of nanofluids

The viscosity of CNT nanofluids as a function of shear rate was measured under various conditions. Shear rate is the rate of change of velocity at which one layer of fluid passes over an adjacent layer. Shown in Figure 5.2 are results for two different temperatures and pH = 6.0 (a) and 11.0 (b). A clear shear thinning behaviour is seen under all conditions. At a given shear rate, the viscosity of nanofluids increases with increasing CNT concentration and decreasing temperature. The shear thinning behaviour was also observed by Kinloch et. al. (2002) for which highly concentrated aqueous suspensions of multi-walled carbon nanotubes were studied. The dispersion also exhibit shear thinning behaviour in steady shear measurement. Yang et. al. (2005) and Yang et. al. (2006) also reported that CNT nanofluids shear thinned with increasing shear rates.

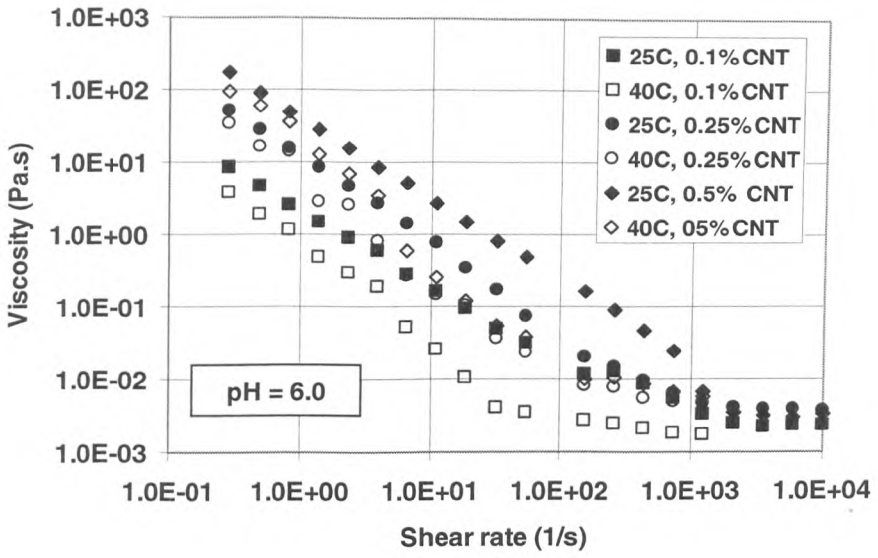

(a) Viscosity of CNT nanofluids (pH = 6.0) at 25°C and 40°C.

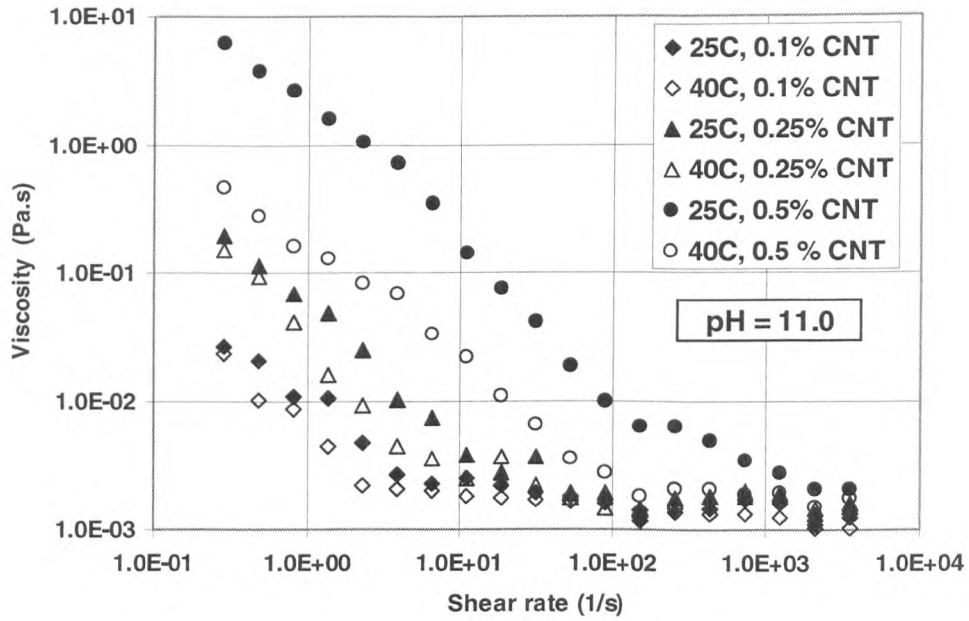

(b) Viscosity of CNT nanofluids (pH = 11.0)

Figure 5.2: Viscosity as a function of shear rate at 25°C and 40C °for CNT nanofluids: (a) at pH = 6.0 and (b) at pH = 11.0.

Furthermore, Yang et. al. (2006) reported that addition of polyisobutene succinimide, as the dispersant, reduced the viscosity from ($5x10^5$ Pa·s) at low stress (0.1 Pa) to < 0.5 Pa·s at a stress of 0.07Pa.

The results shown in Figure 5.2 have very important implication to CNT nanofluids flowing through the tubular geometry used in this work as the shear rate at the wall region is higher than that at the core region, hence lower viscosity at the wall region and better lubrication effect. The results also bear important implications to heat transfer as the heat transfer coefficient depends on the flow behaviour. More discussions will be made in Section 5.2.3.

The viscosity of pure water is shown in Figure 5.3(a). It is clearly shows that the viscosity of CNT nanofluids is much higher than that of water. There may be doubts that the shear thinning behaviour is due to the presence of gum arabic dispersant. A few rheological experiments were therefore carried out on gum arabic solutions. The results are illustrated in Figure 5.3, which clearly shows the shear thinning behaviour at low shear rate but slightly shear thickening is seen at shear rates greater than ~200 s^{-1}. A comparison of Figure 5.2 and Figure 5.3 shows that, at low shear rates the viscosity of gum arabic solutions is several orders of magnitude lower than that of the CNT nanofluids. The gap is narrowed down at high shear rates but the difference is still several-folds. This suggests that the presence of gum arabic affects little on the viscosity of CNT nanofluids at low shear rates but may play a role at high shear rates. Further discussion will be made in Section 5.2.3.

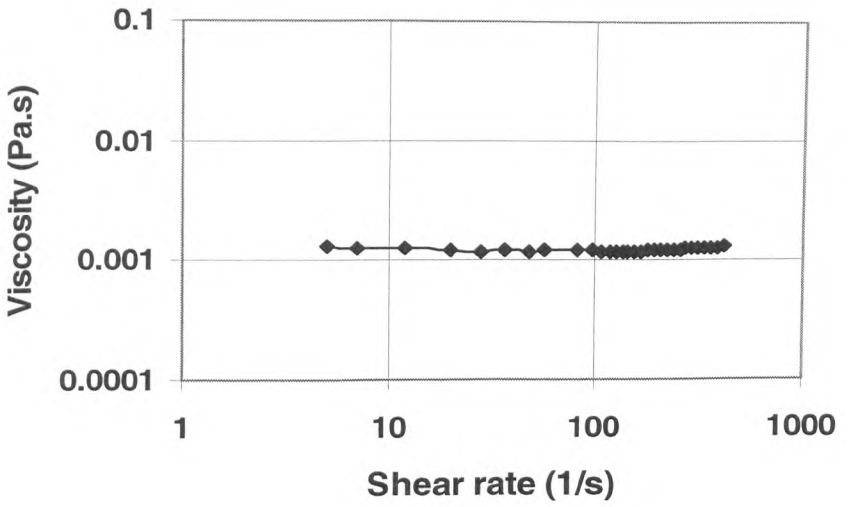

(a) Viscosity of pure water at 25°C.

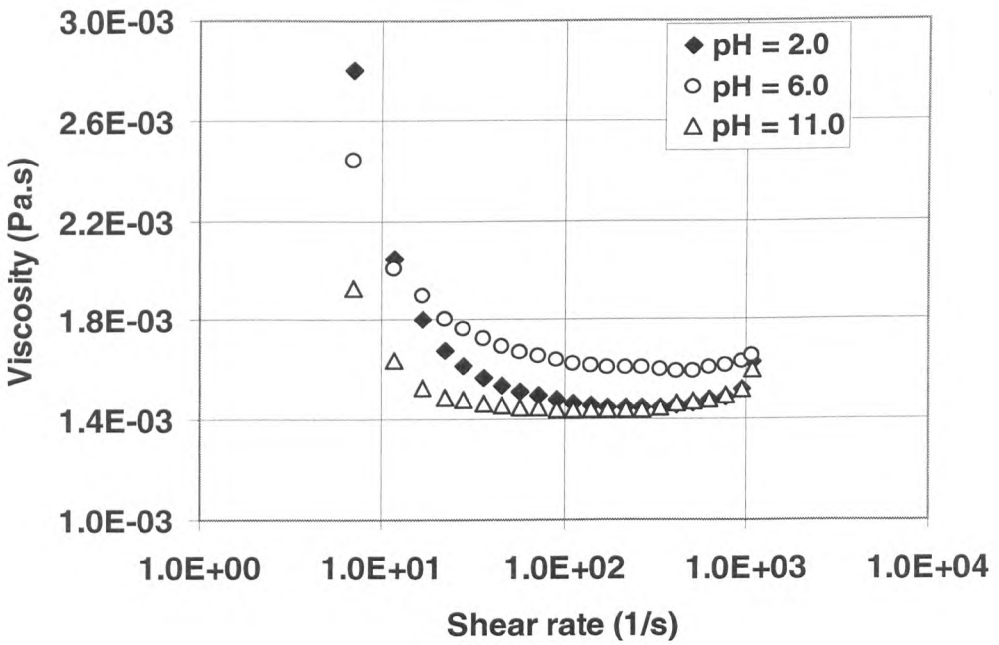

(b) Viscosity of gum arabic-water solution at 25°C.

Figure 5.3: Viscosity of pure water and gum arabic-water solution at 25°C.

5.2.3 Convective heat transfer coefficient

5.2.3.1 Convective heat transfer coefficient of pure water

Before conducting systematic experiments with CNT nanofluids, the reliability and accuracy of the experimental system were tested using distilled water as the working fluid. The results are shown in Figure 5.4, together with predictions of the following well-known Shah equation for laminar flow under the constant heat flux boundary (Shah, 1975);

$$Nu = \begin{cases} 1.953\left(RePr\frac{D}{x}\right)^{1/3} & \left(RePr\frac{D}{x}\right) \geq 33.3 \\ 4.364 + 0.07722RePr\frac{D}{x} & \left(RePr\frac{D}{x}\right) < 33.3 \end{cases} \qquad \text{Eq. 5-2}$$

The Nusselt Number is between 2.0 – 14.0 for both Reynolds Number of 850 and 1100, thus the values are reasonable for flow in the laminar regime. Reasonably good agreement has been achieved between the Shah equation and the measurements over the Reynolds Number range used in this work.

5.2.3.2 Convective heat transfer coefficient of CNT nanofluids

Having established confidence in the experimental system, systematic experiments were performed at different flow conditions (Reynolds numbers), different CNT concentrations and pH levels. The results are presented and discussed in this sub-section.

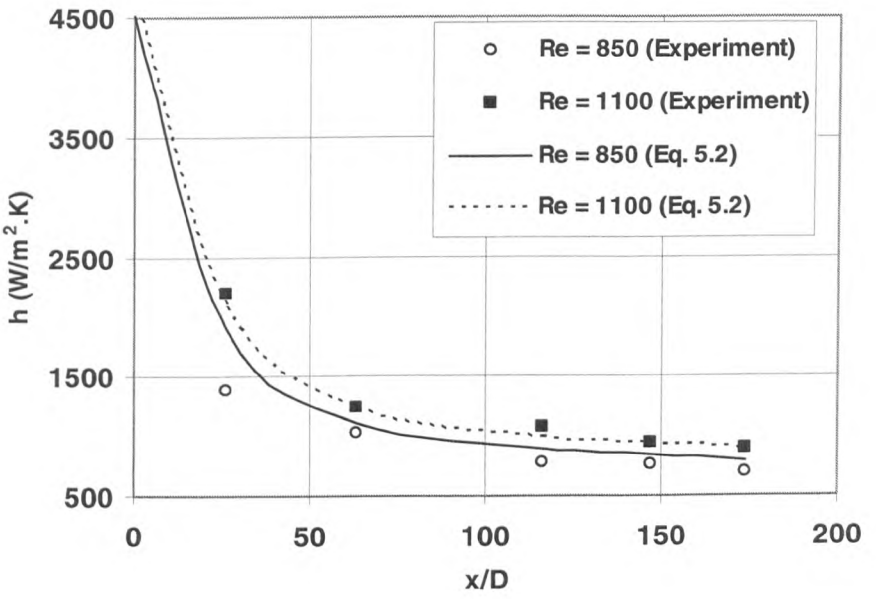

Figure 5.4: Initial test of the experiment rig using distilled water.

As the viscosity is not well defined due to non uniform shear rate across the pipe cross section, the Reynolds number is calculated based on viscosity of the host liquid at zero-shear rate. However, it may be possible to use an alternative non- dimensionless group based on non-Newtonian models for the viscosity to replace the Reynolds number as described above.

5.2.3.2.1 Effect of CNT concentration on the convective heat transfer

Figure 5.5(a) shows the effect of CNT concentration on the local heat transfer coefficient at various axial distances from the entrance of the test section at $Re = 800 \pm 50$ and pH = 6.0. Also included in the figure are results of pure distilled water and gum arabic-water solution for comparison purposes. Figure 5.5(b) shows the enhancement of the heat transfer coefficient, with reference to pure distilled water, as a function of axial distance at different CNT concentrations. The following observations can be made from the two figures:

- The presence of gum arabic only gives a marginal enhancement on the heat transfer performance at $x/D <\sim 100$, but the enhancement approaches to zero at $x/D >\sim 100$ (Figures 5.5a and 5.5b).

- At a given CNT concentration, the heat transfer coefficient decreases with axial distance (Figure 5.5a). This is as expected for heat transfer in the entrance region..

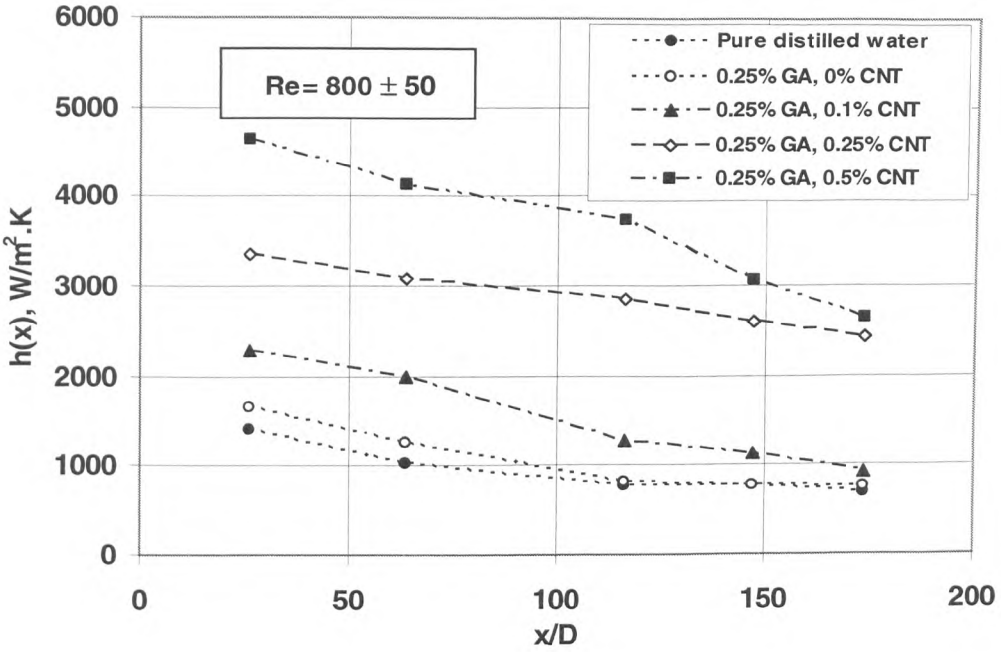

(a)

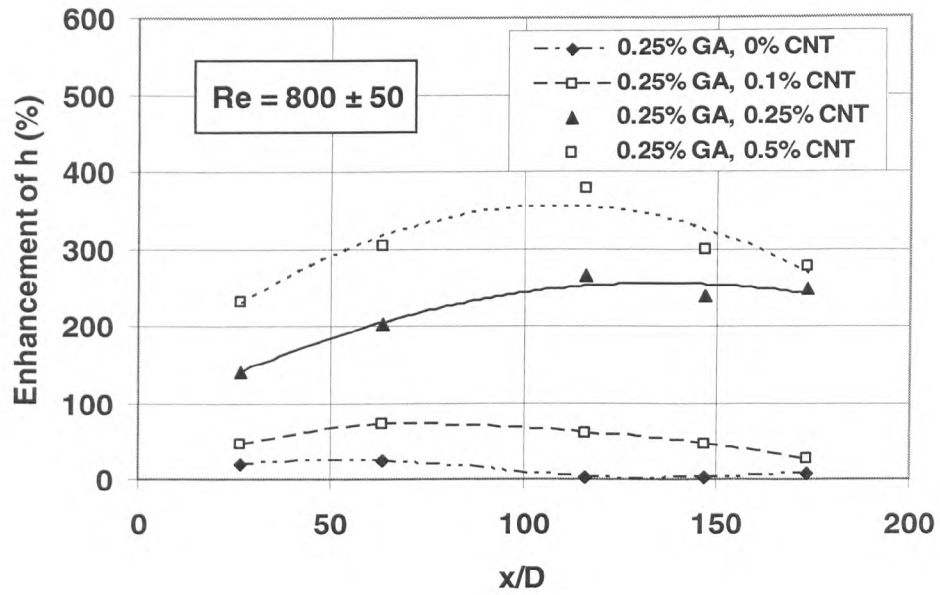

(b)

Figure 5.5 Axial profile of heat transfer coefficient (a) and enhancement of heat transfer coefficient (b) for different CNT concentrations (pH = 6.0) at *Re* ~ 800.

- The enhancement of heat transfer coefficient increases with x/D initially, reaches a maximum at a value of x/D depending on CNT concentration, and then decreases with a further increase in x/D. The value of x/D at which the enhancement is maximum increases with CNT concentration (Figure 5.5).

Figure 5.6 (a) shows the effect of CNT concentration on the local heat transfer coefficient at various axial distances from the entrance of the test section at Re = 1100 and pH = 6.0. The results of water and gum arabic are also included. Figure 5.6 (b) shows the enhancement of the heat transfer coefficient, with reference to pure distilled water, as a function of axial distance at different CNT concentrations. The same observation was seen for the heat transfer coefficient. However, for higher Reynolds Number, the enhancement of heat transfer coefficient reached a maximum value at the same x/D of ~63.3. Several conclusions can be drawn based on Figure 5.5 and Figure 5.6:

- The presence of carbon nanotubes increases the convective heat transfer coefficient significantly, and the increase is more considerable at high CNT concentrations (Figure 5.5).

- The enhancement of heat transfer coefficient increases with increasing Reynolds Number.

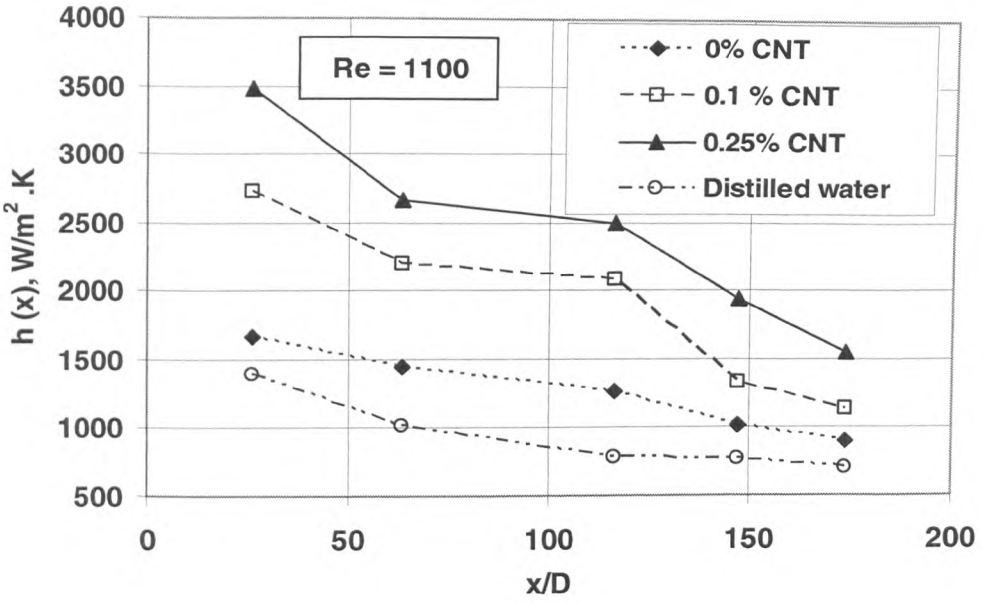

(a)

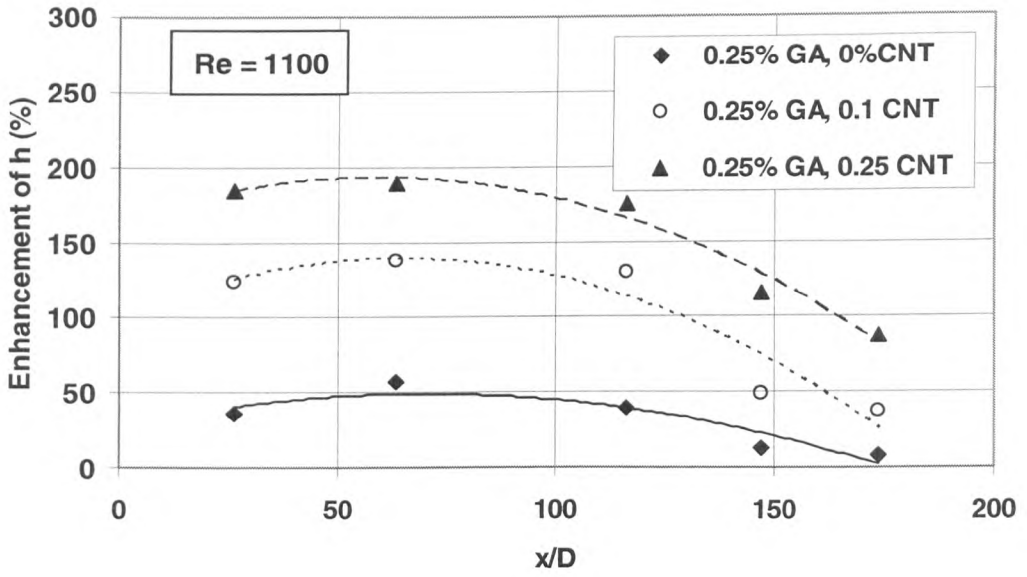

(b)

Figure 5.6 Axial profile of heat transfer coefficient (a) and enhancement of heat transfer coefficient (b) for different CNT concentrations (pH = 6.0) at *Re* = 1100.

- A discrepancy was observed for CNT concentration of 0.25% where higher enhancement was observed for $Re \sim 800$. This may result from particle migration effect, which will be discussed later.

Nevertheless, Figures 5.5 and 5.6 suggest a possible smart measure to keep the high heat transfer coefficient - creation of many 'artificial entrance' regions along a pipeline. The use of artificial length will inevitably increase the pressure drop hence optimisation is needed. A comparison of Figure 5.5 and Figure 5.6 with Figure 5.1 indicates that the enhancement of the convective heat transfer coefficient is much more dramatic than that purely due to the enhancement of effective thermal conductivity. A similar trend but with less significant enhancement was also observed by Xuan and Li (2003) in the turbulent flow regime and Wen and Ding (2004b) at the entrance region in the laminar flow regime. Xuan and Li (2003) showed that the heat transfer coefficient was increased by ~60% for an aqueous based nanofluid containing 2% Cu nanoparticles by volume, but the nanofluid only had an effective thermal conductivity approximately 12.5% higher than that of the base liquid. Wen and Ding (2004b) investigated heat transfer of aqueous γ-alumina nanofluids and observed a ~ 47% increase in the convective heat transfer coefficient at x/D~60 for 1.6 vol. % nanoparticle loading and $Re = 1600$, which was much greater than that due to the enhancement of thermal conduction (~10%). More discussion on this will be made later.

5.2.3.2.2 Effects of Reynolds number on the convective heat transfer

Figure 5.7(a) shows the effect of the Reynolds number, which clearly indicates that the heat transfer coefficient increases with increasing Reynolds number. There is a large difference between the heat transfer coefficient at Re = 1200 and that at Re <~ 1100, which will be discussed further in the following. Figure 5.5(b) shows the enhancement of the heat transfer coefficient with reference to pure water. It can be seen that the heat transfer enhancement increases with increasing Reynolds number at Re = 1000-1200, but a more complex case occurs at Re = 800. At x/D <~ 110, the enhancement for Re = 800 is higher than that for Re = 1000 and 1100, but this is reversed at x/D >~ 110. To identify how the heat transfer enhancement changes with Reynolds number, the data shown in Figure 5.7(b) are presented in a different format in Figure 5.8. It is seen that the effect of Reynolds number is small at Re <~ 1100 but a big increase occurs when the Reynolds number becomes greater than 1100. The reason for this requires further investigation, but the effect of shear rate on the viscosity could be a reason. At Re = 1100, the shear rate at the wall is approximately 500 s^{-1}, which corresponds to the transition from the strong shear thinning region to the region with approximately constant viscosity.

It is recognised that measurements of pressure drop across the tube length under different conditions could provide some information for relating directly the observed heat transfer behaviour to the flow behaviour. As shown in Figure 5.9, the pressure drop along the pipe was low and can be negligible in this work.

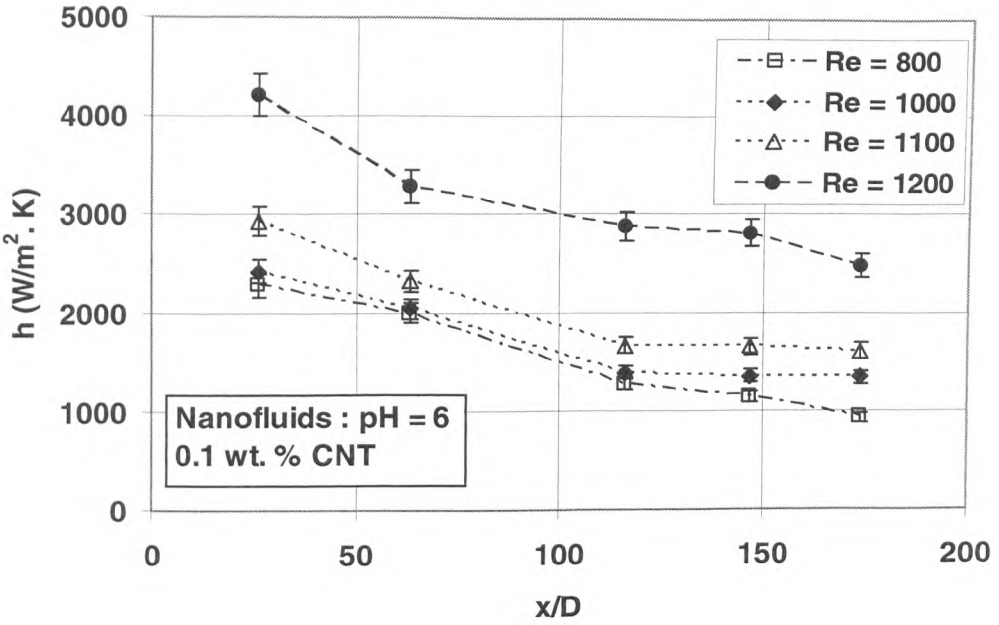

(a)

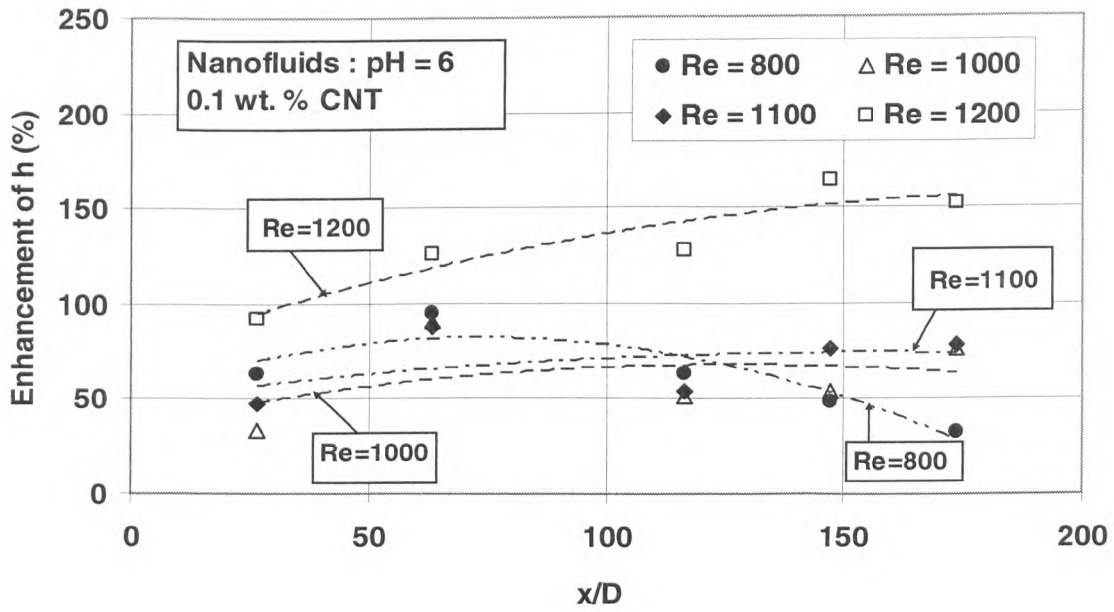

(b)

Figure 5.7: Effect of Reynolds number on the convective heat transfer coefficient (a) and heat transfer enhancement (b) for 0.1 wt.% CNT at pH = 6.0.

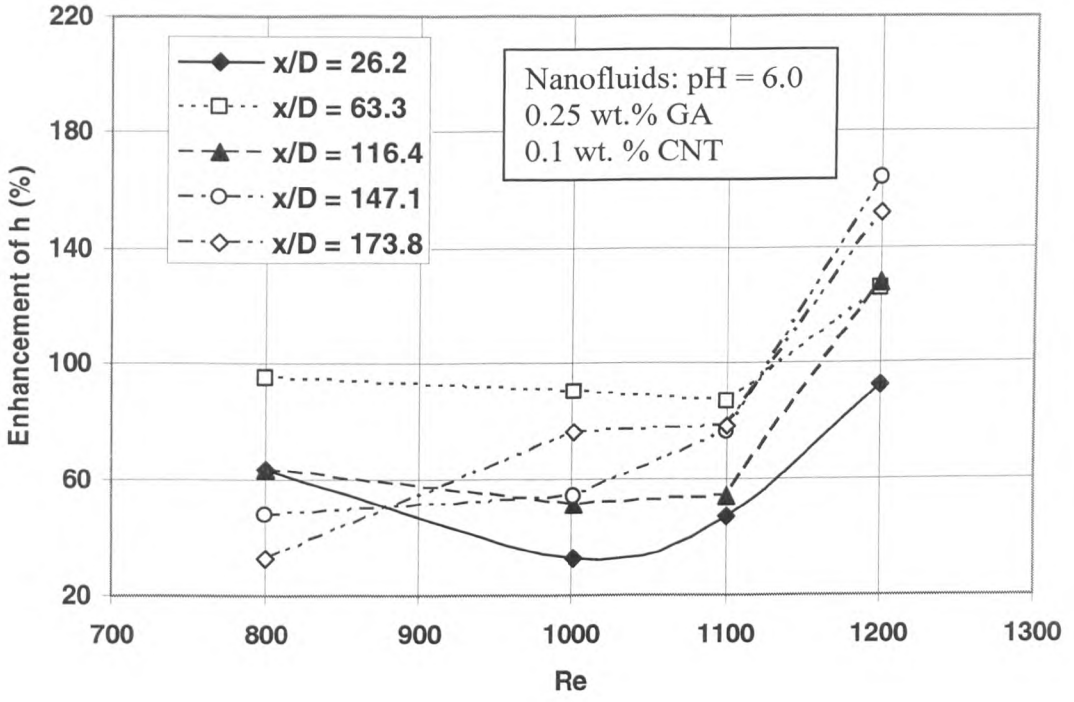

Figure 5.8: Enhancement of heat transfer coefficient as a function of Reynolds number at a different axial positions

5.2.3.2.3 Effect of pH on the convective heat transfer

Figure 5.10 compares the axial profiles, at two Reynolds numbers, of the convective heat transfer coefficient under two pH conditions. The convective heat transfer coefficient at pH = 6 is slightly higher than that at pH = 10.5. It is unclear if the effect of pH is actually very small under other pH conditions. If the small effect of pH is proven, excellent opportunities will be provided for future industrial taking-up of the technology as both very acidic and alkaline suspensions would increase both the capital and operating costs and also have significant safety implications.

5.2.3.2.4 Mechanisms of heat transfer enhancement

The heat transfer coefficient, h, is a macroscopic parameter describing heat transfer when a fluid flowing across a solid surface of different temperature. It is not a material property but can be approximately given by k/δ_t with δ_t the thickness of thermal boundary layer. At the entrance (x/D = 0), the theoretical boundary layer thickness is zero, hence the heat transfer coefficient approaches infinity. The boundary layer increases with axial distance until fully developed after which the boundary layer thickness and hence the convective heat transfer coefficient is constant. The above simple argument addresses the problem qualitatively and does not give much insight into the mechanisms for the observed large heat transfer enhancement. However, it does provide a starting point for looking at possible underlying mechanisms.

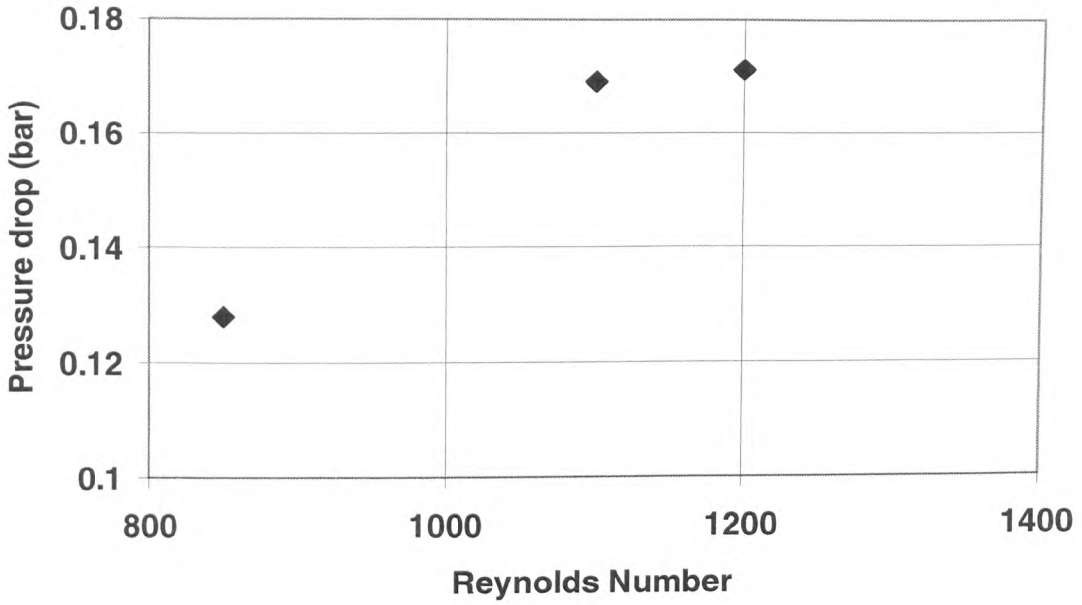

Figure 5.9: Pressure drop of 0.1 wt.% CNT nanofluids in the pipe for various Reynolds Number.

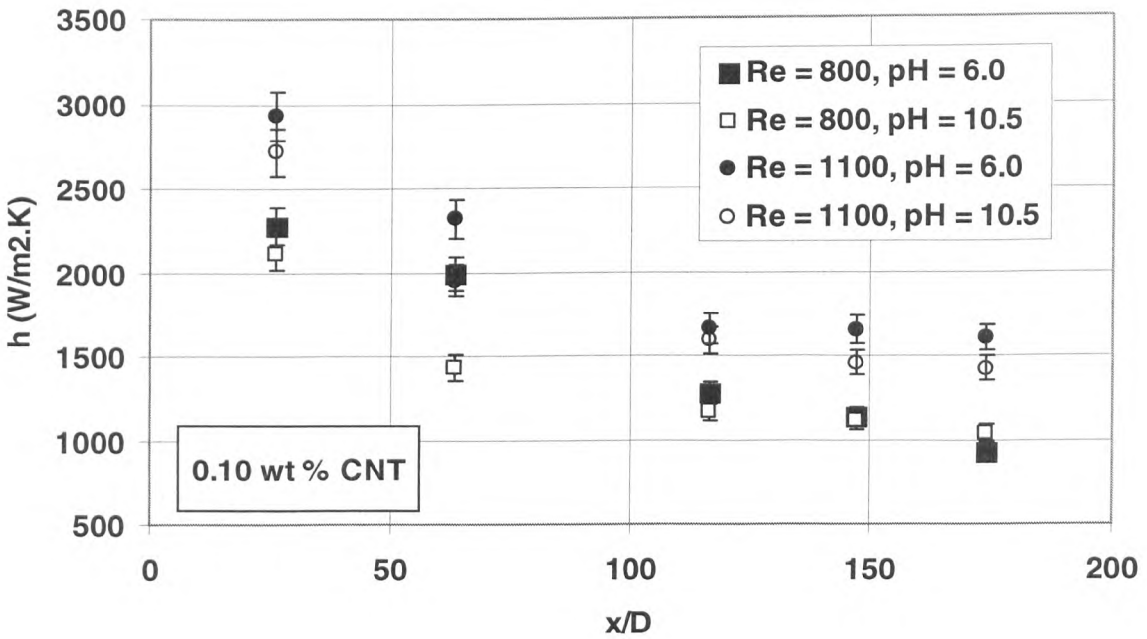

Figure 5.10: Effect of pH on the convective heat transfer.

The above simplified theory suggests that both an increase in k and/or a decrease in δ_t increase the convective heat transfer coefficient. As can be seen from Figure 5.1, the maximum enhancement of the thermal conductivity under the conditions of the convective heat transfer experiments in this work does not exceed 18% for 0.1% CNT nanofluids and 37% for 0.5% CNT nanofluids. The enhancement of the convective heat transfer coefficient, however, is much greater than that due to the increase in the thermal conductivity, particularly at high CNT concentrations and high Reynolds numbers; see Figures 5.5-5.10. One may therefore simply attribute the large enhancement purely to a decrease in the thermal boundary layer thickness. No doubt, the reduction in the thermal boundary layer thickness could be an important factor, but further enhancement on the thermal conduction under dynamic conditions could be another important factor. The effective thermal conductivity shown in Figure 5.1 was obtained under the static conditions, whereas significant shear exists under the conditions of the convective heat transfer experiments. In this research, the effective thermal conductivity is defined as the ratio of the thermal conductivity of nanofluid over the thermal conductivity of the base liquid. As shown in Figure 5.2, CNT nanofluids exhibit a significant shear thinning behaviour, the effective thermal conductivity under dynamic shear conditions may therefore be much higher than that shown in Figure 5.1. Such behaviour has indeed been observed previously by Sohn and Chen (1981) who measured the effective thermal conductivity in a rotating Couette flow apparatus at low Reynolds number but high Peclet number conditions, where the Peclet number is defined as $\dot{\gamma} \cdot d_p^2 / v$ with $\dot{\gamma}$ is the shear rate, and d_p is the particle diameter. Significant enhancement on effective thermal conductivity was observed at Peclet numbers over 300, and the shear-dependent behaviour fitted well into a power law relationship. A similar trend was also reported by Ahuja (1975), who

used a shell-and-tube heat exchanging arrangement, and employed the Graetz solutions at the entrance region to evaluate the effective thermal conductivity of a saline / polystyrene latex suspension. These researchers attributed the enhancement to the high Peclet number, which represents a measure of the eddy scale convection as compared to conduction, and therefore is associated with self-rotating and/or micro-convection (Ahuja 1975a, 1975b). For CNT nanofluids, Peclet number is of an order of 1 under the conditions of this work if the shear rate at the wall and the volume based equivalent particle diameter are used in the calculation. This seems to suggest little contribution of enhanced thermal conduction to the observed large enhancement of the convective heat transfer coefficient. However, CNTs are likely to form structures, which may have an effective particle size much larger than the volume based equivalent particle diameter, and hence lead to a much higher Peclet number and significant further enhancement on the thermal conduction.

As shown in Figures 5.4-5.8, the convective heat transfer coefficient decreases with axial distance, and the decay for pure water is much quicker than that for CNT nanofluids. This indicates that the presence of CNTs affects the development of boundary layers. The effect of particles on the boundary layer development has also been suggested to be the main mechanism for heat transfer enhancement in particulate flows under the turbulent flow regime (Hetsroni and Rozenblit, 1994). For a pure Newtonian fluid flowing in a straight pipe, the boundary layer develops smoothly and the flow is hydrodynamically and thermally fully developed at $x/D \geq \sim(0.05Re)$ and $x/D \geq \sim(0.05RePr)$, respectively. The criterion for the thermal boundary layer development does not apply to CNT nanofluids as clearly shown in Figures 5.4-5.7.

The above discussion is mostly from the macroscopic point of view. Microscopically, particle migration and re-arrangement due to non-uniform shear rate over the pipe cross-section could also be a reason for the observed large heat transfer enhancement. In normal pipe flows, the highest shear rate occurs at the wall, whereas the lowest shear rate takes place at the centre. The non-uniform shear rate implies non-uniformity in both viscosity and thermal conductivity; see Phillips et al. (1992), Ding and Wen (2004), and Wen and Ding (2005b). Wen and Ding (2005b), by using a theoretical model, showed that the non-uniform thermal conductivity profile resulting from particle migration could lead to a higher Nusselt number. They also found that the average particle concentration has a considerable effect on the particle concentration distribution. A more non-uniform particle distribution occurred for higher average particle concentration. A higher average particle concentration also weakens the fluid velocity distribution. This is most likely be the case of the discrepancy observed for 0.25wt% CNT as seen in Figure 5.5b and Figure 5.6b. This suggests that for utilizing nanofluids for heat intensification, an optimal particle concentration may exist.

A final point is the effect of particle shape on the heat transfer performance. Previously studies using nearly spherical nanoparticles by Pak and Cho (1999), Xuan and Li (2003) and Wen and Ding (2004b) showed an enhancement of the convective heat transfer of up to ~60%. Recently, Yang et. al. (2004) studied the laminar flow heat transfer of nanofluids made from disc-like graphitic nanoparticles with an aspect ratio of ~0.02. They found very small enhancement in the heat transfer coefficient, and the enhancement is even lower than that due to thermal conductivity. These observations seem to suggest that the observed high heat transfer enhancement in this

work be (at least partially) associated with the very high aspect ratio (> 100) of CNTs.

In summary, the observed large enhancement of the convective heat transfer coefficient is associated with a) enhancement of the thermal conductivity under the static conditions, b) further enhancement on the thermal conduction under the dynamic conditions (shear induced), c) reduction of the boundary layer thickness and delay in the boundary layer development, d) particle re-arrangement due to non-uniform shear-rate across the pipe cross-section, and e) high aspect ratio of CNTs.

5.3 Conclusions

This chapter discussed the study on the heat transfer behaviour of aqueous suspensions of multi-walled carbon nanotubes (CNT nanofluids). Stable CNT nanofluids are produced by using both ultrasonification and high shear homogenisation methods in the presence of a small percentage of gum arabic. Systematic experiments were performed on the produced nanofluids to obtain the (static) effective thermal conductivity, viscosity and convective heat transfer coefficient. The following conclusions are obtained:

- Significant enhancement was observed of the convective heat transfer in comparison with pure water as the working fluid. The enhancement depended on the flow conditions, CNT concentration, Reynolds Number and the pH level, and the effect of pH is observed to be small.
- Given other conditions, the enhancement is a function of the axial distance from the inlet of the test section; the enhancement increased first, reached a

maximum, and then decreased with increasing axial distance. The position at which the maximum enhancement occurred increased with CNT concentration and Reynolds number.

- Given CNT concentration and pH level, there seems to be a Reynolds number above which a big increase in the convective heat transfer coefficient occurs. Such a big increase seems to correspond to the shear thinning behaviour.
- For nanofluids containing 0.5 wt % CNTs, the maximum enhancement is over 350% at Re = 800, and the maximum occurs at an axial distance of approximately 110 times the tube diameter.
- The observed large enhancement of the convective heat transfer could not be attributed purely to the enhanced thermal conduction under the static conditions. Particle re-arrangement, shear induced thermal conduction enhancement, reduction of thermal boundary layer thickness due to the presence of nanoparticles, as well as the very high aspect ratio of CNTs are proposed to be possible mechanisms.

CHAPTER SIX

CONVECTIVE HEAT TRANSFER OF NANOFLUIDS CONTAINING TIO_2 NANOPARTICLES

6.1 Introduction

This chapter will discuss the investigation of convective heat transfer coefficient of TiO_2-water nanofluids. Very few publications discussed on the work of TiO_2 nanofluids. Murshed et. al. (2005) and Wen and Ding (2006) studied the enhanced thermal conductivity of TiO_2-water nanofluids, while Pak and Cho (1998) investigated the convective heat transfer of TiO_2-water nanofluids. Therefore, thorough investigation and understanding of nanofluids containing TiO_2 is essential and that has motivated this part of research. This research was different from that of Pak and Cho (1998) in terms of the experimental set up. Table 6.1 describes the difference between the two experimental rigs set up.

The procedures and data processing for this work is similar to that of CNTs nanofluids (Chapter 5) and the details have been described in Chapter 4. Therefore, this chapter will focus only on the results and discussion of heat transfer study of TiO_2-water. This chapter is organized in the following manner. Section 2 presents and discusses the results. And finally Section 3 summaries the main conclusions. Reviews of relevant work in the literature will also be included where appropriate.

Table 6.1: Comparison between Pak and Cho (1998) and current work.

Researcher	Pipe type	Test section axial distance (x)	Pipe inner diameter (D)	Nanoparticle size (nm)	Method of production	Stabilization technique	Nanofluids pH value
Pak and Cho (1998)	Stainless steel	351 cm	1.066 cm	27	High speed mixing (10000 rpm)	Electrostatic repulsion	10.0
Current work	Copper	97 cm and 184 cm	0.45 cm	90, 120, 180, 570	Beads milling	Electrostatic repulsion	11.0

6.2 Results and Discussion

6.2.1 Effective thermal conductivity

Figure 6.1 shows the effective thermal conductivity of TiO_2-water nanofluids at five different temperatures, 20°C, 23°C, 25°C, 28°C, and 30°C. Note that the concentration of nanofluids was 0.2 wt % and the pH value was at 11.0. It is interesting to see that the effective thermal conductivity increases slightly with increasing particle size and temperature. However, the increase is significant given that the error bar is ~3%, particularly due to particle size. The temperature effects on the thermal conductivity enhancement were more considerable albeit still small with the maximum enhancement observed was ~4%. Wen and Ding (2006) observed that at ~2.5 wt % (pH = 2.0) TiO_2 nanofluid gave an enhancement of ~ 5%.

Figure 6.2 shows a comparison of the effective thermal conductivity between the previous works on TiO_2-water nanofluids. It clearly shows that the thermal conductivity enhancement depends on pH value, temperature and concentration. The current results are comparable to previous work (Pak and Cho, 1998; Wen and Ding, 2006). Since this work limits to more dilute systems, a direct comparison cannot be made to those by others. However, the data point falls within the same order of magnitude of the reported data by previous studies. An inspection of the results of Pak and Cho (1998) and Murshed et. al. (2005) showed that the pH value seems to play an important role in thermal conductivity enhancement of TiO_2-water nanofluids. This implies that the electrostatic charges hence extent of particle clustering could affect the thermal conductivity. This seems to be consistent with a recent study by Lee et. al.

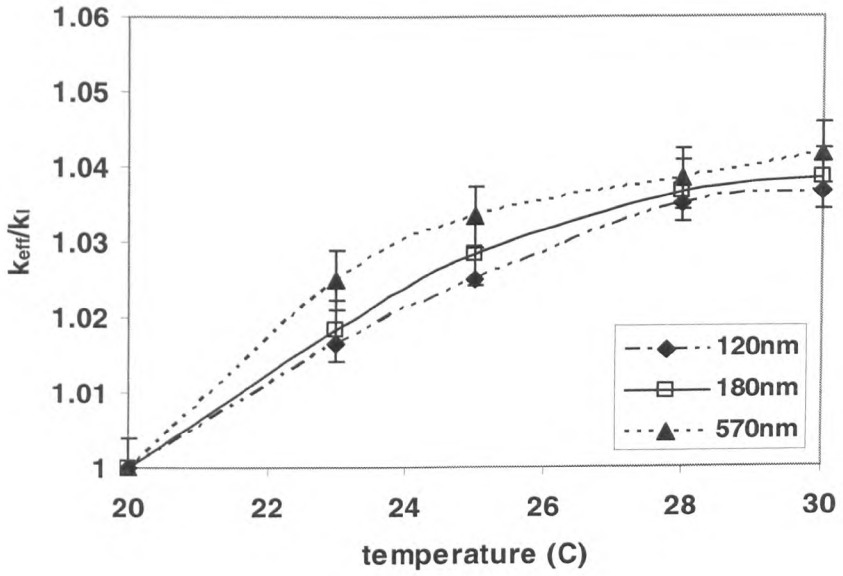

Figure 6.1: Effective thermal conductivity of 0.2 wt.% of TiO_2-water nanofluids at pH 11.0.

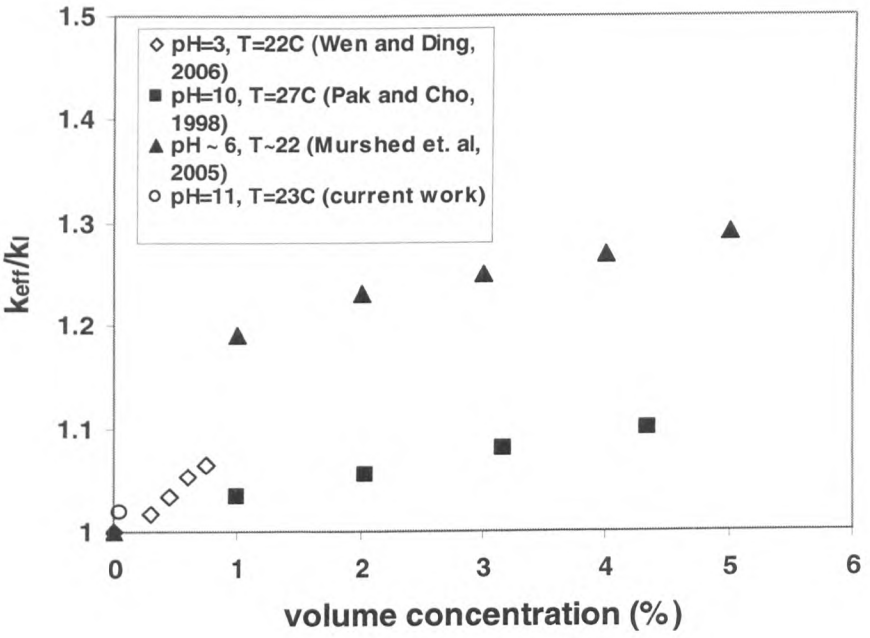

Figure 6.2: Comparison of effective thermal conductivity of TiO_2-water nanofluids.

(2006) who found a strong correlation between thermal conductivity and surface charges. Note also that the CTAB surfactant was used in Murshed et. al. (2005) work. The difference may therefore be partially due to the use of surfactant.

6.2.2 Viscosity of TiO_2-water nanofluids

Figure 6.3 shows the viscosity results for the TiO_2-water nanofluids. In general the viscosities of TiO_2-water nanofluids showed shear thinning behaviour at 0.2 wt %. The particle size did not have a significant impact on the viscosities, all sizes of particles showed similar viscosities values. The viscosity of TiO_2 nanofluid is higher than that of water by ~1.3 times. The viscosity difference was obvious only at low shear rate (< 100 s^{-1}). At shear rate greater than 150 s^{-1} the viscosity values approached a constant. Pak and Cho (1998) observed constant viscosities for 1 vol. % of TiO_2-water nanofluids. Shear thinning behaviour of TiO_2 suspensions was observed at 10 vol. % nanofluids. Wen and Ding (2006) observed shear thinning behaviour for 1 wt. % and 2 wt. % of TiO_2-water nanofluids and the viscosities approached a constant value at shear rate greater than 200s^{-1}.

Figure 6.4 shows the temperature-dependent behaviour of viscosity for TiO_2-water nanofluids. The viscosity decreases with increasing temperature which is expected for liquid suspensions.

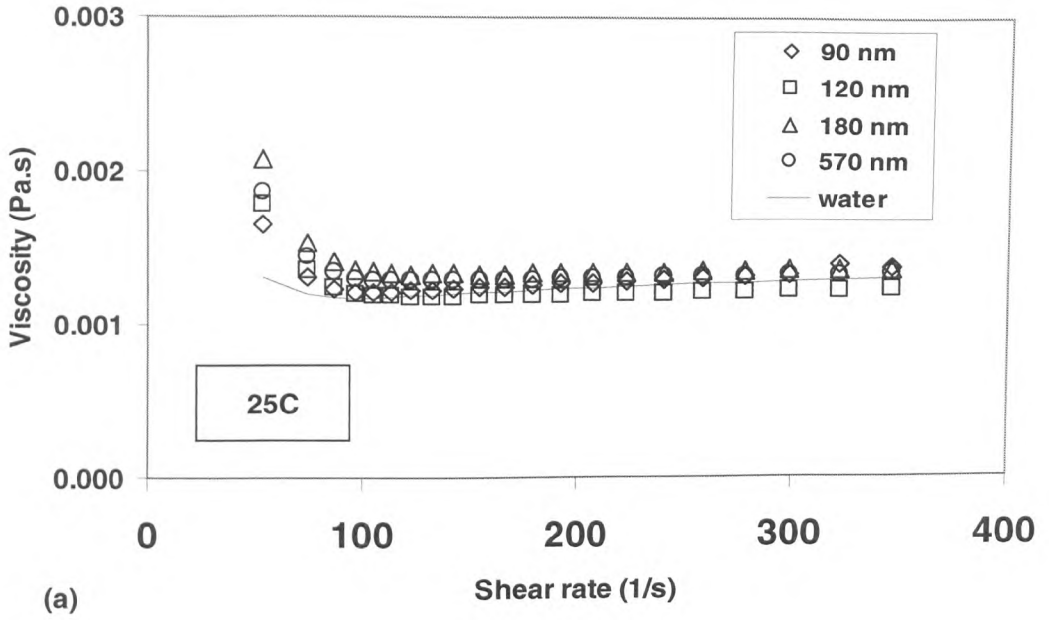

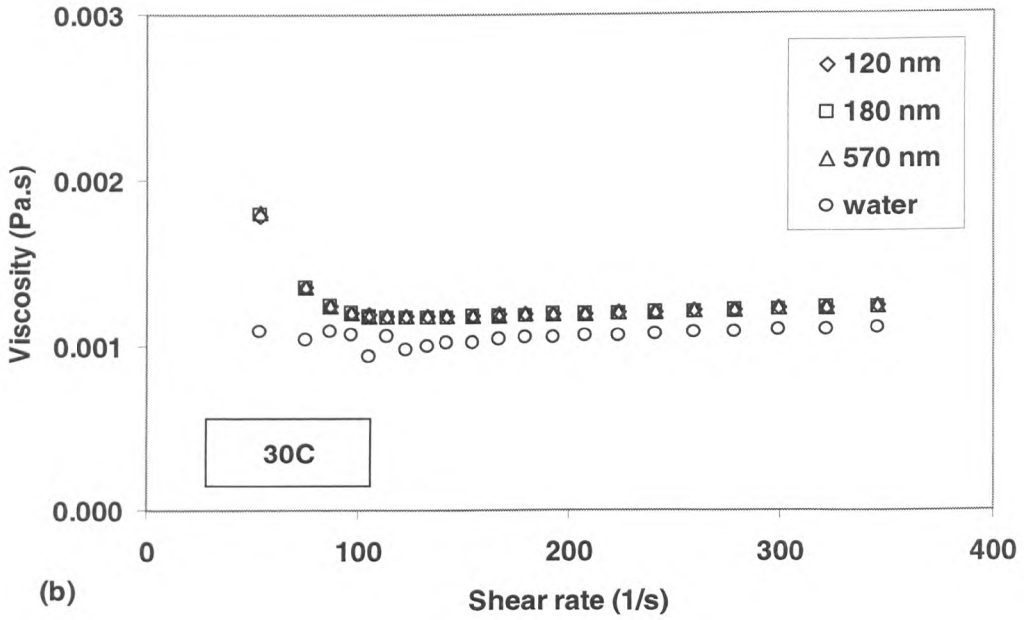

Figure 6.3: Viscosity of 0.2 wt % TiO_2-water nanofluids (pH=11.0) at 25°C (a) and 30°C (b).

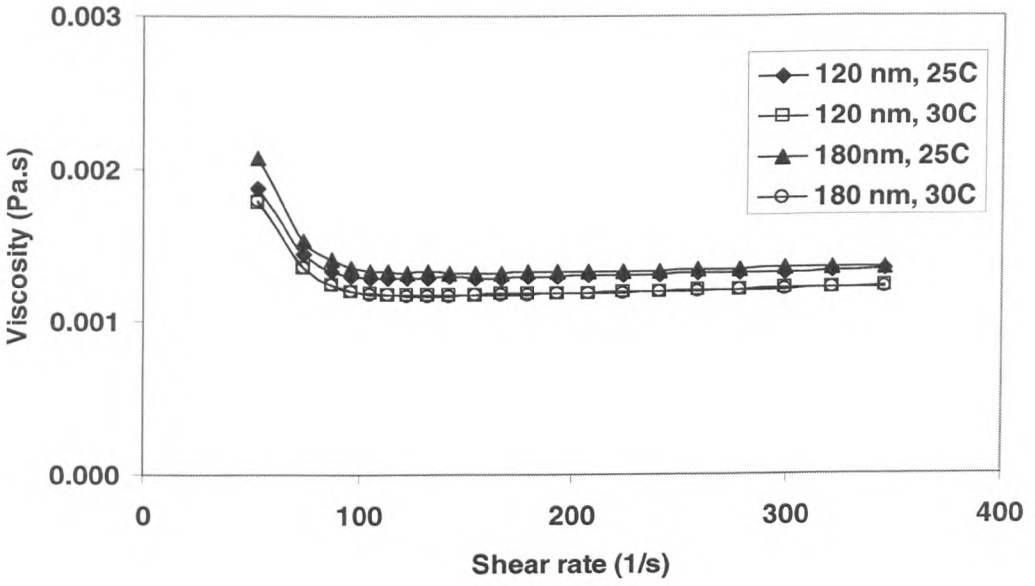

Figure 6.4: Temperature effects on viscosity of TiO_2-water nanofluids.

6.2.3 Convective heat transfer coefficient of TiO2-water nanofluids

The reliability and accuracy of the experimental system were tested in the same manner as was described in Section 5.2.3.1. Predictions using Shah's equation (Shah, 1975) was used for laminar flow under the constant heat flux boundary condition:

$$Nu = \begin{cases} 1.953\left(Re \cdot Pr\frac{D}{x}\right)^{1/3} & \left(Re \cdot Pr\frac{D}{x}\right) \geq 33.3 \\ 4.364 + 0.07722 Re \cdot Pr\frac{D}{x} & \left(Re \cdot Pr\frac{D}{x}\right) < 33.3 \end{cases} \qquad \text{Eq. 6-1}$$

The results are shown in Figure 6.5. The heat transfer coefficient values using Shah's Equation and from the experiments are in reasonably good agreement. Having established the confidence in the experimental set up, experiments were performed at different flow conditions (Reynolds Number) and different sizes of nanoparticles.

6.2.3.1 Effect of Reynolds Number (flow condition) on the convective heat transfer

In these experiments, the difference between the inlet and outlet temperatures as well as between the bulk temperature and the wall was maintained to be less than 10 K (between 3-5 K). This is to minimize the effect of temperature-dependent viscosity on the heat transfer coefficient. The inlet temperature of the nanofluids was kept at 28°C-30°C for all runs.

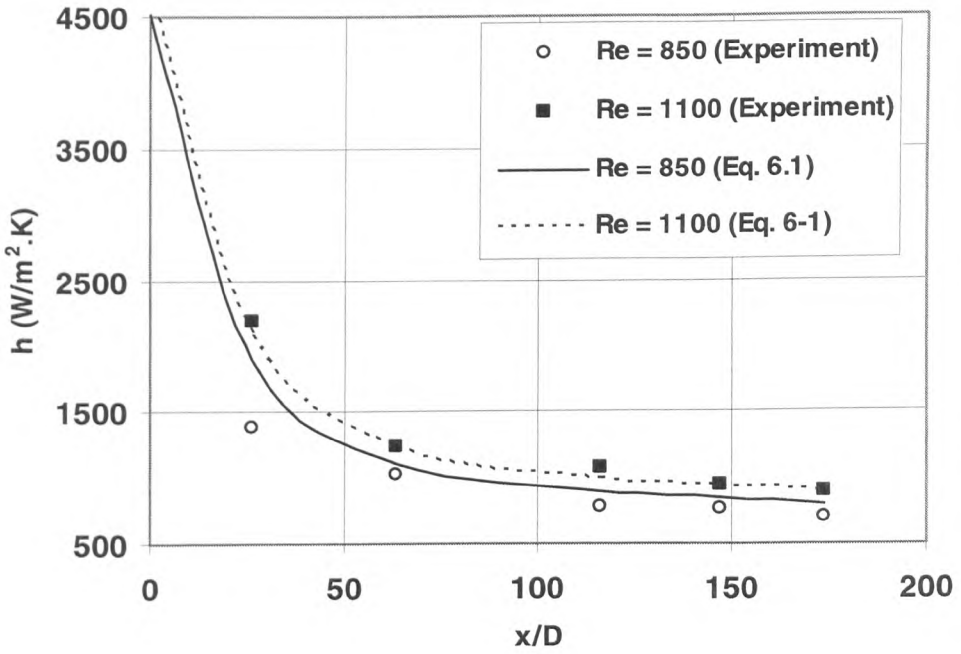

Figure 6.5: Initial test of the experiment rig using distilled water.

Figure 6.6 shows the axial profile of convective heat transfer coefficient of distilled water for different Reynolds Numbers. Figure 6.7 shows the effect of Reynolds Number on the axial profile of the heat transfer coefficient for; (a) 90 nm and (b) 120 nm (b), and Figure 6.8 shows the effects of Reynolds Number for; (a) 180 nm and (b) 570 nm. These figures clearly show that the convective heat transfer increases with increasing Reynolds Number. The heat transfer coefficient decreases with increasing axial direction. This is as expected for heat transfer in the entrance region. Figure 6.7a and Figure 6.8a also show that the convective heat transfer coefficient reached to a similar value towards the exit if the pipe was long enough ($x/D > 400$). Wen and Ding (2004) also observed that the heat transfer coefficient of Al_2O_3-water nanofluids reached to a similar value towards the exit.

The enhancement of the heat transfer coefficient was calculated with reference to water. Figure 6.9 shows the enhancement of heat transfer coefficient, as a function of axial distance. The following observation can be made from the two figures:

- The enhancement of heat transfer coefficient increased with x/D initially, reaches a maximum, decreased with further increase in x/D.
- The maximum enhancement was observed at $x/D = 150$ for the Reynolds Number studied. This observation is different from that of CNT nanofluids where the maximum enhancement occurred increased with concentration and Reynolds Number. This is due to particle shape effect. The average diameter of multi- wall CNT was 20-60nm and the length was a few tens of micrometers. Thus the aspect ratio (L/D) of CNT is > 1000 while the average diameter of TiO_2 was 20 nm. The different

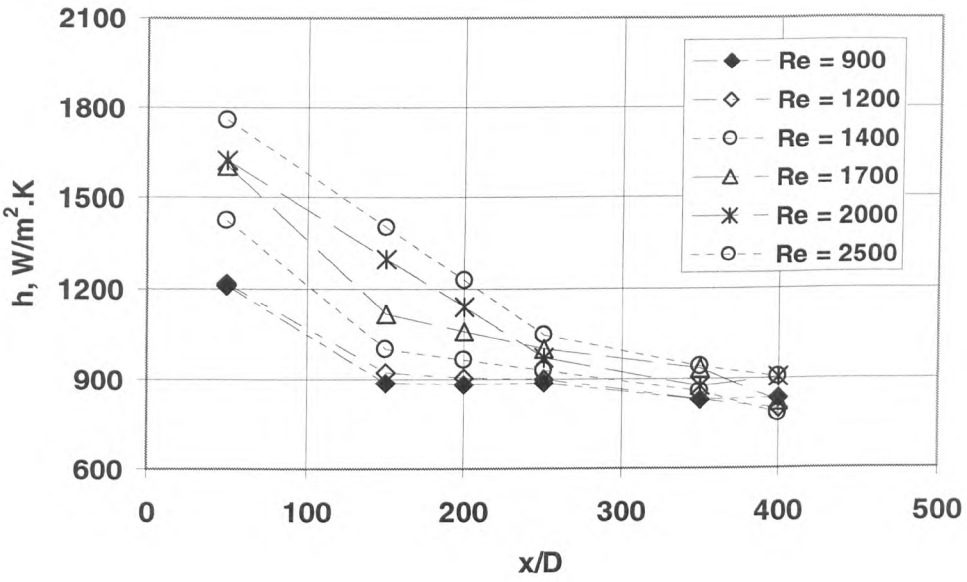

Figure 6.6: Axial profiles of heat transfer coefficient of water for different Reynolds Number.

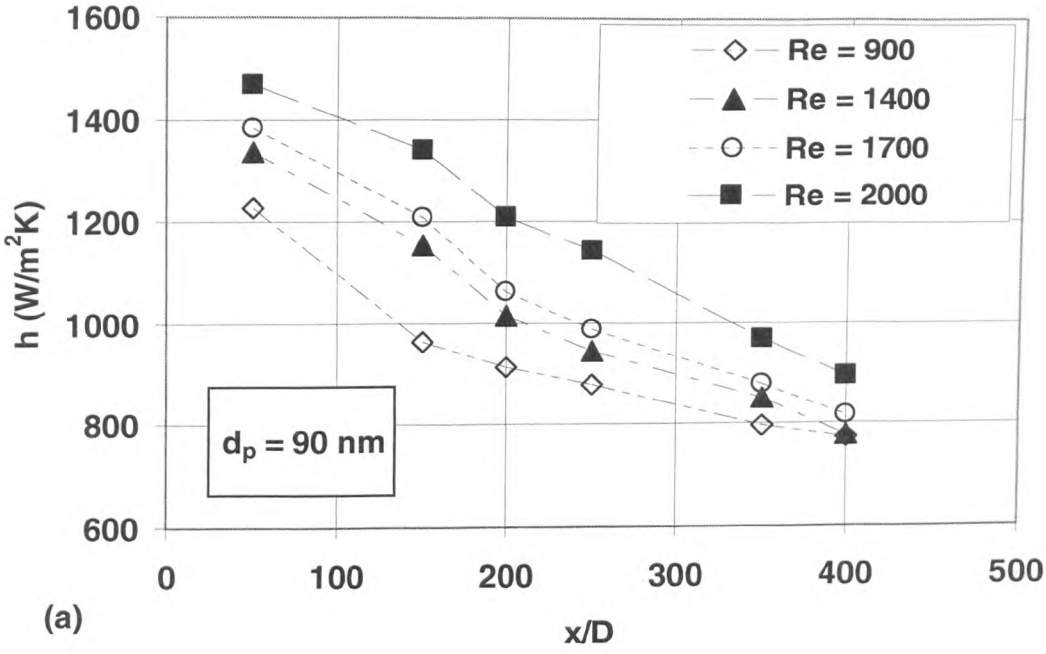

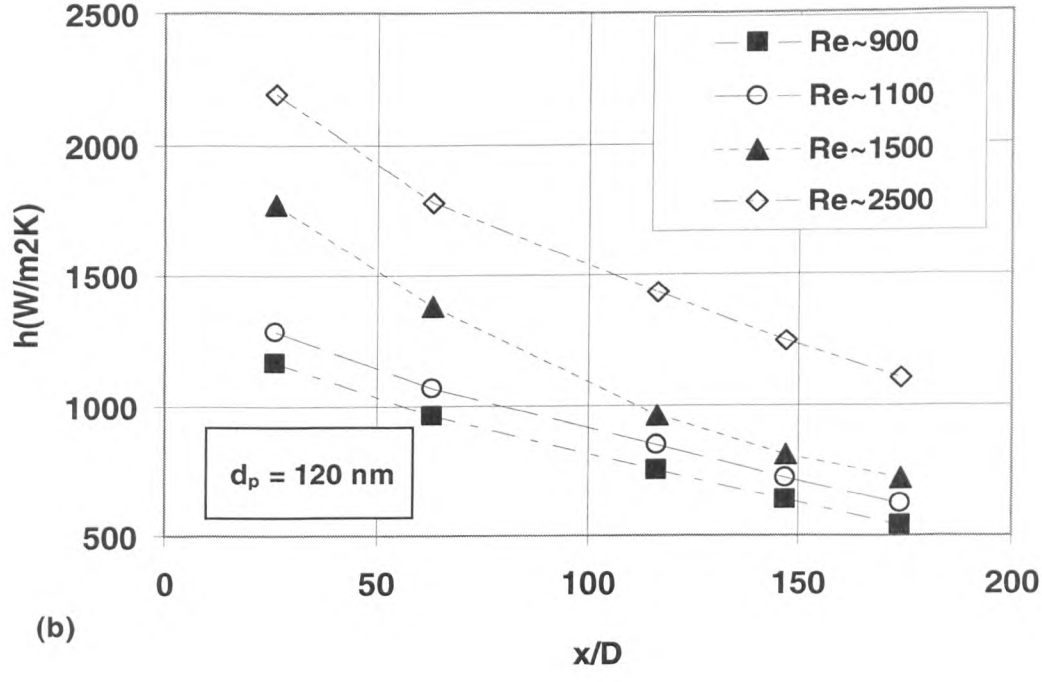

Figure 6.7: Effect of Reynolds Number on heat transfer coefficient for (a) 90 nm and (b) 120 nm of TiO_2-water nanofluids.

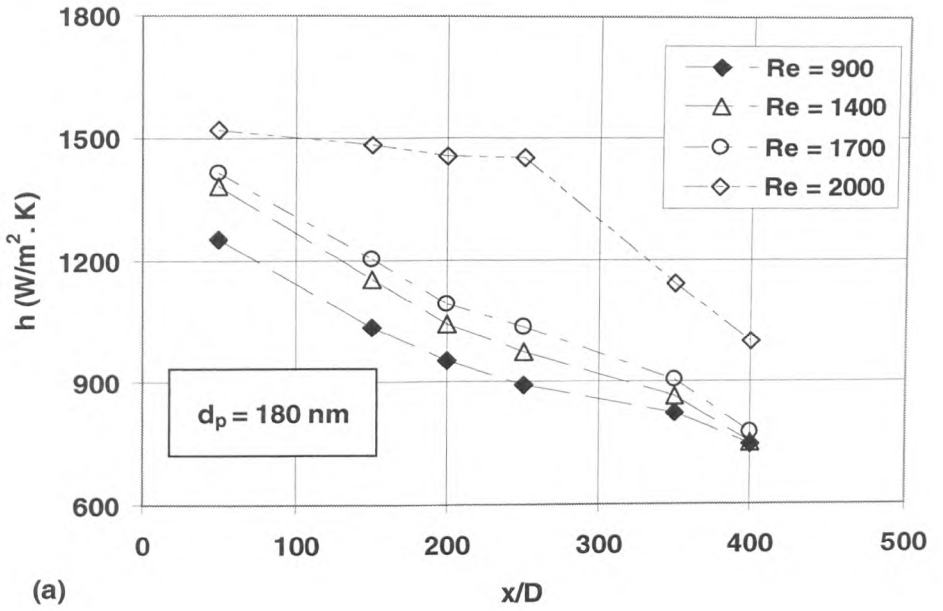

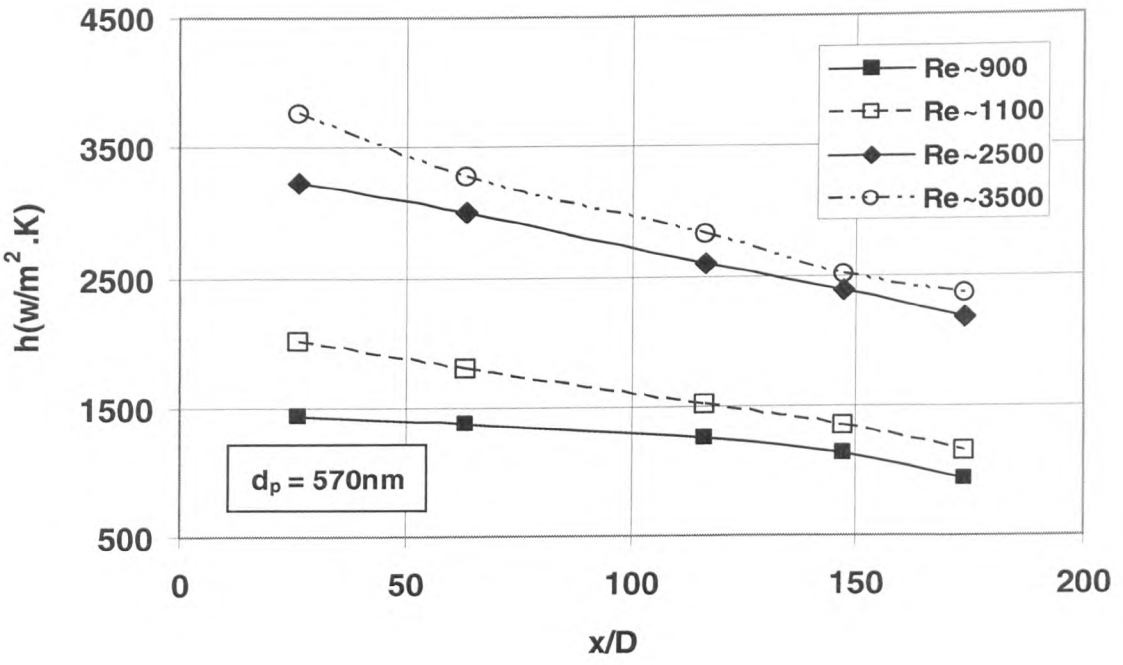

Figure 6.8: Effect of Reynolds Number on heat transfer coefficient for (a) 180 nm and (b) 570 nm of TiO2-water nanofluids.

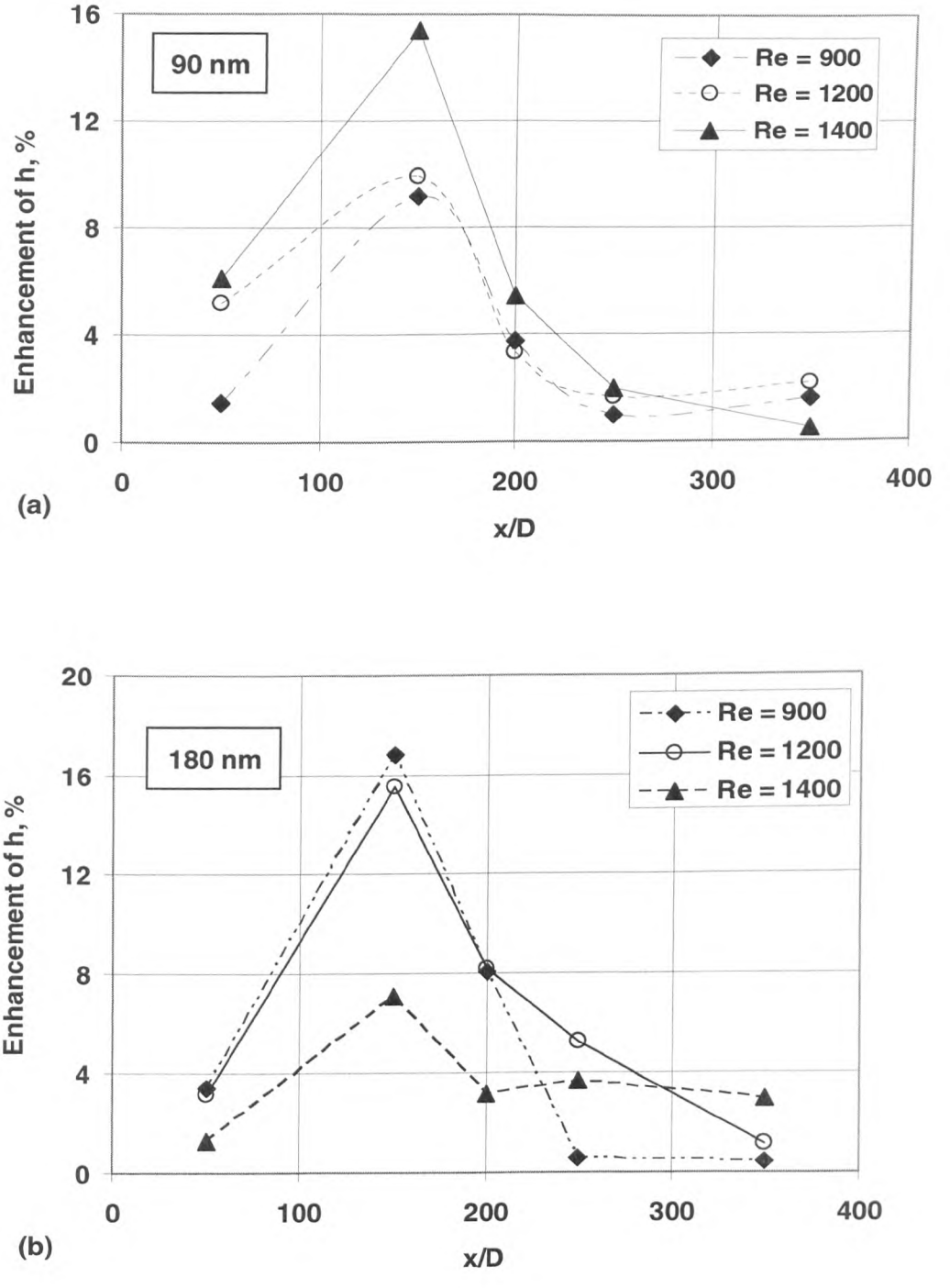

Figure 6.9: The enhancement of heat transfer coefficient for 0.2 wt %, pH = 11.0 of TiO2-water nanofluids.

particle shape will alter the fluid flow in the pipe. The velocity distribution of TiO_2 nanofluids is more uniform than that of CNT nanofluids. Thus, the position at which the maximum enhancement was achieved is similar. Moreover, the TiO_2 concentration was lower than that of CNT nanofluids, hence creates a better particle concentration distribution in the pipe.

- The maximum enhancement achieved was about 16 %.

A similar trend was observed by Xuan and Li (2003) and Wen and Ding (2004b) but with more significant enhancement. Xuan and Li observed that the turbulence heat transfer coefficient of Cu-water nanofluids was increased by 60%. Pak and Cho (1998) investigated the turbulent ($Re > 10^4$) heat transfer coefficient of Al_2O_3-water and TiO_2-water nanofluids. They observed that the enhancement of heat transfer coefficient was ~45% for additional of 1.3% vol. concentration of Al_2O_3 and 75% at the concentration on 2.78%. They also observed that the heat transfer enhancement of TiO_2 was less than that of Al_2O_3. Wen and Ding (2004b) observed ~47% increase in the heat transfer coefficient for 1.6 vol % of Al_2O_3-water nanofluids. This indicates that particle concentration affects the extent enhancement of convective heat transfer of nanofluids. Wen and Ding (2004b) also observed that the maximum enhancement was observed at $x/D \sim 63$, which was closer to the entrance.

The enhancement of heat transfer coefficient for TiO_2-water nanofluids was much lower than that of CNT-water nanofluids where >100% enhancement was observed. This suggests that the enhancement of heat transfer coefficient is associated with the enhancement of thermal conduction. This can be seen from Figure 6.1 where

the enhancement for TiO_2-water nanofluids was much lower than that of CNT-water nanofluids (Figure 5.1). Thus, in order to utilize nanofluids as working medium to enhance heat transfer performance, selecting particles with higher effective thermal conductivity should be considered. However, as discussed in Chapter 5, the thermal conduction only contributes a small part of the enhanced convective heat transfer. Other factors such as particle shape and viscosity may play a role; more detail discussions will be made in later section.

6.2.3.2 Effect of nanoparticle size on the convective heat transfer

Figure 6.10 shows the nanoparticle size effect on the convective heat transfer coefficient for different Reynolds Number. The figures show that at a Reynolds Number of 900 and 1700 the size of nanoparticles does not contribute a significant impact on the convective heat transfer of nanofluids. Figure 6.11 shows the effects of particle size on the convective heat transfer for $Re = 2000$. It shows that the convective heat transfer increased with decreasing particles size. A discrepancy occurred for the 570 nm particles where the heat transfer coefficient increased with Reynolds Number. As discussed by Wen and Ding (2005a), the Peclet Number increases with particle size and Reynolds Number. This is most likely the case for the 570 nm nanofluids, hence this implies that the 570nm TiO_2 nanofluids dose not possess nanofluids feature where Peclet Number is in the order of 1. However, Pak and Cho (1998) suggested the use of bigger size of particles to enhanced heat transfer performance. To resolve the controversy, further experimental work is strongly recommended.

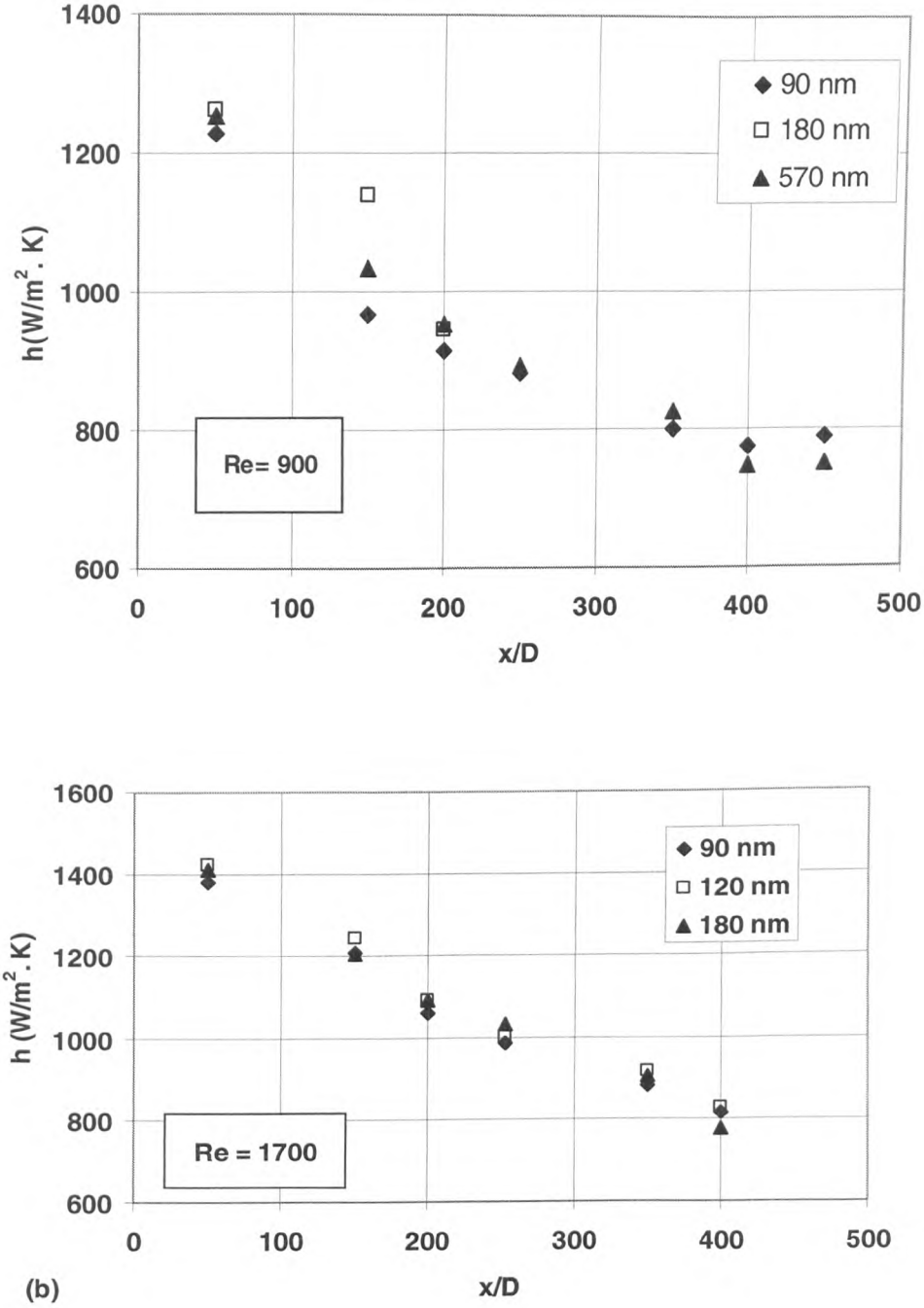

Figure 6.10: Size effect on the convective heat transfer of TiO_2-water nanofluids for Reynolds Number = 900 (a) and 1700(b).

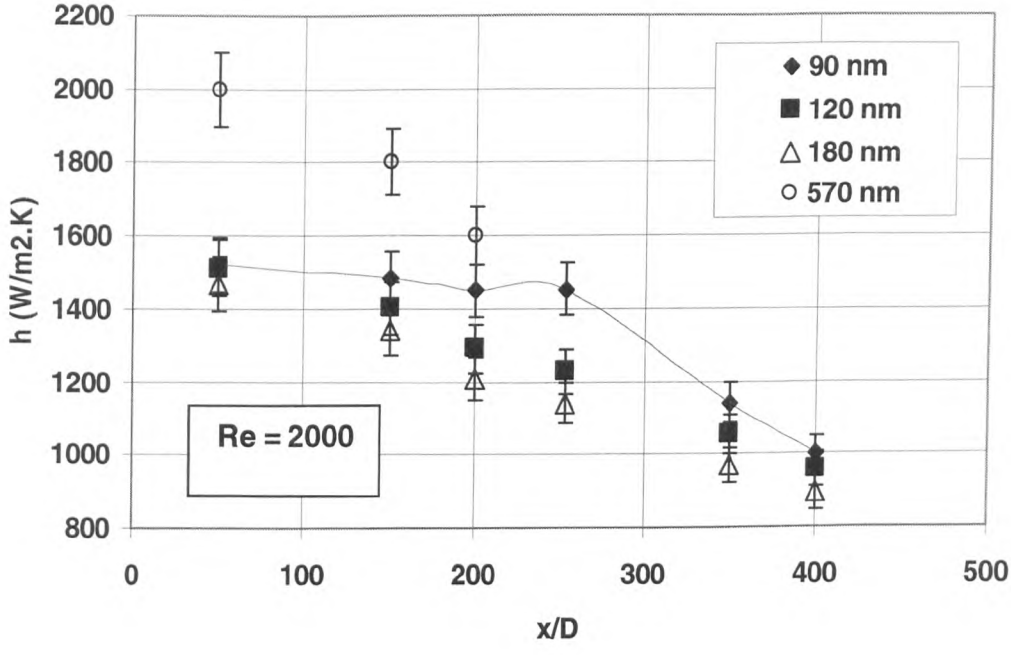

Figure 6.11 Size effect on the convective heat transfer of TiO_2-water nanofluids for Reynolds Number = 2000.

6.2.3.3 Mechanism for heat transfer

As discussed in Chapter 5, the enhancement of heat transfer coefficient is associated with several possible mechanisms, a) enhancement of the thermal conductivity under the static conditions, b) further enhancement on the thermal conduction under the dynamic conditions (shear induced), c) reduction of the boundary layer thickness and delay in the boundary layer development, d) particle shape and e) particle migration and re-arrangement due to non-uniform shear-rate across the pipe cross-section. The following discussions will be based on these mechanisms.

The enhancement of thermal conductivity under static condition contributes to the enhancement of heat transfer coefficient of the TiO_2-water nanofluids. In this work, the maximum enhancement observed was ~ 4% at 30°C. However, the enhancement of convective heat transfer is much greater than that due to the thermal conductivity. Hence, further enhancement of thermal conductivity may be due to the dynamic shear conditions. As shown in Figure 6.3, the nanofluids showed a shear thinning behaviour, and therefore the effective thermal conductivity should be higher than that shown in Figure 6.1. Such behaviour has been observed by Sohn and Chen (1981) and Ahuja (1975a). These researchers attributed the enhancement to the high Peclet Number ($Pe = \dot{\gamma} \cdot d_p^2 / v$), where $\dot{\gamma}$ is the shear rate, and d_p is the particle diameter. However, for TiO_2 nanofluid, the Peclet Number is of an order of 1. Consequently, the enhancement of heat transfer coefficient cannot solely lie on such argument. On the other hand, if the nanoparticle were to form clusters that are much larger than the particles sizes, then it would be possible that the Pe Number were much larger under the conditions of this

work. This argument is in contradiction to the results shown in Figure 6.11 where small particles give a higher heat transfer coefficient.

The enhancement may be due to presence of thermal boundary thickness. The heat transfer coefficient, h, can be approximately given by k/δ_t where δ_t is the thickness of the thermal boundary layer. This indicates that the heat transfer coefficient increases with an increase k and/or decreasing δ_t. Therefore, the maximum enhancement at the entrance region occurred as a result of decreasing thermal boundary thickness. The presence of nanoparticles affects the development of boundary layer in the pipe. For Newtonian fluids, the boundary layer develops smoothly and hydrodynamically developed at $x/D \geq (0.05Re)$ and thermal fully developed at $x/D \geq (0.05Re \cdot Pr)$. However, Figures 6.7 and 6.8, show the existence of a greater thermal developing length for nanofluids. Therefore, the presence of nanoparticles affects the boundary layer development in the pipe flow.

Wen and Ding (2005b) suggested that the enhancement is due to the particle migration and rearrangement due to non-uniform shear rate over the pipe cross section. Consequently, there would be a non-uniformity in the viscosity and the thermal conductivity of nanofluids. For TiO_2-water nanofluids, the particle migration may have a significant impact on the thermal conductivity but not the viscosity. As seen in Figure 6.3, the viscosity of TiO_2-water nanofluids reaches a constant value at higher shear rate.

6.3 Conclusions

This chapter discussed the study on the heat transfer behaviour of TiO_2-water nanofluids. Stable TiO_2 nanofluids of various size, were produced by beads milling technique and the electrostatic mechanism was employed to stabilize nanoparticles. Experiments were performed on the produced nanofluids to obtain the (static) effective thermal conductivity, viscosity and convective heat transfer coefficient. The following conclusions are obtained:

- A small enhancement (4%) was observed for the effective thermal conductivity.

- A significant enhancement was observed of the convective heat transfer in comparison with pure water as the working fluid. The enhancement depended on the flow conditions and nanoparticle size.

- Given other conditions, the enhancement is a function of the axial distance from the inlet of the test section; the enhancement increases first, reaches a maximum, decreases with increasing axial distance. The position at which the maximum enhancement occurred was at $x/D = 150$.

- The maximum enhancement achieved was ~ 16% under the conditions of this work ($Re = 900$, 1200 and 1400).

- The observed large enhancement of the convective heat transfer could not be attributed purely to the enhanced thermal conduction under the static conditions.

- Particle shape, particle re-arrangement, shear induced thermal conduction enhancement, reduction of thermal boundary layer thickness due to the presence of nanoparticles, are proposed to be possible mechanisms.

CHAPTER SEVEN

CONCLUSIONS

7.1 Nanofluids formulation and characterization

The procedures and formulations for preparation of nanofluids are presented. The dry CNTs and TiO_2 samples (before suspended) were characterised using scanning electron microscope (SEM). The microscopy images showed that the CNTs were entangled into a spaghetti-like network and the TiO_2 nanoparticles were agglomerated and form aggregates that are bigger than the corresponding primary particles.

Several methods were employed to formulate and produce stable nanofluids systems. The sonication and high-shear mixing methods were applied in the production of CNT-water nanofluids. This method was simple and inexpensive, thus suitable for a lab scale production. Beads milling technique was employed to formulate TiO_2-water nanofluids systems. This method allowed more control on the nanoparticle size desired depending on the time of milling engaged. The longer process gave smaller nanoparticle size in the suspension. Nanofluids produced by these methods remained stable for months in a stationary state.

To further enhance the stability of CNT-water nanofluids, gum arabic was chosen as the surfactant after a series of trial and error with other surfactants. The stability of CNTs nanofluids showed that surfactant can modify the surface of the nanoparticles and prevent aggregation over certain period of time.

On the other hand, the TiO_2-water was stabilized by means of electrostatic repulsion mechanism. Sodium hydroxide was used for the purpose and the pH was adjusted to 11.0.

7.2 Heat transfer investigation of CNTs-water nanofluids

The thermal conductivity of CNT nanofluids was higher than that of water. The effective thermal conductivity increases with increasing particle loading and temperature. At 20°C and 25°C , the effective thermal conductivity reached a constant value for particle concentration greater than 0.5 wt %. At 30°C the thermal conductivity enhancement was ~30% at o.25 wt. % and reached as high as 80% for 1.0 wt. %. The enhancement, however, was higher than several previous works (Assael et. al, 2003; Xie, et. al, 2003; Wen and Ding, 2004a), but much lower than that reported by Choi et. al. (2001).

Viscosity analysis showed that CNT nanofluids shear thinned (decreased) with increasing shear rates. The viscosity decreased with increasing temperature. These observations are consistent with previous works (Kinloch et. al, 2002; Yang et. al, 2005; Yang et. al, 2006). The viscosities of CNT nanofluids were much higher than that of pure water. For instances at 25°C, the lowest viscosity of 0.1% CNT was 0.003 Pa·s which is approximately 3 times higher than that of water.

The convective heat transfer investigation showed that a significant enhancement in comparison with pure water as the working fluid. The enhancement depended on the flow conditions, CNT concentration and the pH level, and the effect of

pH is observed to be small. The enhancement increased first, reached a maximum, and then decreases with increasing axial distance. For nanofluids containing 0.5 wt % CNTs, the maximum enhancement is over 350% at Re = 800, and the maximum occurs at an axial distance of approximately 110 times the tube diameter.

7.3 Heat transfer investigation of TiO_2-water nanofluids

The thermal conductivity of TiO_2 nanofluids was higher than that of water. The enhancement was not significant; ~4% enhancement was observed. Note that the concentration of TiO_2 nanoparticle in this work is 0.2 wt. % which can be considered as very dilute. Therefore the contribution of the thermal conductivity of TiO_2 towards the thermal conductivity of nanofluids is not expected to be large. The nanoparticle size was not seen to play a major role in the effective thermal conductivity. A comparison with previous researchers' results (Pak and Cho, 1998; Murshed et. al, 2005; Wen and Ding, 2006) shows that the effective thermal conductivity of TiO_2 nanofluids is likely to depend on particle loading, size, shape and pH.

The viscosity of TiO_2 nanofluids was 3% higher than that of water. TiO_2 nanofluids showed a shear thinning behaviour at low shear rates and behaved like a Newtonian fluids at shear rate > 150 s^{-1}. The viscosity difference between different sizes of nanoparticle was insignificant. The viscosity decreased with increasing temperature. However, the viscosity did not differ in large amount as temperature increase was < 10%.

A significant enhancement was observed for the heat transfer coefficient. The enhancement of heat transfer coefficient increased with *x/D* initially, reached a maximum, and decreased with further increase in *x/D*. The maximum enhancement of ~16% was observed at *x/D* = 150. At low Reynolds Number, the size effect did not show a significant impact on the heat transfer coefficient. At higher Reynolds Number the heat transfer decreased with increasing particle size (90, 120, 180 nm). The discrepancy for the 570 nm TiO_2 nanofluids suggests that it does not possess the feature of nanofluids where Peclet Number is in the order of 1.

7.4 Overall conclusions

The heat transfer coefficient of nanofluids depends on the thermal conductivity of the nanoparticles. The experimental results have shown that, the enhancement of heat transfer coefficient of CNT nanofluids was very high as compared to TiO_2 nanofluids. This is because CNTs have a much higher thermal conductivity. An investigation of Al_2O_3 nanofluids (Wen and Ding, 2004b), showed that the enhancement of heat transfer coefficient was higher than that of this work. Another study by Pak and Cho (1998), also observed that the heat transfer coefficient of TiO_2 nanofluids was lower than of Al_2O_3. This is at least partially because, the thermal conductivity of Al_2O_3 (35 W/m·K) is higher than that of TiO_2 (11 W/m·K). This suggests that, to utilize nanofluids as heat transfer medium, the thermal conductivity of solid nanoparticles is one of the crucial factors. The viscosity also play a role in the enhancement of heat transfer coefficient since there exist shear inside the tube and therefore changes the thermal conductivity which arise from the shear induced.

This work shows that the size effect as suggested by Pak Cho (1998) did not seem to be significant. Further investigation is crucial to justify the argument. The thermal conduction is not the only factor that contributes to the enhancement of heat transfer coefficient. There are other mechanisms that could be possible such as thermal conduction due to dynamics conditions, particle re-arrangement, particle-surface interactions, and the reduction of thermal boundary layer thickness.

CHAPTER EIGHT

RECOMMENDATIONS FOR FUTURE RESEARCH

This research has shown reliable results and findings. However, there are still plenty of areas where this research could be improved and further investigation is highly recommended. The current publications on convective heat transfer of nanofluids are limited. However, the findings have reported a range of results that are worth looking into. This chapter recommends possible future research that can be done to improve the understanding of convective heat transfer of nanofluids. Among the activities include nanofluids samples preparation, convective heat transfer study and investigation of heat transfer enhancement mechanism.

8.1 Nanofluids samples preparation

The method of nanofluids preparation in this study could be improved in order to have better property. The raw materials used in the study are agglomerates with much bigger size than the primary particles when received. This is due to the fact the attractive forces between the particles are very strong so that they may be sintered at high temperature. Therefore, they have to be broken into the desired size using some mechanical means. One possible technique is to use the two-step process where the nanoparticles are produced in situ. In this method the nanoparticles size can be better controlled.

One direction that can be look into is to use different base liquid such as oil, refrigerants, and ionic liquid mixed with nanoparticles of various sizes and

concentrations. This work will indicate the trend and will give a better insight view of the heat transfer process of nanofluids.

8.2 The measurements of nanoparticle physical properties

Due to the lack of information on the actual thermal conductivity of nanoparticles, in most studies, the bulk properties of particles were used. It would be beneficial if the actual properties such as thermal conductivity and density of nanoparticles are known. Therefore, extensive experiments are recommended in future to measure the actual properties nanofluids, which are crucial for better understanding of behaviour of flowing nanofluids.

8.3 Convective heat transfer investigation

The study of TiO_2 nanofluids was restricted to very dilute system. The behaviour of TiO_2 nanofluids behaviour can be better understood if more concentrated systems are also looked into. So far, no work on heat transfer has been done for concentration of greater than 3.5 vol. %. At present conditions, the research of convective heat transfer is limited to only water as the based fluids. It would be of great interest if convective heat transfer of other based liquids is investigated such as oil and ionic liquid.

BIBLIOGRAPHY

Ahuja, A.S. (1975a). Augmentation of heat transport in laminar flow of polystyrene suspension: I - experiments and results. *Journal of Applied Physics.*, **46**(8), 3408-3416.

Ahuja, A.S. (1975b). Augmentation of heat transport in laminar flow of polystyrene suspension: II – analysis of data. *Journal of Applied Physics.*, **46**(8), 3417-3425.

Aitcheson, N., Fickes, D., and Lloyd, J.R. (2002). Fundamental effects of boundary structure on nano-scale conductive heat transfer. *Proceedings of IMECE2002, ASME International Mechanical Engineering Congress & Exposition*, New Orleans.

Ali, A.A. (2003). Analysis of heat and mass transfer between air and falling film desiccant for different flow configuration in the ultra-fine particles, The Ohio State University, PhD Thesis.

Ali,, A., Vafai, K., and Khaled, A.R.A. (2003). Comparative study between parallel and counter flow configurations between air and falling film desiccant in the presence of nanoparticles suspensions. *International Journal of Energy Research,* **27**, 725-745.

Alias, H., Ding, Y., and Williams, R.A. (2003). On the rheology of carbon nanotubes suspensions. *Proceedings of 2nd Asian Particle Technology Symposium*, **(I)**, Penang, Malaysia, 421-425.

Andres, R.P., Bowles, R.S., Kolstad, J.J., and Calo, J.M. (1981). Generation of molecular clusters of controlled size, *Surface Science*, **106**, 117-124.

Ashly, S. (1994). Small-scale structure yields big property payoffs, *Mechanical Engineering*, **116** (2), 52-57.

Assael M.J., Chen C.F., Metaxa L and Wakeman W.A. (2004). Thermal conductivity of suspensions of carbon nanotubes in water. *International Journal of Thermophysics*, **25** (4), 971-985.

Assael M.J., Metaxa, I.N., Arvanitidis, J., Christofilos, D. and Lioutas C. (2006). Thermal conductivity enhancement in aqueous suspension of carbon multi-walled and double-walled nanotubes in the presence of two different dispersants. *International Journal of Thermophysics*, **26** (3), 647-664.

Bandyopadhyaya, R., Nativ-Roth, E., Regev, O., and Yerushalmi-Rozen, R. (2002). Stabilization of individual carbon nanotubes in aqueous solutions. *Nano Letters*, **2**(1), 25-28.

Bang, I.C. and Chang, S.H. (2005). Boiling heat transfer performance and phenomena of Al_2O_3-water nano-fluids from plain surface in a pool, *International Journal of*

Heat and Mass Transfer, **48**(12), 2407-2419.

Berber S., Kwon Y.K. And Tomanek D. (2000). Unusually high thermal conductivity of carbon nanotubes. *Physical Review Letters*, **84**, 4613-4616.

Bhattacharya, P. (2005). Thermal conductivity and colloidal stability of nanofluids, Arizona State Univeristy, PhD Thesis.

Bhattacharya, P., Saha, S.K., Yadav, A. and Phelan, P.E. (2004). Brownian dynamics simulation to determine the effective thermal conductivity of nanofluids, *Journal of Applied Physics*, 95(11), 6492-6494.

Biercuk, M.J., Llaguno, M.C., Radosavijevic, M., Hyun, J.K., Johnson, A.T., and Fischer, J.E. (2002). Carbon nanotubes composites for thermal management, *Applied Physics Letters*, **80**(15), 2767-2769.

Bonnecaze, R.T., and Brady, J.F. (1990). A method for determining effective conductivity of dispersions of particles. *Proceeding of the Royal Society of London, Series A*, **430**(1879), 285-313.

Bonneman, H., Botha, S.S., Bladergroen, B., Linkov, V.M. (2005), Monodisperse copper –And silver-nanocolloids suitable for heat conductive fluids, *Applied Organometallic Chemistry*, **19**(6), 768-773.

Bruggeman, D.A.G. (1935). Berechnung vershiedener physikalischer Konstanten von

heterogenen Subtanzen, I. Dielektrizitatskonstanen und Leitfahigkeiten der Mischkorper aus isotropen Substanzen, *Annalen der Physik*, Leipzig 24, 636-679.

Buongiorno, J. (2006). Convective transport in nanofluids. *Journal of Heat Transfer*, Transaction of ASME, **28**, 240-250.

Chein, H.T., Tsai, C.I., Chen, P.H. and Chen, P.Y. (2003). Improvement on thermal performance of a disk-shaped miniature heat pipe with nanofluid. *Proceedings of 5th International Conference on Electronic and Packaging Technology*, 389-391.

Chein, R., and Huang, G. (2005). Analysis of microchannel heat sink performance using nanofluids. *Applied Thermal Engineering*, **25** (17-18), 3104-3114.

Chen, G. (2000). Phonon heat conduction in nanostructures. *International Journal of Thermo Science*, 39, 471-480.

Chen, X., Cheng, H. and Ma, J. (1998). A study on the stability and rheological behaviour of concentrated TiO_2 dispersions. *Powder Technology*, **99**, 171-176.

Choi S.U.S. and Eastman, J.A. (2001). Enhanced heat transfer using nanofluids. United States Patent, US 6,221,275 B1, April 24, 2001.

Choi, S.U.S, Zhang, Z.G., Yu, W., Lockwood, F.E., and Grulke, E.A. (2001).

Anomalous thermal conductivity enhancement in nanotube suspensions. *Applied Physics Letters*, **79**(14), 2252-2254.

Choi, S.U.S. (1995). Enhancing thermal conductivity of fluids with nanoparticles. *American Society of Mechanical Engineers, Fluids Engineering Division (Publication) FED, **v 231**, Developments and Applications of Non-Newtonian Flows*, 99-105.

Choi, S.U.S. (2002). Nanofluids could help open door to advanced truck designs. *TransForum Research Review*,. **3**(4), 5.

Choi, S.U.S., Xu, X., Keblinski, P., and Yu, W. (2002). Nanofluids can take the heat. *DOE BES 20th Symposium on Energy Engineering Sciences*; Argonne, IL.

Chon, C.H., Kihm, K.D., Lee, S.P., Choi, S.U.S. (2005). Empirical correlation finding the role of temperature and particle size for nanofluid (Al_2O_3) thermal conductivity enhancement, *Applied Physics Letters*, **87**, 153107(1-3).

Chopkar, M., Das, P.K. and Manna, I. (2006). Synthesis and characterization of nanofluids for advanced heat transfer applications, *Scripta Materialia*, **55**, 549-552.

Daungthongsuk, W, and Wongwises, S. (2005). A critical review of convective heat transfer of nanofluids. *Renewable and Sustainable Energy Reviews*, Article in Press.

Das, S.K., Putra, N., and Roetzel, W. (2003a). Pool boiling characteristics of nano-fluids. *International Journal of Heat and Mass Transfer*, **46**, 851-862.

Das S.K., Putra N. and Roetzel W. (2003b). Pool boiling of nano-fluids on horizontal narrow tubes. *International Journal of Multiphase Flow*, **29**, 1237-1247.

Das, S.K., Putra, N., Thiesen, P., and Roetzel W. (2003c). Temperature dependence of thermal conductivity enhancement for nanofluids. *Journal of Heat Transfer*, **125**, 567-574.

Davis, R.H. (1986). The effective thermal conductivity of composite material with spherical inclusions. *Journal of Thermophysics*, **7**(3), 609-620.

Ding, Y. and Wen, D. (2005). Particle migration in a flow of nanoparticle suspensions. *Powder Technology,* **149**, 84-92.

Ding, Y., Alias, H, Wen, D, and Williams, R.A. (2006). Heat transfer of aqueous suspensions of carbon nanotubes (CNT nanofluids). *International Journal of Heat and Mass Transfer,***49**, 240-250.

Deiss, J.L., Anizan, P., Hadigui, S.El. and Wecker, C. (1996). Steric stability of TiO2 nanoparticles in aqueous dispersions, *Colloids and Surfaces A:Physicochemical and Engineering Aspects*, **106**, 59-62.

Eastman, J.A. Choi, S.U.S., Li, S. (2002). Development of energy-efficient nanofluids for heat transfer application, Research Briefs, 1-6. (http://www.msd.anl.gov/highlights/Eastman.html)

Eastman, J.A. Choi, S.U.S., Li, S., Thompson, L.J., and Lee, S. (1997). Enhanced thermal conductivity through the development of nanofluids. Materials Research Society Symposium - Proceedings, **v 457**, *Nanophase and Nanocomposite Materials II*, 3-11.

Eastman, J.A., Choi, S.U.S, Li, S., Soyez, G., Thompson, L.J., and DiMelfi, R.J. (1999). Novel thermal properties of nanostructured materials. *Material Science Forum*, **312-314**, 629-634.

Eastman, J.A., Choi, S.U.S., Li, S., Yu, W., and Thompson, L.J. (2001). Anomalously increased effective thermal conductivities of ethylene glycol-based nanofluids containing copper nanoparticles. *Applied Physics Letters,* **78**(6), 718-720.

Eastman, J.A., Phillpot, S.R., Choi, S.U.S. and Keblinski, P. (2004). Thermal transport in nanofluids, Annual Review of Material Research, **34**, 219-246.

Esumi, K., Ishigami, M., Nakajima, A., Sawada, K. and Honda, H. (1996). Chemical treatment of carbon nanotubes. *Carbon*, **24**, 279-281.

Evans, W., Fish, J. and Keblinski, P. (2006). Role of brownian motion hydrodynamics on nanofluid thermal conductivity, Applied Physics Letters, **88**, 093116 (1-3).

Faulkner, D., Khotan, M., and Shekarriz. (2003). Practical design of a 1000 W/cm^2 cooling system. 19th *IEEE Semiconductor Thermal Measurement and Management Symposium*, 223-230.

Gibson, S.L., Pathak, J.A., Grulke, E.A., Wang, H., and Hobbie, E.K. (2004). Elastic flow instability in nanotubes suspension, *Physical Review Letters*, **92**(4), 048302(1-4).

Gleiter, H. (1989). Nanocrystalline materials, *Progress of Material Science*, **33**, 223-315.

Gosselin, L. and Da Silva, A. (2004). Combined "heat transfer and power dissipation" optimization of nanofluid flows, *Applied Physics Letters*, **85**(18), 4160-4162.

Hamilton, R.L. and Crosser, O.K. (1962). Thermal conductivity of heterogeneous two-component systems, *Industrial and Engineering Chemistry Fundamaentals I*, **1**(3), 182-191.

Healy, J.J. de Groot, J.J., and Kestin, J. (1976). A theory of the transient hot-wire method for measuring thermal conductivity, *Physica 82C*, 392-408.

Heris, S.Z., S., Etemad, S. G., and Nasr Esfahany, M. (2006). Experimental investigation of oxide nanofluids laminar flow convective heat transfer. *International Communications in Heat and Mass Transfer*, **33**(4), 529-535.

Hernadi, K. (2002). Catalytic synthesis of multiwall carbon nanotubes from methylacetylene, *Chemical Physics Letters*, **363** (1-2), 169-74.

Hetsroni G. and Rozenblit R. (1994). Heat transfer to a liquid-solid mixture in a flume. *International Journal of Multiphase Flow*, **20**, 671-689.

Hilding, J., Grulke, E.A., Zhang, Z.G., and Lockwood, F. (2003). Dispersion of carbon nanotubes in liquid. *Journal of Dispersion Science and Technology*, **24**(1), 1-41.

Hirai, H., and Yakura, N. (2001). Protecting polymer in suspension of metal nanoparticles. *Polymer Advanced Technology*, **12**, 724-733.

Hong, T.K., Yang, H.S., and Ghoi, C.J. (2005). Study of the enhanced thermal conductivity of Fe nanofluids. *Journal of Applied Physics*, **97(6)**, 64311-1-4.

Hwang,Y.J., Ahn, Y.C.,Shin, H.S., Lee, C.G., Kim, G.T., Park, H.S. and Lee, J.K. (2005). Investigation on characteristics of thermal conductivity enhancement of nanofluids. *Current Applied Physics,* Article in Press.

Hwang,Y. Park, H.S., Lee, J.K. and Jung, W.H. (2006). Thermal conductivity and lubrication characteristics of nanofluids, Current Applied Physics, Article in Press.

Iijima, S. (1991). Helical microtubules of graphitic carbon, *Nature*, **354**, 56-58.

Islam, M.F., Rojas, E., Bergey, D.M., Johnson, A.T., and Yodh, A.G. (2003). High weight fraction surfactant solubilization of single-wall carbon nanotubes in water. *Nano Letters*, **3**(2), 269-273.

Jang, S. P., and Choi, S. U. S. (2004). Role of Brownian motion in the enhanced thermal conductivity of nanofluids, *Applied Physics Letters*, **84**(21), 4316-4318.

Jang, S. P., and Choi, S. U. S. (2006). Cooling performance of a microchannel heat sink with nanofluids. *Applied Thermal Engineering*, **26**(17-18), 2457-2463.

Jiang, L., Gao, L., and Sun, J. (2003). Production of aqueous colloidal dispersion of carbon nanotubes. *Journal of Colloid and Interface Science*, **260**(1), 89-94..

Jou, R.-Y., and Tzeng, S.-C. (2006). Numerical research of nature convective heat transfer enhancement filled with nanofluids in rectangular enclosures. *International Communications in Heat and Mass Transfer*, **33**(6), 727-736.

Khanafer, K., Vafai, K., and Lightstone, M. (2003). Bouyancy-driven heat transfer enhancement in a two-dimensional enclosure utilizing nanofluids. *International Journal of Heat and Mass Transfer*, **46**(19), 3639-3653.

Keblinski, P., Phillpot, S.R., Choi, S.U.S., and Eastman, J.A. (2002). Mechanisms of heat flow in suspensions of nano-sized particles (nanofuids). *International Journal of Heat and Mass Transfer*, **45**, 855-863.

Keblinski, P., Eastman, J.A. and Cahill, D.G. (2005). Nanofluids for thermal transport, *Materials Today*, June 2005, 36-44.

Kim, J., Choi, C.K., Kang, Y. T., Kim, M.G. (2006). Effects of thermodiffussion and nanoparticles on convective instabilities in binary nanofluids. *Microscale Thermophysical Engineering*, **10**(1), 29-39.

Kim, J.K., Kang, Y.T. and Choi, C.K. (2004). Analysis of convective instability and heat transfer characteristics of nanofluids, *Physics of Fluids*, **16**(7), 2395-2401.

Kim, J.K., Jung, J.Y. and Kang, Y.T. (2006), The effect of nano-particles on the bubble absorption performance in a binary nanofluid, *International Journal of Refrigeration*, **29**, 22-29.

Kim P., Shi L., Majumdar A., and McEuen P.L. (2001). Thermal transport measurements of individual multi walled nanotubes. *Physical Review Letters*, **87**(21), 215502/1-4.

Kinloch, I.A., Roberts, S.A., and Windle, A.H. (2002). A rheological study of concentrated aqueous nanotube dispersions. *Polymer*, **43**, 7483-7491.

Koo, J. (2005). Computational nanofluid flow and heat transfer analysis applied to micro-systems, North Carolina University, PhD Thesis.

Koo, J. and Kleinstreuer, C. (2004). A new thermal conductivity model for nanofluids,

Journal of Nanoparticle Research, **6**, 577-588.

Koo, J. and Kleinstreuer, C. (2005). Impact analysis of nanoparticle motion mechanism on the thermal conductivity of nanofluids, *International Communications in Heat and Mass Transfer*, **32**, 1111-1118.

Krishnamurthy, S., Bhattacharya, P., Phelan, P. E., and Prasher, R. S. (2006). Enhanced mass transport in nanofluids. *Nano Letters*, **6**(3), 419-423.

Kumar, D.H, Patel, H.E, Rajeev Kumar, V.R., Sundarajan, T., Pradeep, T, and Das, S.K. (2004). Model for heat conduction in nanofluids, *Physical Review Letters*, **93**(14), 144301(1-4).

Kwak, K. and Kim, C. (2005). Viscosity and thermal conductivity of copper oxide nanofluid dispersed in ethylene glycol, *Korea-Australia Rheology Journal*, **17**(2), 35-40.

Lee.D, Kim, J.W. and Kim, B.G. (2006). A new parameter to control heat transport in nanofluids: surface charge state of the particle in suspension, *Journal of Physical Chemistry B*, **110**, 4323-4328.

Lee, S., and Choi, S.U.S. (1996). Application of metallic nanoparticle suspensions in advanced cooling systems. *American Society of Mechanical Engineers, Pressure Vessels and Piping Division (Publication) PVP*, v 342, *Recent Advances in Solids/Structures and Application of Metallic Materials*, 227-234.

Lee, S., Choi, S.U.S., Li, S., Eastman, J.A. (1999). Measuring thermal conductivity of fluids containing oxide nanoparticles. *Journal of Heat Transfer*, Transactions ASME, **121**, 280-289.

Li, Q. and Xuan, Y. (2000). Experimental investigation on transport properties of nanofluids. *Heat Transfer Science and Technology*, 757-762.

Li, Q. and Xuan, Y. (2002). Convective heat transfer and flow characteristics of Cu-water nanofluid. *Science, Series E*, **45**(4), 408-416.

Lo, C.-H., Tsung, T.-T., and Chen, L.-C. (2005). Shape-controlled synthesis of Cu-based nanofluid using submerged arc nanoparticle synthesis system (SANSS). *Journal of Crystal Growth*, **277** (1-4), 636-642.

Liu, C.H., Huang, H., Wu, Y. and Fan, S.S. (2004). Thermal conductivity improvement of silicone elastomer with carbon nanotubes loading. *Applied Physics Letters*, **84**(21), 4248-4250.

Liu, M.-S., Ching-Cheng Lin, M., Huang, I..T., and Wang, C.-C. (2005), Enhancement of thermal conductivity with carbon nanotube for nanofluids. *International Communications in Heat and Mass Transfer*, 32(9), 1202-1210.

Liu, M.-S., Lin, M. C.-C., Tsai, C. Y., and Wang, C.-C. (2006). Enhancement of thermal conductivity with Cu for nanofluids using chemical reduction method. *International Journal of Heat and Mass Transfer*, **49** (17-18), 3028-3033.

Lu, S. and Lin, H. (1996). Effective conductivity of composites containing aligned spherical inclusions of finite conductivity. *Journal of Applied Physics*, **79**(9), 6761-6769.

Ma, H. B., Wilson, C., Borgmeyer, B., Park, K., Yu, Q., Choi, S. U. S., and Tirumala, M. (2006). Effect of nanofluid on the heat transport capability in an oscillating heat pipe. *Applied Physics Letters*, 88 (14).

Maiga, S.E. B., Nguyen, C.T., Galanis, N., and Roy, G. (2004). Heat transfer behaviours of nanofluids in a uniformly heated tube. *Superlattices and Microstructures,* **35**(3-6), 543-557.

Maiga, S.E. B., Palm, S.J., Nguyen, C.T., Roy, G., and Galanis, N. (2005). Heat transfer enhancement by using nanofluids in forced convection flows, *International Journal of Heat & Fluid Flow*, **26**, 530-546.

Mamut, E. (2006). Characterization of heat and mass transfer properties of nanofluids, *Romania Journal of Physics*, **51**(1-2), 5-12.

Manna, I., Chopkar, M., and Das, P. K. (2005). Nanofluid - A new concept in heat transfer and thermal management. *Transactions of the Indian Institute of Metals*, 58(6), 1045-1055.

Masuda, H., Ebata, A., Teramae, K., and Hishinuma, N. (1993). Alteration of thermal conductivity and viscosity of liquid by dispersing ultra-fine particles

(Dispersion of γAl_2O_3, SiO_2, and TiO_2 ultra-fine particles). *Netsu Bussei*, **7**(4), 227-233.

Maxwell, J.C. (1904). *Electricity and Magnetism, Part II*, 3rd ed., Clarendon, Oxford, 440.

Momoda, L.A., and Phelps, A.C. (2002). Nanometer sized phase change materials for enhanced heat transfer fluid performance. US Patent, US6447692B1.

Moy, D., Niu, C., Tennent, H., and Hoch, R. (2001). Carbon nanotubes in fuels and lubricants. International Patent, WO 0170915 A1.

Müller, F., Peukert, W., Polke, R. and Stenger, F. (2004). Dispersing nanoparticles in liquids, *International Journal of Mineral Processing*, **74** (1), S31-S41.

Mushed, S.M.S., Leong, K.C. and Yang, C. (2005). Enhanced thermal conductivity of TiO_2-water based nanofluids, *International Journal of Thermal Sciences*, **44**, 367-373.

Nan, C.W., Birringer, R., Clarke, D.R. and Gleiter, R. (1997). Effective thermal conductivity of particulate composites with interfacial thermal resistance, *Journal of Applied Physics*, **81**(10), 6692-6699.

Nan, C.W. Shi, Z. and Lin, Y. (2003). A simple model for thermal conductivity of carbon nanotube-based composites, *Chemical Physics Letters*, **375**, 666-669.

Pak B.C. and Cho Y.I. (1998). Hydrodynamic and heat transfer study of dispersed fluids with submicron metallic oxide particles. *Experimental Heat Transfer*, **11**(2), 151-170.

Palm, S. J., Roy, G., and Nguyen, C. T. (2006). Heat transfer enhancement with the use of nanofluids in radial flow cooling systems considering temperature-dependent properties. *Applied Thermal Engineering*, **26** (17-18), 2209-2218.

Pan, Z.W., Xie, S.S., Chang, B.H., Sun, L.F., Zhou, W.Y., and Wang, G. (1999). Direct growth of aligned open carbon nanotubes by chemical vapor deposition, *Chemical Physics Letters*, **299** (1), 97-102.

Patel, H.E., Das, S.K., Sundarajan, T., Nair, A.S., George, B. and Pradeep, T. (2003). Thermal conductivities of naked and monolayer protected metal nanoparticle based nanofluids: Manifestation of anomalous enhancement and chemical effects, *Applied Physics Letters*, **83**(14), 2931-2933.

Philips, R.J., McGaughey, A.J.H. (2005). Introduction to thermal transport, *Materials Today*, **8**(6), 18-20.

Prasher, R., Battacharya, P. and Phelan, P.E. (2005). Thermal conductivity of nanoscale colloidal solution (nanofluids), *Physical Review Letters*, **94**, 025901(1-4).

Prasher, R., Battacharya, P. and Phelan, P.E. (2006). Brownian-motion-based

convective-conductive model for the effective thermal conductivity of nanofluids, *Transactions of the ASME*, **128**, 588-595.

Putnam, S.A., Cahill, D.G., Ash, B.J. and Schadler, S. (2003). High precision thermal conductivity measurements as a probe of polymer/nanoparticle interfaces, *Journal of Applied Physics*, **94**(10), 6785-6788.

Putnam, S. A., Cahill, D. G., Braun, P. V., Ge, Z. B., and Shimmin, R. G. (2006). Thermal conductivity of nanoparticle suspensions. *Journal of Applied Physics*, **99** (8).

Putra, N. (2002). Heat transfer in dispersed media. University derBundeswehr, Hamburg, PhD Dissertation,

Putra, N., Roetzel, W., and Das. S.K. (2003). Natural convection of nano-fluids. *Heat and Mass Transfer*, **39**(8-9), 775-784.

Ren, Y., Xie, H., and Cai, A. (2005). Effective thermal conductivity of nanofluids containing spherical nanoparticles. *Journal of Physics D-Applied Physics*, 38(21), 3958-3961.

Romano, S.D., Acosta, E.O., Durrschmidt, T., and Kurlat. D.H. (2001). Rheological and optical properties in systems containing TiO_2 nanoparticles. *Colloid and Surfaces A: Physicochemical and Engineering Aspects*, **183-185**, 595-605.

Roy, G., Nguyen, C. T., and Lajoie, P.-R. (2004). Numerical investigation of laminar flow and heat transfer in a radial flow cooling system with the use of nanofluids. *Superlattices and Microstructures*, 35(3-6), 497-511.

Saito, T., Matsushige, K. and Tanaka, K. (2002). Chemical treatment and modification of multi-walled carbon nanotubes. *Physica B*, **323**, 280-283.

Scott, C.D., Arepalli, S., Nikolaev, P., and Smalley, R.E. (2001). Growth mechanism for single-wall carbon nanotubes in a laser ablation process. *Applied Physics A*, **72**, 573-580.

Shaffer, M.S.P., Fan, X., and Windle, A.H. (1998). Dispersion and packing of carbon nanotubes. *Carbon*, **36**(11), 1603-1612.

Shaffer, M.S.P., and Windle, A.H. (1999). Analogies between polymer solutions and carbon nanotube dispersion. *Macromolecules*, **32**, 6864-6866.

Shah, R.K. (1975). Thermal entry length solutions for the circular tube and parallel plates. in Proceedings of 3rd National Heat and Mass Transfer Conference, Indian Institute of Technology, Bombay, 1, Paper No. HMT-11-75.

Shin, S. and Lee, S.H. (2000). Thermal conductivity of suspensions in shear flow fields. *International J ournal Heat & Mass Transfer*, **43**, 4275-4282.

Sohn C.W. and Chen M.M. (1981). Microconvective thermal conductivity in disperse

two phase mixtures as observed in a low velocity Couette flow experiment. *Journal of Heat Transfer*, Transaction ASME, **103**, 47-51.

Tadros, T.F. (1993). Industrial applications of dispersion, *Advances in Colloid and Interface Science*, **46**, 1-47.

Tepei, U. and Forter-Barth. U. (2001). Rheology of nano-scale aluminium suspension. *Propellants, Explosives, Polytechnics*, **26**, 268-272.

Trisaksri, V. and Wongwises, S. (2005). Critical review of heat transfer characteristics of nanofluids. *Renewable and Sustainable Energy Reviews*, in Press.

Tsai, C.Y., Chien, H.T., Ding, P.P., Chan, B., Luh, T.Y. and Chen, P.H. (2004). Effect of structural character of gold nanoparticles in nanofluids on heat pipe thermal performance, Materials Letters, 58, 1461-1465.

Tseng, W.J. and Lin, K.C. (2003). Rheology and colloidal structure of aqueous TiO_2 nanoparticle suspensions. *Material, Science and Eng*ineering, **A355**, 186-192.

Tseng, W.J. and Wu, C.H. (2002). Aggregation, rheology and electrophoretic packing structure of aqueous Al_2O_3 nanoparticles suspensions. *Acta Materialia*, **50**, 3757-3766.

Vadasz, P. (2006). Heat conduction in nanofluid suspension, *Journal of Heat Transfer*, **128**(5), 465-477.

Wang, B.X., Zhou, L.P., and Peng, X.F. (2003). A fractal model for predicting the effective thermal conductivity of liquid with suspension of nanoparticles. *International Journal of Heat and Mass Transfer*, **46**(14), 2665-2672.

Wang, X.B., Liu, Z.M., Hu, P.A., Liu, Y.Q., Han, B.X., and Zhu, D.B. (2005). Nanofluids in carbon nanotubes supercritical CO_2: a first step towards nanochemical reaction. *Applied Physics A*, **80**, 637-639.

Wang, X., Xu, X. and Choi, S.U.S. (1999). Thermal conductivity of nanoparticle-fluid mixture. *Journal of Thermophysics and Heat Transfer*, **13**(4), 474-480.

Wasan, D.T. and Nikolov, A.D. (2003). Spreading of nanofluids on solids. *Nature*, **423**, 156-159.

Wen, D., and Ding, Y. (2004a). Effective thermal conductivity of aqueous suspensions of carbon nanotubes (Nanofluids). *International Journal of Thermophysics and Heat Transfer*, **18**(4), 481-485.

Wen, D., and Ding, Y. (2004b). Experimental investigation into convective heat transfer of nanofluids at the entrance region under laminar flow conditions. *International Journal Heat and Mass Transfer,* **47**(24), 5181-5188.

Wen, D., and Ding, Y. (2005). Formulation of nanofluids for natural convective heat transfer applications. *International Journal of Heat and Fluid Flow, special*

issue of the 6th World Conference on Experimental Heat Transfer, Fluid Mechanics, and Thermodynamics (ExHFT-6), **26** (6), 855-864.

Wen, D., and Ding, Y. (2005b). Effect on heat transfer of particle migration in suspensions of nanoparticles flowing through minichannels, Microfluidics and Nanofluidics, **1** (2), 183-189.

Wen, D and Ding, Y. (2006). Natural convection heat transfer of suspensions of titanium dioxide nanoparticles (nanofluids), *IEEE Transactions on Nanotechnology*, **5** (3), 220-227.

Werth, J.H., Linsenbuhler, M., Dammer, S.M., Farkas, Z., Hinrichsen, H., Wirth, K.-E and Wolf, D.E. (2003). Agglomeration of charged nanopowders in suspensions, *Powder Technology*, **133**, 106-112.

Withers, J. C. and Loutfy, R.O. (2003). Nano carbon materials for enhancing thermal transfer in fluids. *International Patent*, WO 03004944 A2.

Xie, H., Fujii, M., and Zhang, X. (2005). Effect of interfacial nanolayer on the effective thermal conductivity of nanoparticle-fluid mixture, *International Journal of Heat and Mass Transfer,* **48**, 2926-2932.

Xie, H., Lee, H., Youn, W., and Choi, M. (2003). Nanofluids containing multiwalled carbon nanotubes and their enhanced thermal conductivities. J*ournal of Applied Physics*, 94(8), 4967-4971.

Xie, H., Wang, J., Xi, T., and Liu, Y. (2002a). Thermal conductivity of suspensions containing nanosized SiC particles. *International Journal of Thermophysics*, **23**(2), 571-580.

Xie, H., Wang, J., Xi, T., Liu, Y., and Ai, F. (2002b). Dependence of the thermal conductivity of nanoparticle-fluid mixture on the base fluid. *Journal of Material Science Letter,* **21**, 1469-1471.

Xie, H., Wang, J., Xi, T., Liu, Y, and Ai, F. (2002c). Thermal conductivity enhancement of suspensions containing nanosized alumina particles. *Journal of Applied Physics*, **91**(7), 4568-4572.

Xie, H., Wang, J., Xi, T., Liu, Y, and Ai, F. (2002d). Thermal conductivity of suspension containing SiC particles. *Journal of Material Science Letter,* **21**, 193-195.

Xie, S. Li, W., Pan, Z., Chang, B. and Sun, L. (2000). Mechanical and physical properties on carbon nanotubes, *Journal of Physics and Chemistry of Solids*, **61**, 1153-1158.

Xue, L. (2004). Role of interfaces on thermal conductivity, Rensselaer Polytechnic Institute, PhD Thesis.

Xuan, Y. and Li, Q. (2000). Heat transfer enhancement of nanofluids. *International Journal of Heat and Fluid Flow*, **21**, 58-64.

Xuan, Y. and Li, Q. (2003). Investigation on convective heat transfer and flow features of nanofluids. *Journal of Heat Transfer*, **125**(1), 151-155.

Xuan, Y. and Roetzel, W. (2000). Conception for heat transfer correlation of nanofluid. *International Journal of Heat and Mass Transfer*, **43**, 3701-3707.

Xuan,Y., Li, Q., and Hu, W. (2003). Aggregation structure and thermal conductivity of nanofluids. *AIChE*, **49**(4), 1038-1043.

Xuan, Y. and Yao, Z. (2005). Lattice Boltzmann model for nanofluids. *Heat and Mass Transfer*, **41(3),** 199-205.

Xuan, Y., Yu, K. and Li, Q.m (2005). Investigation on flow and heat transfer of nanofluids by the thermal Lattice Boltzmann model. *Progress in Computational Fluids Dynamics*, **5**(1-2), 13-19.

Xue, Q., and Xu, W.-M. (2005). A model of thermal conductivity of nanofluids with interfacial shells. *Materials Chemistry and Physics*, **90** (2-3), 298-301.

Xue, Q.Z. (2003). Model for effective thermal conductivity of nanofluids. *Physical Letter A*, **307**, 313-317.

Xue, Q. Z. (2006). Model for the effective thermal conductivity of carbon nanotube composites. *Nanotechnology*, **17** (6), 1655-1660.

Xue, L., Keblinski, P., Phillpot, S.R., Choi, S.U.S., Eastman, J. (2003). Two-regimes of thermal resistance at a liquid-solid resistance. *Journal of Chemical Physics*, **118**(1), 337-339.

Xue, L., Keblinski, P., Phillpot, S.R., Choi, S.U.S., Eastman, J. (2004). Effect of liquid layering at the liquid–solid interface on thermal transport. *International Journal of Heat and Mass Transfer*, **47**, 4277-4284.

Yang, Y., Grulke, E.A., Zhang, Z.G. and Wu, G. (2005). Rheological behaviour of carbon nanotubes and graphite nanoparticle dispersions, *Journal of Nanoscience and Nanotechnology*, **5**, 571-579.

Yang, Y., Grulke, E.A., Zhang, Z.G. and Wu, G. (2006). Thermal and rheological properties of carbon nanoyube-in-oil dispersion, *Journal of Applied Physics*, **99**, 114307(1-7).

Yang, Y., Zhang, Z. G., Grulke, E. A., Anderson, W. B., and Wu, G. (2005). Heat transfer properties of nanoparticle-in-fluid dispersions (nanofluids) in laminar flow. *International Journal of Heat and Mass Transfer*, **48** (6), 1107-1116.

Yatsuya, S., Tsukasaki, Y., Mihama, K. and Uyeda, R. (1978). Preparation of extremely fine particles by vacuum evaporation onto a running oil substrate. *Journal of Crystal Growth*, **45**, 490-494.

Yerushalmi-Rozen, R., and Regev, O. (2002). Method for the preparation of stable

suspensions and powders of single carbon nanotubes. International Patent.,WO 02076888A1.

You, S.M., Kim, J.H., and Kim, K.H. (2003). Effect of nanoparticles on critical heat flux of water in pool boiling heat transfer. *Applied Physics Letters*, **83(16)**, 3374-3376.

Yu, W. and Choi, S.U.S. (2002). Analysis of thermal conductivity and convective heat transfer in nanotube suspension. ASME International Mechanical Engineering Congress & Exposition, New Orleans.

Yu, W. and Choi, S.U.S. (2003). The role of interfacial layers in the enhanced thermal conductivity of nanofluids: A renovated Maxwell model. *Journal of Nanoparticle Research*, **5**(1-2), 167-171.

Yu, W. and Choi, S.U.S. (2004). The role of interfacial layers in the enhanced thermal conductivity of nanofluids: A renovated Hamilton-Crosser model. *Journal of Nanoparticle Research*, **6**(4), 355-361.

Yu, W. and Choi, S.U.S. (2005). An effective thermal conductivity model of nanofluids with a cubical arrangement of spherical particles, *Journal of Nanoscience and Nanotechnology*, **5**, 580-586.

Zaman, A.A., Singh, P., and Moudgil, B.M. (2002). Impact of self-assembled

surfactant structures on rheology of concentrated nanoparticles dispersions. *Journal of Colloid and Interface Science*, **251**, 381-387.

Zhang, Z., and Lockwood, F. E. (2004). Preparation of stable nanotubes dispersions in liquids. US Patent US6783746B1, August 31, 2004.

Zhou, D. W. (2004). Heat transfer enhancement of copper nanofluid with acoustic cavitation. *International Journal of Heat and Mass Transfer*, **47**(14-16), 3109-3117.

Zhou, X. F. and Gao, L. (2006). Effective thermal conductivity in nanofluids of nonspherical particles with interfacial thermal resistance: Differential effective medium theory. *Journal of Applied Physics*, **100**, 024913 (1-6).

Zhou, D. W. and Liu, D.Y. (2004). Heat transfer characteristics of nanofluids in an acoustic cavitation field, *Heat Transfer Engineering*, **25**(6), 54-61.

Zhu, H.T., Lin. Y.S. and Yin Y.S. (2004). A novel one-step chemical method for preparation of copper nanofluids, *Journal of Colloid and Interface Science*, **277** (1), 100-103.

APPENDIX A

IMAGES OF NANOPARTICLES

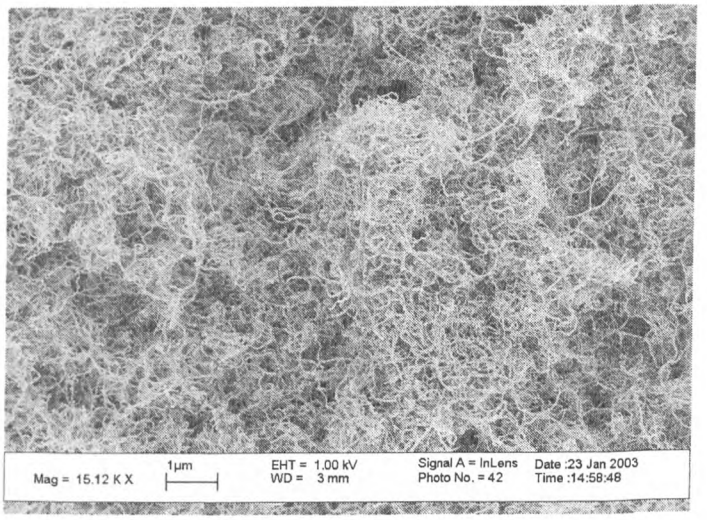

Figure A.1 : SEM image of carbon nanotubes under FEGSEM Leo 1500.

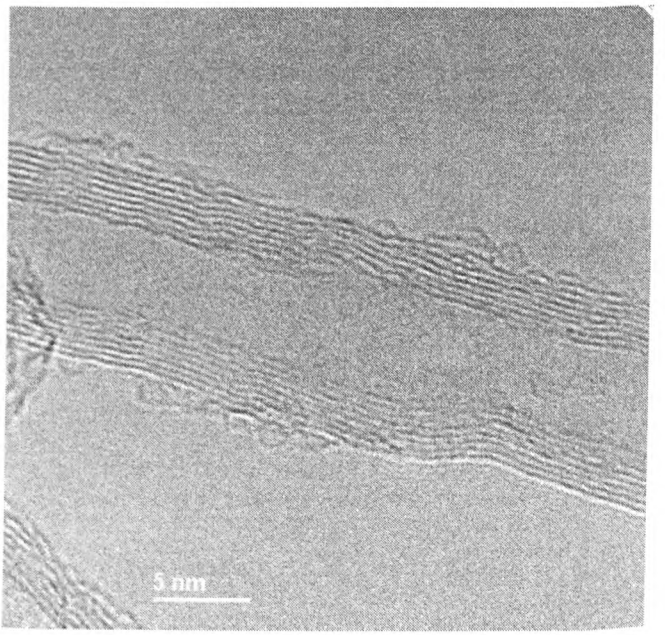

Figure A.2: TEM images of carbon nanotube suspension.

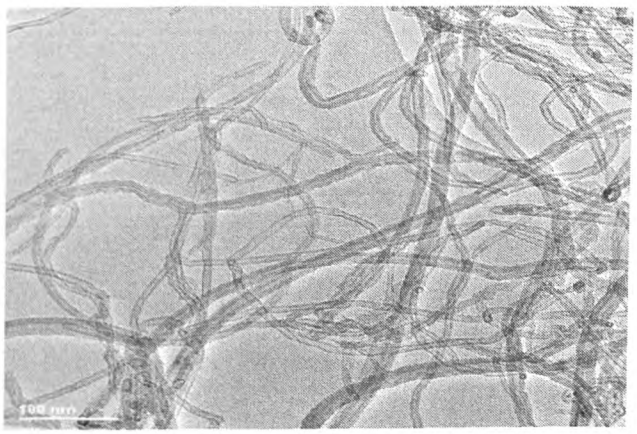

Figure A.3: TEM images of carbon nanotube suspension.

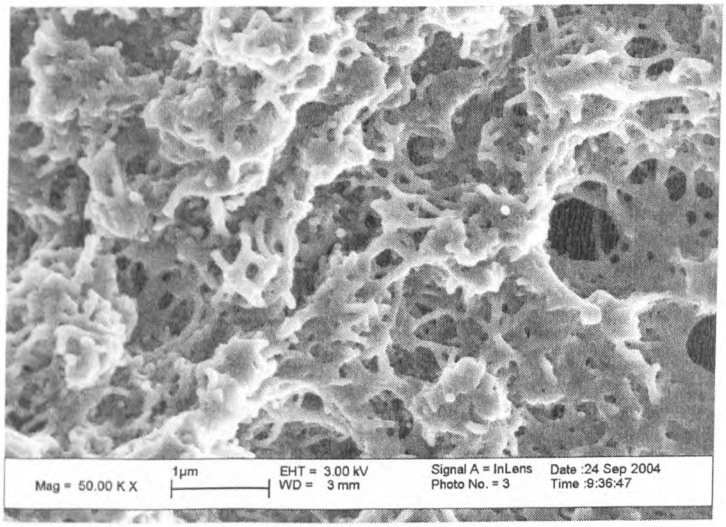

Figure A.4: SEM image of dispersed carbon nanotube nanofluids.

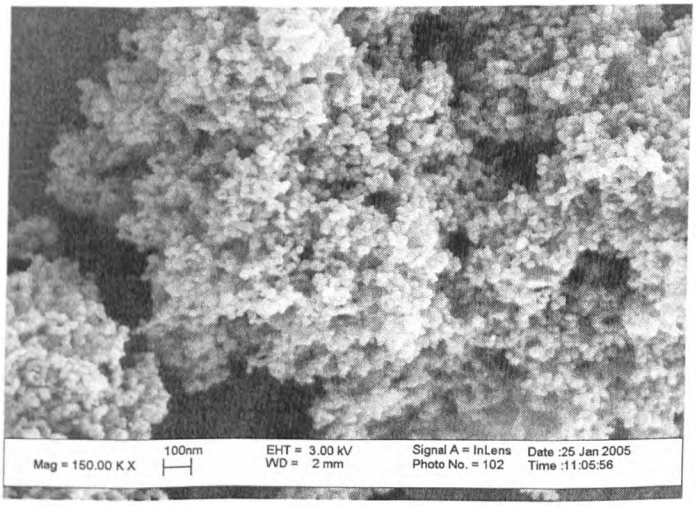

Figure A.5: SEM image of TiO_2 nanoparticles.

APPENDIX B1

RHEOLOGY DATA OF CARBON NANOTUBES SUSPENSIONS

Temperature = 25C
pH ~6.00

Conc= 0.10%		Conc = 0.25%		Conc =0.50%	
Shear Rate '(1/s)	Viscosity '(Pas)	Shear Rate '(1/s)	Viscosity '(Pas)	Shear Rate '(1/s)	Viscosity '(Pas)
2.86E-01	8.44E+00	2.86E-01	5.21E+01	2.86E-01	1.77E+02
4.83E-01	4.77E+00	4.83E-01	2.80E+01	4.83E-01	8.92E+01
8.15E-01	2.61E+00	8.15E-01	1.54E+01	8.15E-01	4.96E+01
1.38E+00	1.48E+00	1.38E+00	8.56E+00	1.38E+00	2.79E+01
2.32E+00	9.19E-01	2.32E+00	4.79E+00	2.32E+00	1.55E+01
3.91E+00	5.93E-01	3.91E+00	2.70E+00	3.91E+00	8.58E+00
6.60E+00	2.84E-01	6.60E+00	1.45E+00	6.60E+00	5.18E+00
1.11E+01	1.66E-01	1.11E+01	7.64E-01	1.11E+01	2.68E+00
1.88E+01	9.28E-02	1.88E+01	3.56E-01	1.88E+01	1.51E+00
3.17E+01	4.92E-02	3.17E+01	1.70E-01	3.17E+01	8.31E-01
5.35E+01	3.10E-02	5.35E+01	7.26E-02	5.35E+01	4.90E-01
1.52E+02	1.17E-02	1.52E+02	2.05E-02	1.52E+02	1.64E-01
2.57E+02	1.26E-02	2.57E+02	1.50E-02	2.57E+02	8.83E-02
4.33E+02	8.51E-03	4.33E+02	9.48E-03	4.33E+02	4.74E-02
7.31E+02	5.54E-03	7.31E+02	6.52E-03	7.31E+02	2.51E-02
1.23E+03	3.36E-03	1.23E+03	4.72E-03	1.23E+03	6.66E-03
2.08E+03	2.48E-03	2.08E+03	3.97E-03	2.08E+03	3.48E-03
3.51E+03	2.23E-03	3.51E+03	3.91E-03	3.51E+03	3.16E-03
5.92E+03	2.32E-03	5.93E+03	3.79E-03	5.92E+03	3.08E-03
1.00E+04	2.35E-03	1.00E+04	3.73E-03	1.00E+04	3.26E-03

APPENDIX B1 (CONTINUED)

Temperature = 40C
pH = 6

Conc=0.10% Shear Rate '(1/s)	Viscosity '(Pas)	Conc=0.25% Shear Rate '(1/s)	Viscosity '(Pas)	Conc=0.50% Shear Rate '(1/s)	Viscosity '(Pas)
2.86E-01	3.78E+00	2.86E-01	3.51E+01	2.86E-01	9.69E+01
4.83E-01	1.95E+00	4.83E-01	1.63E+01	4.83E-01	5.91E+01
8.15E-01	1.17E+00	8.15E-01	1.41E+01	8.15E-01	3.65E+01
2.32E+00	4.97E-01	2.32E+00	2.83E+00	2.32E+00	1.28E+01
3.91E+00	3.00E-01	3.91E+00	2.55E+00	3.91E+00	6.89E+00
6.60E+00	1.96E-01	6.60E+00	8.02E-01	6.60E+00	3.49E+00
1.88E+01	5.34E-02	1.88E+01	2.79E-01	1.88E+01	5.97E-01
3.17E+01	2.55E-02	3.17E+01	1.53E-01	3.17E+01	2.55E-01
5.35E+01	1.05E-02	5.35E+01	1.04E-01	5.35E+01	1.24E-01
1.52E+02	4.02E-03	1.52E+02	3.59E-02	1.52E+02	5.57E-02
2.57E+02	3.53E-03	2.57E+02	2.37E-02	2.57E+02	3.94E-02
7.31E+02	2.70E-03	7.31E+02	8.39E-03	7.31E+02	9.90E-03
1.23E+03	2.41E-03	1.23E+03	7.70E-03	1.23E+03	1.06E-02
3.51E+03	2.12E-03	3.51E+03	5.58E-03	3.51E+03	8.68E-03
5.93E+03	1.85E-03	5.93E+03	4.92E-03	5.93E+03	6.69E-03
1.00E+04	1.74E-03	1.00E+04	4.65E-03	1.00E+04	5.66E-03

APPENDIX B2

RHEOLOGY DATA OF TiO_2 NANOFLUIDS

Shear Rate '(1/s)	119nm 25C Viscosity '(Pas)	119nm 30C Viscosity '(Pas)	90nm 25C Viscosity '(Pas)
53.432	1.87E-03	1.79E-03	0.001653
74.68	1.45E-03	1.36E-03	0.001314
87.024	1.34E-03	1.24E-03	0.001234
96.433	1.31E-03	1.20E-03	0.001212
104.93	1.30E-03	1.19E-03	0.001209
113.45	1.29E-03	1.18E-03	0.001212
122.39	1.29E-03	1.18E-03	0.001217
132.37	1.29E-03	1.18E-03	0.001224
141.9	1.30E-03	1.18E-03	0.001232
154.26	1.29E-03	1.18E-03	0.00124
166.27	1.30E-03	1.19E-03	0.001247
179.05	1.30E-03	1.19E-03	0.001255
192.8	1.30E-03	1.19E-03	0.001263
207.51	1.31E-03	1.20E-03	0.001271
223.42	1.31E-03	1.20E-03	0.001279
240.57	1.31E-03	1.20E-03	0.001288
258.9	1.32E-03	1.21E-03	0.001298
278.53	1.32E-03	1.21E-03	0.001308
299.58	1.33E-03	1.22E-03	0.001317
322.04	1.33E-03	1.23E-03	0.001391
346.16	1.34E-03	1.23E-03	0.001369

APPENDIX B2 (CONTINUED)

Shear Rate '(1/s)	180nm 25C Viscosity '(Pas)	180nm 30C Viscosity '(Pas)	570nm 25C Viscosity '(Pas)	570nm 30C Viscosity '(Pas)
53.432	2.08E-03	1.80E-03	1.87E-03	1.81E-03
74.68	1.53E-03	1.36E-03	1.45E-03	1.36E-03
87.024	1.42E-03	1.24E-03	1.34E-03	1.24E-03
96.433	1.36E-03	1.20E-03	1.30E-03	1.20E-03
104.93	1.34E-03	1.18E-03	1.29E-03	1.19E-03
113.45	1.33E-03	1.18E-03	1.29E-03	1.18E-03
122.39	1.33E-03	1.17E-03	1.29E-03	1.18E-03
132.37	1.33E-03	1.17E-03	1.28E-03	1.18E-03
141.9	1.33E-03	1.17E-03	1.29E-03	1.18E-03
154.26	1.33E-03	1.18E-03	1.29E-03	1.18E-03
166.27	1.33E-03	1.18E-03	1.29E-03	1.18E-03
179.05	1.33E-03	1.18E-03	1.29E-03	1.19E-03
192.8	1.33E-03	1.19E-03	1.30E-03	1.19E-03
207.51	1.33E-03	1.19E-03	1.30E-03	1.19E-03
223.42	1.34E-03	1.19E-03	1.30E-03	1.20E-03
240.57	1.34E-03	1.20E-03	1.31E-03	1.20E-03
258.9	1.34E-03	1.20E-03	1.31E-03	1.21E-03
278.53	1.35E-03	1.21E-03	1.32E-03	1.21E-03
299.58	1.35E-03	1.21E-03	1.32E-03	1.22E-03
322.04	1.36E-03	1.22E-03	1.33E-03	1.23E-03
346.16	1.36E-03	1.22E-03	1.33E-03	1.23E-03

APPENDIX B2 (CONTINUED)

Shear Rate '(1/s)	water 25C Viscosity '(Pas)	water 30C Viscosity '(1/s)
53.432	0.00131	0.001089
74.68	0.001204	0.001042
87.024	0.001174	0.00109
96.433	0.001168	0.001066
104.93	0.00117	0.000934
113.45	0.001176	0.001063
122.39	0.001184	0.0009762
132.37	0.001191	0.0009952
141.9	0.001198	0.001012
154.26	0.001206	0.001021
166.27	0.001214	0.001033
179.05	0.001222	0.001043
192.8	0.001229	0.00105
207.51	0.001237	0.001057
223.42	0.001246	0.001062
240.57	0.001255	0.001068
258.9	0.001263	0.001075
278.53	0.001272	0.00108
299.58	0.001281	0.001086
322.04	0.001289	0.001091
346.16	0.001296	0.001098

APPENDIX C

DATA FOR PARTICLE SIZE DISTRIBUTION MEASUREMENTS FROM NANOSIZER

90nm Size d.nm	Mean Intensity %	Size d.nm	Mean Intensity %	Size d.nm	Mean Intensity %	Size d.nm	Mean Intensity %
0.4	0	5.61	0	78.8	10.6	1110	0
0.463	0	6.5	0	91.3	12.1	1280	0
0.536	0	7.53	0	106	12.6	1480	0
0.621	0	8.72	0	122	12.2	1720	0
0.719	0	10.1	0	142	10.8	1990	0
0.833	0	11.7	0	164	8.7	2300	0
0.965	0	13.5	0	190	6.3	2670	0
1.12	0	15.7	0	220	3.9	3090	0
1.29	0	18.2	0	255	1.9	3580	0
1.5	0	21	0	295	0.6	4150	0
1.74	0	24.4	0	342	0	4800	0
2.01	0	28.2	0	396	0	5560	0
2.33	0	32.7	0	459	0	6440	0
2.7	0	37.8	0.5	531	0	7460	0
3.12	0	43.8	1.7	615	0	8630	0
3.62	0	50.7	3.6	712	0	1.00E+04	0
4.19	0	58.8	6	825	0		
4.85	0	68.1	8.4	955	0		

APPENDIX C (CONTINUED)

120 nm

Size d.nm	Mean Intensity %	Size d.nm	Mean Intensity %	Size d.nm	Mean Intensity %	Size d.nm	Mean Intensity %
0.4	0	5.61	0	78.8	7.3	1110	0
0.463	0	6.5	0	91.3	9.6	1280	0
0.536	0	7.53	0	106	11.4	1480	0
0.621	0	8.72	0	122	12.4	1720	0
0.719	0	10.1	0	142	12.4	1990	0
0.833	0	11.7	0	164	11.4	2300	0
0.965	0	13.5	0	190	9.7	2670	0
1.12	0	15.7	0	220	7.4	3090	0
1.29	0	18.2	0	255	5	3580	0
1.5	0	21	0	295	2.9	4150	0
1.74	0	24.4	0	342	1.2	4800	0
2.01	0	28.2	0	396	0.3	5560	0
2.33	0	32.7	0	459	0	6440	0
2.7	0	37.8	0	531	0	7460	0
3.12	0	43.8	0.3	615	0	8630	0
3.62	0	50.7	1.1	712	0	1.00E+04	0
4.19	0	58.8	2.7	825	0		
4.85	0	68.1	4.9	955	0		

180 nm

Size d.nm	Mean Intensity %	Size d.nm	Mean Intensity %	Size d.nm	Mean Intensity %	Size d.nm	Mean Intensity %
0.4	0	5.61	0	78.8	1.3	1110	0
0.463	0	6.5	0	91.3	1.6	1280	0
0.536	0	7.53	0	106	2.6	1480	0
0.621	0	8.72	0	122	4.3	1720	0
0.719	0	10.1	0	142	6.6	1990	0
0.833	0	11.7	0	164	9	2300	0
0.965	0	13.5	0	190	11	2670	0
1.12	0	15.7	0	220	12.1	3090	0
1.29	0	18.2	0	255	12.1	3580	0
1.5	0	21	0	295	11	4150	0
1.74	0	24.4	0	342	9	4800	0
2.01	0	28.2	0	396	6.4	5560	0
2.33	0	32.7	0	459	3.8	6440	0
2.7	0	37.8	0.5	531	1.7	7460	0
3.12	0	43.8	1.3	615	0.4	8630	0
3.62	0	50.7	1.9	712	0	1.00E+04	0
4.19	0	58.8	1.9	825	0		
4.85	0	68.1	1.6	955	0		

APPENDIX C (CONTINUED)

570nm

Size d.nm	Mean Intensity %	Size d.nm	Mean Intensity %	Size d.nm	Mean Intensity %	Size d.nm	Mean Intensity %
0.4	0	5.61	0	78.8	0	1110	0
0.463	0	6.5	0	91.3	0	1280	0
0.536	0	7.53	0	106	0	1480	0
0.621	0	8.72	0	122	0	1720	0
0.719	0	10.1	0	142	0	1990	0
0.833	0	11.7	0	164	0	2300	0
0.965	0	13.5	0	190	0	2670	0
1.12	0	15.7	0	220	0	3090	0
1.29	0	18.2	0	255	0	3580	0
1.5	0	21	0	295	9.9	4150	0
1.74	0	24.4	0	342	30.5	4800	0
2.01	0	28.2	0	396	36.9	5560	0
2.33	0	32.7	0	459	21.2	6440	0
2.7	0	37.8	0	531	1.5	7460	0
3.12	0	43.8	0	615	0	8630	0
3.62	0	50.7	0	712	0	1.00E+04	0
4.19	0	58.8	0	825	0		
4.85	0	68.1	0	955	0		

APPENDIX D1

PAPER PRESENTED FOR ORAL PRESENTATION AT

The 2nd Asian Particle Technology Symposium, Penang Malaysia,

ON THE RHEOLOGY OF CARBON NANOTUBES SUSPENSION

Hajar Alias, Yulong Ding, Richard A. Williams
Leeds Institute of Particle Science and Engineering,
School of Process, Environmental and Materials Engineering,
University of Leeds, Leeds LS2 9JT, United Kingdom.

Keywords : agglomerate breakage, dispersion, multiwall carbon nanotubes (MWNTs), nanofluids

ABSTRACT

Since its discovery, carbon nanotubes (CNTs) materials have inspired engineers for a range of potential applications. Some applications have been limited due to difficulties in dispersing the CNTs in liquid. To obtain a fully dispersed carbon nanotubes suspension is a significant problem. In this paper, a procedure to prepare nanofluids which consists of multi-wall carbon nanotubes (MWNTs) and a base liquid is discussed. Some sample suspensions were prepared using several different types of dispersant. The microscopy images are shown to illustrate morphology of the suspension. The rheological behaviour of the suspensions for various CNTs concentration is investigated. The steady shear test is applied to the suspension for analysis.

INTRODUCTION

Since their discovery by Iijima in 1991, carbon nanotubes have attracted considerable attention in fundamental and applied research. According to many experimental efforts and theoretical calculations, carbon nanotubes have extraordinary mechanical, thermal and electrical properties. These excellent properties of carbon nanotubes are due to their unique carbon structure as well as the nanosize scale. Carbon nanotubes have been expected to have a variety applications based on their remarkable properties. Unfortunately, achievement of these applications has been hindered, mainly by the poor processability of carbon nanotubes. Furthermore, carbon nanotubes are insoluble in many organic solvent because of the pure carbon element and their stable structure. They also have tendency to aggregate together due to the strong Van der Waals interaction between the tubes, and it is very difficult to disperse them uniformly.

EXPERIMENTAL SECTION

The multi-walled carbon nanotubes used in this study are obtained from Tsinghua-Nafine Nano-Powder Commercialization Engineering Centre. These nanotubes are produced catalytically from hydrocarbon materials on nano-catalyst under high pressure. The average diameter of the nanotubes is 20-60nm. The SEM images of the raw materials are shown in Figure 1 below.

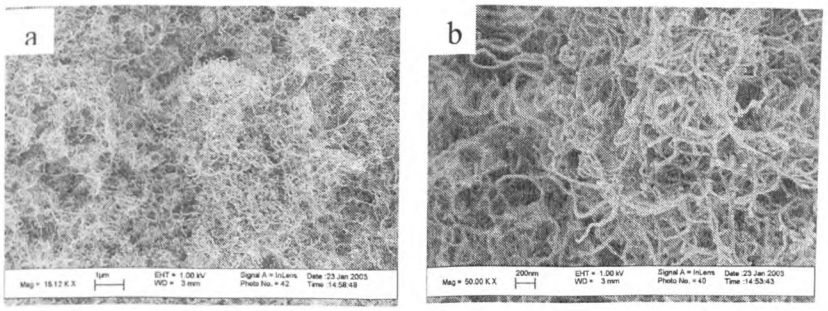

FIGURE 1 : The SEM images of the raw materials as obtained.

The possibility of producing stable dispersion has been reported (Bandyopadhyaya et al. 2002; Islam et al. 2003; Jiang et al.), and dispersion have been made stable by using surfactants, dispersing agent, stabilizing agents or by means of chemical treatment and modification (Esumi et al. 1996; Saito et al. 2002). In this study, gum arabic (GA), sodium dodecyl benzene sulfonate (NaDDBS), laurate salt and succinimide were used to enhance stabilization of the carbon nanotubes. Gum Arabic and NaDDBS have been used as dispersant in other research as well (Bandyopadhyaya et al. 2002; Islam et al. 2003; Yerushalmi-Rozen and Regev 2002).

Prior to the preparation of suspension, the CNTs are sonicated for 20 minutes to break up the tangled aggregates. The dispersant was dissolved in the base liquid and sonicated for 15 minutes to obtain homogenous mixture and enhance dispersivity. The carbon nanotubes are then added to the sample. Each of the samples was sonicated for 1 hour. A homogeneous dispersion of MWNT was obtained. All the suspensions, that had an ink-like appearance, were stored at ambient temperature and checked periodically for visual changes. After more than 1 month at stationary state, the dispersion remained unchanged (Figure 3). However the suspension using succinimide as the dispersant show sign of settlement (Figure 2).

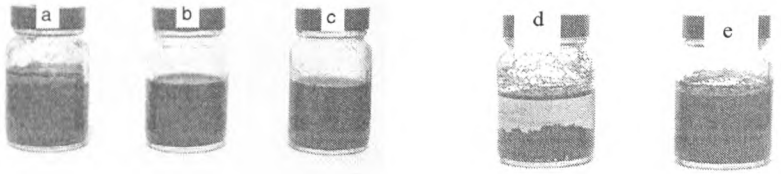

FIGURE 2: Vials containing aqueous dispersion of MWNTs (0.05 wt% CNT in 0.5 wt % dispersant) after more than one month in stationary state. Dispersant used are (a) laurate salt, (b) NaDDBs and (c) gum arabic and (d and e) succinimide. Note that the dispersion in (d) settle after one month in stationary state and (e) is the sample at the beginning of observation.

A high resolution C-VOR Bohlin Instruments rheometer was used to analyse the dispersions. A mooney geometry was predominantly used as this applies a homogeneous shear rate across the sample (75μm gap). This geometry is excellent in preventing water loss evaporation during the experiments.

RESULTS AND DISCUSSION

Measurements were taken in steady mode at 20°C. Steady shear sweeps were used to investigate the flow properties of the suspensions by recording the shear stress(σ) and viscosity(η) at increasing shear rate($\dot{\gamma}$). The shear rate was increased in a stepwise manner,

with the samples being held as each step for typically 120 seconds. The results for the flow behaviour of the dispersions are shown in Figure 3. The dispersion shows a shear thinning behaviour. Rheological analysis was not done to the samples in succinimide due to the unstable dispersion obtained.

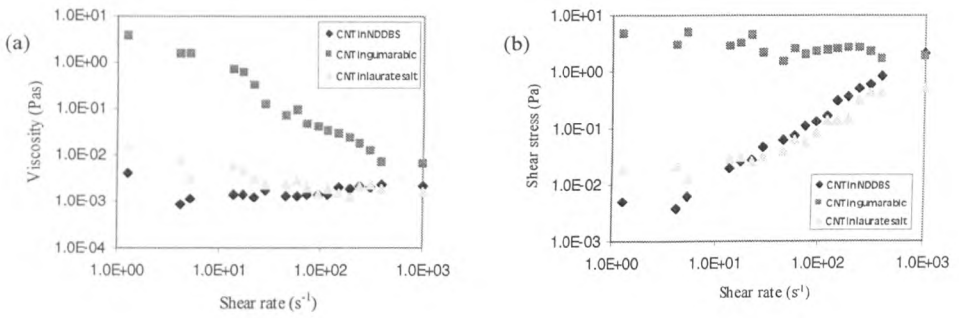

Figure 3 The steady flow behaviour of the dispersion.

CONCLUSION

A method of preparing a nanofluid consisting of carbon nanotubes in a base liquid is presented.

NOTATION

σ shear stress
η viscosity
$\dot{\gamma}$ shear rate

ACKNOWLEDGEMENT

The author would like to thanks the Ministry of Science and Technology and Environment of Malaysia for sponsoring her PhD study.

REFERENCES

Bandyopadhyaya, R., Nativ-Roth, E., Regev, O., and Yerushalmi-Rozen, R. 2002. Stabilization of Individual Carbon Nanotubes in Aqueous Solutions, *Nano Letters*, **2**(1), 25-28.

Esumi, K., Ishigami, M., Nakajima, A., Sawada, K., and Honda, H. 1996. Chemical treatment of carbon nanotubes, *Carbon*, **24**, 279-281.

Islam, M. F., Rojas, E., Bergey, D. M., Johnson, A. T., and Yodh, A. G. 2003. High weight fraction surfactant solubilization of single-wall carbon nanotubes in water, *Nano Letters*, **3**(2), 269-273.

Jiang, L., Gao, L., and Sun, J. 2003. Production of aqueous colloidal dispersion of carbon nanotubes, *Journal of Colloid and Interface Science*, **260**(1), 89-94.

Bandyopadhyaya, R., Nativ-Roth, E., Regev, O., and Yerushalmi-Rozen, R. (2002). "Stabilization of Individual Carbon Nanotubes in Aqueous Solutions." *Nano Letters*, 2(1), 25-28.

Esumi, K., Ishigami, M., Nakajima, A., Sawada, K., and Honda, H. (1996). "Chemical treatment of carbon nanotubes." *Carbon*, 24, 279-281.

Islam, M. F., Rojas, E., Bergey, D. M., Johnson, A. T., and Yodh, A. G. (2003). "High weight fraction surfactant solubilization of single-wall carbon nanotubes in water." *Nano Letters*, 3(2), 269-273.

Jiang, L., Gao, L., and Sun, J. (2003). "Production of aqueous colloidal dispersion of carbon nanotubes." *Journal of Colloid and Interface Science*, 260(1), 89-94.

Saito, T., Matsushige, K., and Tanaka, K. (2002). "Chemical treatment and modification of multi-walled carbon nanotubes." *Physica B*, 323, 280-283.

Yerushalmi-Rozen, R., and Regev, O. (2002). "Method for the preparation of stable suspensions and powders of single carbon nanotubes." The World Intellectual Property Organization (PCT), 1-23.